Investigation of the Photocatalytic and Hydrophilic properties of the thermally reduced Graphene Oxide/TiO2 Membranes

| Chemical Engineering |

Master thesis
Spring/Autumn 2017

Birgit Wright

Title:

Investigation of the Photocatalytic and hydrophilic properties of the thermally reduced Graphene Oxide/TiO2 Membranes

Semester:

10th semester

Project period:

1st February- 8st of December 2017

ECTS:

30

Supervisor:

Morten E. Simonsen

Birgit Wright (20151458)

Year of Publication

2017

Aalborg University Esbjerg

PREFACE AND ACKNOWLEDGEMENT

This Master's thesis is prepared by a student of chemical engineering at Aalborg University Esbjerg. The purpose of the project is to produce graphene oxide (GO) /TiO_2 membranes and to explore their photocatalytic and hydrophilic properties and the pore size dependence on the conditions of thermal reduction. Several experimental tools have been used to characterize the membranes. This report contains a theoretical part, introduction of used methods and results with discussion, conclusion and recommendations.

I would like to show my gratitude to my supervisor Morten E. Simonsen for his guidance and patience throughout the long project. The laboratory personnel; Dorte Spangsmark, Linda B. Madsen and Morten Strandgaard, who are always ready to answer my questions and help me when needed. In addition, Mette Skjød Hartvigsen for her understanding attitude and kindness.

ABSTRACT

The aim of the project is to investigate the photocatalytic and hydrophilic properties of the GO/TIO2 membranes. In addition, the effect of thermal reduction on the pore size of the membrane is explored.

In total seven synthesis of graphene oxide with Tour's method were done, where only 4 out of 7 batches were useable for membrane production. The sensitivity of GO concerning the size of the particles was found as one of the successful patches was ruined with exfoliation process.

A change in the behavior of the graphene oxide over time was registered, where an unsuccessful product turned into a usable gel after resting in a fume hood for a couple of months. It could be an indication GO is a dynamic material, which slowly changes its properties.

The composition of graphene oxide gel was investigated with Elemental Analysis. The content of sulfur degreases from 2.3% to 0.78% due to hydrolysis of sulphates if the gel is firstly washed with water and left to rest for a few days before the acid wash.

The successful GO gel was characterized with TGA, where GO's average concentration was found to be 2.1%. All the most common functional groups such as carboxyl, hydroxyl and ketones were found in the material with FT-IT analysis.

XRD identified a defined change from the reactant graphite into graphene oxide. A possible deoxidation was detected when the d-value of one of the gels decreased over few months from 0.8504 nm to 0.8346 cm.

Thermal reduction at 120°C was found to be occurring at a very slow pace. No signs of reduction on the XRD was noticed after 30-minute reduction, but first signs of conversion was seen on the results from 120 minute. The slow speed of reduction was also registered by analysis the membranes with DSA, where the polarity and the surface energy did not change within the first hour of reduction. The thermal reduction at 140°C on the other was registered on the XRD plots and in the results from DSA from 30 minutes and onwards. Thermal reduction duration at 140°C affected the zeta potential, where the membrane reduced for 30 minutes had higher value (average -25 mV) compared to 60-minute reduction (-40 mV). Varying the thermal reduction did not affect the pore size distribution of the membranes.

The GO and GO/TiO2 were tested for its photocatalytic property using a standard method with methylene blue solution and UV-Vis. All of the experiments – UV lamp irradiated and non-irradiated membranes - ended up decreasing the concentration of methylene blue, which was unexpected. The rate of the concentration change of the dye was also calculated to be very similar in all cases. An explanation of adsorption of methylene blue onto GO surface due to electrostatic interactions was proposed.

The photocatalytic and hydrophilic property of graphene oxide was investigated by measuring the zeta potential with and without UV exposure. The zeta potential value was measured to be lower after the irradiation. DSA analysis did not registered any increase in hydrophilicity due to UV exposure, leaving the conclusion of GO's photocatalytic properties unsettled.

Superhydrophilicity was induced by exposure to UV light with GO/TiO2 membranes, where the contact angle with water decreased noticeably.

The swelling of the GO/TiO2 membranes in aqueous was registered during the characterization.

CONTENTS

1 INTRODUCTION

About 1.2 billion people, that is a fifth of the Earth's habitants, must deal with water scarcity due to the area's natural water shortage. This deficit can be caused by several reasons: the climate of the place, climate change or a high density of habitants in the region. Hence, the demand of water cannot be met. An additional 1.6 billion people, a quarter of the world's population, experience a lack of clean drinking water because of economic shortage, which causes the countries to not be able to build the necessary infrastructure to draw water from rivers or aquifers [1, 2]. Each year, thousands of people, mostly children, lose their lives due to preventable diseases caused by a lack of access to clean water and adequate sanitation [3]. Thus, the issue of water scarcity has been caused as a combination of both – natural inclination and human activity.

The Earth has enough freshwater for its 7 billion habitants, but the resource is distributed unevenly, where most of it is mistreated and wasted. The unbalance has led to a situation where millions of people across the globe must spend their day searching for water, while people who have access to clean drinking water take it for granted and don't use it wisely. The amount of water being used has been growing more than twice the rate of the population growth in the last century. Although, globally, water scarcity is not yet a pressing issue, but the number of regions which chronically lack of water is increasing at an alarming rate.

The way the reserve of freshwater is being used is showing a serious lack of sustainability. For example, freshwater is withdrawn from aquifers at a higher rate than nature can recharge, mostly to be overused on privileged people, animals, lands and many more. Reckless behavior as such has already caused several states across the USA, areas in India and European countries to become or be almost water deficit [4, 5, 6]. On top of abusing freshwater reserves, the drawn water is frequently mistreated and ends up being polluted. Pollution can be caused by oil, carcasses, chemicals and fecal matter. Whatever the source, if the spoiled water is not dealt with, it will end up damaging people's health.

Water treatment is a solution to the sustainability concerns mentioned above. In general, there are three aims of water treatment technologies. Firstly, to produce clean drinking water from different sources such as rivers, lakes and seawater. Secondly, to treat wastewater from sewage and lastly, to develop methods for purification of industrial wastewater. There are numerous ways to purify water and during this project membrane technology is mostly focused on.

Membrane technologies have been said to be low-energy separation processes and they can be applied under ambient conditions, but the membrane operation cannot be said to be cheap. The membranes themselves are costly and in case of reverse osmosis high operating pressures raise the cost even more. In addition, membranes have the tendency to decrease in efficiency and need protection for continuous operation. Over the years the membrane separation technology has gained an important role within the subject of water treatment. New materials and production technologies have been used to produce new types of membranes suitable for a wide range of applications. There is pressure-driven microfiltration, ultrafiltration, nanofiltration and more, that can be used to remove contaminants from drinking and wastewater. Membranes have been implemented in drinking water treatment, wastewater treatment, water reclamation and desalination processes. Many novel hybrid and composite membranes with new materials have been reported, one of the examples being graphene oxide. An addition of new control technologies in the membranes against loss of efficiency have been developed, such as implementation of $TiO2$ nanoparticles, and many more exciting novelties are being researched into. The innovation concerning the membrane technology and integration of different membrane units has resulted in greatly enhanced process efficiency, reduced energy consumption, treatment cost and stability in long-term applications, but overall there is still plenty of room for improvement.

To illustrate a recent breakthrough in the water treatment field, the development producing drinking water from seawater should be looked at. The Middle East is one of the areas that suffers under constant water stress. So far, thermal techniques have been implemented to distil safe drinking water from seawater, but the process is energy intensive and costly. The persistent development work on the reverse osmosis method has provided a cheaper alternative to distillation.

The ultimate aim of the research concerning water treatment is of course to create a filtration device that will produce potable water from seawater or wastewater with minimal energy input. A material which shows great potential for membrane production is graphene oxide due to its large surface area, its oxygen rich functional groups making it hydrophilic, and graphene based structure, which can provide particle selectivity [7]. Graphene oxide has shown be a great material to be combined with titanium dioxide (TiO_2) nanoparticles.

$TiO2$ is a commonly used photocatalyst in water treatment. It has great chemical stability, low toxicity and cost-effectiveness. It can completely decompose organic pollutants into $CO2$ and water, and enhance a membrane’s flux, contaminant removal and fouling resistance [8]. Together, the two materials, could possibly create a so called self-cleaning membrane, which can provide great quality water and reduce the cost of operation noticeably.

2 THEORY

In the theory section subjects relevant to the project goals and results are presented. In the first part the introduction to membranes and how they work is outlined. The second part is dedicated to the introduction to the main material used for membrane production during this project – graphene oxide. The section starts off by introducing the reactant graphite and graphene based compounds followed by an overview of common synthesis methods, a detailed description of the formation of the graphene oxide and some of its unique behaviors. The third part is about the thermal reduction of graphene oxide. The fourth part is purely dedicated to titanium dioxide (TiO_2), where its characteristics and properties are discussed. The theory section will be finished by a section where previous work done at the development of the graphene oxide and titanium dioxide membrane is presented up until now.

2.1 MEMBRANES

This part is dedicated to give a brief overview of membranes, their categorization and how they work addition, the recommended. In qualities for a membrane are presented and common weaknesses are discussed.

2.1.1 CLASSIFICATION OF MEMBRANES

Membranes, which are pressure-driven, can be categorized based on their pore size. There are four general categories: microfiltration (MF), ultrafiltration (UF), reverse osmosis (RO) and nanofiltration (NF). The largest pore sized membranes belong to the microfiltration from 5 – 0.05 μm, followed by ultrafiltration 0.1- 0.005 μm, nanofiltration 0.008-0.001 μm and reverse osmosis < 0.001 μm [9]. The type of particles being rejected by different pore sizes can be seen on Figure 2.1.1.1. Schematic diagram of the membrane filtration spectrum .

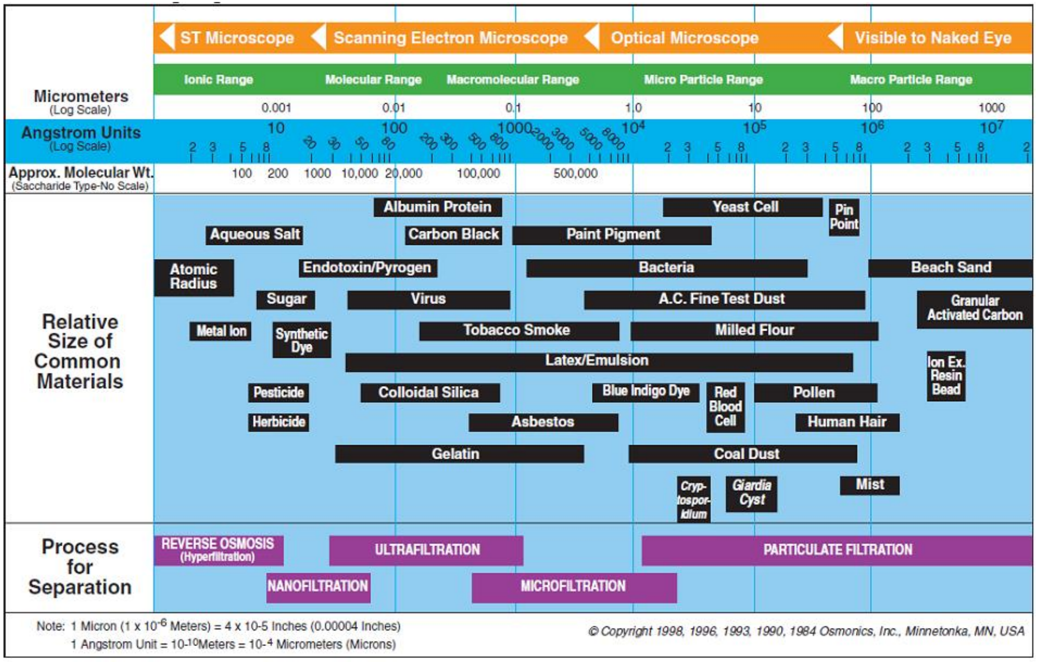

Figure 2.1.1.1. Schematic diagram of the membrane filtration spectrum [10].

Microfiltration membranes are normally applied to separate the microorganisms in drinking water. They can be used in applications such as solid–liquid separation (milled flour), separation of oil/water emulsions, beverage and pharmaceuticals industries, biological wastewater treatment, and as pre-step to remove particles to avoid problems in further treatment steps.

Ultrafiltration (UF) membranes involves removal of suspended solids, viruses, bacteria, and macromolecules. UF finds use in oil–water separation, fruit juice clarification, milk and whey production, purification of pharmaceuticals, potable water production, and secondary or tertiary wastewater reuse.

Nanofiltration (NF) membrane processes can remove most organic molecules, viruses and a range of salts. Monovalent ions can pass through the membrane, but highly charged multi valent salts and low molecular weight organics are rejected. In water treatment processes, NF membranes are used for hard water softening and synthetic dye removal.

Reverse osmosis (RO) membranes are a high-pressure and energy-efficient process, which removes minerals and monovalent ions in water. RO has been applied in seawater desalination, fruit juice concentration, cheese whey concentration, ice-making, applied on ships to clean water and car wash water reclamation. The ranges of pressure, which need to be applied for different membrane separation process are shown in Table 2.1.1.1.

Table 2.1.1.1 Different types of membranes and its application pressures [11].

Classification Type	Applied pressure (bar)
Microfiltration	0.5-3
Ultrafiltration	1-10
Nanofiltration	7-40
Reverse osmosis	25-100

The second way to divide different membranes is the way they are constructed [12]. Membrane filters are usually manufactured as flat sheet stock or as hollow fibers and then formed into several different types of membrane modules. In general, there are four main types of membrane configurations: plate-and-frame (Figure 2.1.1.2 Different membrane modules top left), tubular (Figure 2.1.1.2 top right), spiral wound (Figure 2.1.1.2 bottom left) and hollow fiber (Figure 2.1.1.1a bottom right).

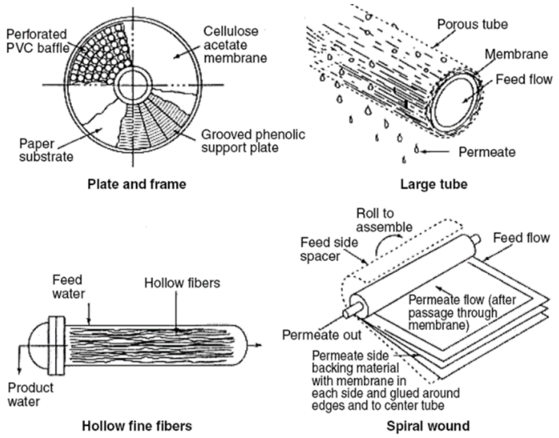

Figure 2.1.1.2 Different membrane modules [13].

The plate-and-frame is the simplest form and is made from two end plates, the flat membrane and spacers. The tubular module has the membrane located in the tube and the feed passes through the tube during the process. The third configuration, the spiral wound, is widely implemented for nanofiltration or reverse osmosis processes. A flat sheet membrane is wrapped around a perforated permeate collection tube, where the feed flows on one side of the membrane and the permeate is collected in the other side while it is spiraling in towards the collection tube. Lastly, the hollow fiber configuration is made of hollow fibers in a pressure vessel. This construction has a couple of ways to flush through the feed. One of them is where the feed moves along the outside of the fibers and exits at the end of them. The second is called a bore-side feed configuration, where the feed is circulated through the fibers.

The third way to classify membranes is based on the membrane material [11]. Most membranes can be split into three groups as shown in Table 2.1.1.2. The material mostly defines the properties the membrane is going to have.

Table 2.1.1.2. Membrane categories based on the membrane material with their advantages and disadvantages [11].

Type	Properties	Advantage	Disadvantage
Ceramic	Brittle, strong	Chemical and thermal resistance	Expensive production
Polymeric	Ductile, flexible	Cheap production and wide range of applications	Bad chemical resistance
Composite	String and flexible	Enhanced properties	Expensive production

Lastly membranes can be categorized based on how many materials are used to build a membrane. Isotropic membranes are dense or porous with a homogeneous composition. On Figure 2.1.1.3 different type of membranes is shown that all fall under isotropic due to their structure.

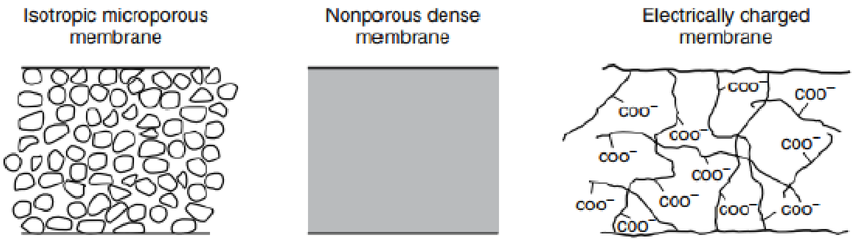

Figure 2.1.1.3. Examples of different commonly used isotropic membranes. [9]

Microporous membranes have a structure of interconnected pores. They are similar to conventional filters. Nonporous membranes are dense films, where transport across the membrane is dependent on the diffusivity and solubility of the filtrate in the membrane material. Electrically charged membrane can be dense or microporous with positive or negative surface charge or ions at the pore walls. The purification process is based on the charge of the ions.

Anisotropic membranes are made using different types of material making them heterogenous membranes with a number of layers with different structures and permeabilities (Figure 2.1.1.4).

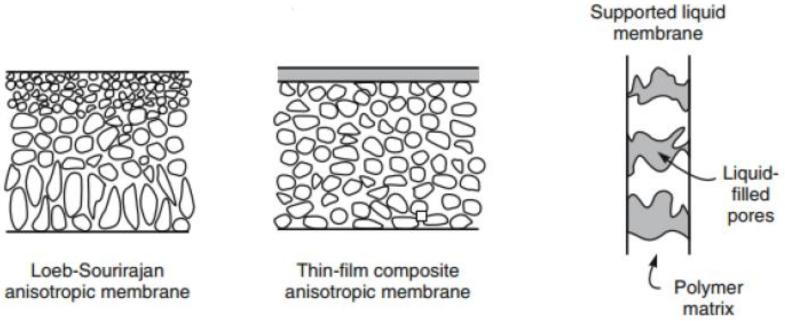

Figure 2.1.1.4. Three widely used anisotropic membranes [9].

Anisotropic membranes often have a thin surface layer referred as skin layer, whose purpose is to define the flux. The skin layer is mechanically supported by a thick porous structure, which should affect the flux. Loeb-Souriajan membranes is made of homogenous material, but its unique layered assembly, which give it pore size variation, makes it anisotropic membrane. The thin-film composite membrane is made of a thin and dense film, that are highly cross-linked polymer mounted on the surface of a microporous support. The cross-linking provides the selectivity. Liquid membranes are often used on pilot scale for removal of heavy-metal ions and organic solvents from industrial waste streams.

2.1.2 MEMBRANE TRANSPORT THEORY

In water treatment, membranes are used for separation processes, which covers a wide spectrum of problems concerning everything ranging from particles to molecules. To solve the issues, a large selection of membranes has been developed over the years. The membranes differ from each other in material, structure and design, but the general mechanism of the separation is common for all types. A membrane is a semipermeable barrier, which allows either molecules or ions to pass through, while everything else is rejected [11, 12]. The separation process is driven by a specific driving force, that is transporting a particle through the membrane, from one phase to another (Figure 2.1.2.1).

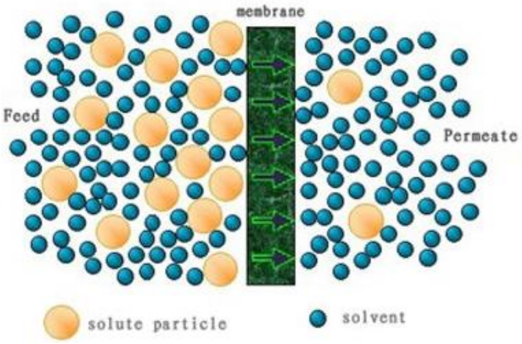

Figure 2.1.2.1. Basic model for membrane filtration [14].

Two important parameters to characterize the membrane separation process is selectivity and flux. Selectivity shows which compound is preferably transported through the membrane. Selectivity is expressed by using the retention factor (R) or separation factor (α).

$$R = \frac{C_{feed} - C_{permeate}}{C_{feed}} = 1 - \frac{C_{permeate}}{C_{feed}}$$

C is the solute concentration in both phases.

$$\alpha = \frac{y_a}{y_b} \div \frac{x_a}{x_b}$$

Compound A and B concentration in feed (x_a, x_b) and permeate (y_a, y_b).

Flux is the flow of a specific component. Flux is defined through the driving force, which makes the transfer from one phase to another happen. Traditionally, for each membrane process a specific flux equation describing that particular membrane transport is employed with a particular driving force. A unified approach regarding the driving forces and flux equations is rarely utilized. For a specific membrane process, an appropriate driving force must be chosen to determine the correct flux equation that describes correctly the membrane transport under investigation. The force acts on the molecule or particle and makes the transportation across the membrane possible. The amount of force depends on the difference or gradient in potential across all the membrane. The main potential differences in membrane processes are chemical ($\Delta\mu$) and electrical potential difference. Common driving forces are pressure, concentration and temperature differences.

2.1.3 MEMBRANE FOULING

By now, the general knowledge of how the membranes work and how they are made brings us to the part about the drawbacks of the technology. The biggest weakness membranes have is fouling. Fouling is a process, where the solute or particles deposit themselves either onto a membrane surface or into a membrane, that disrupts and degrades the membrane's performance. Fouling usually causes flux decline and affects the quality of the produced water [15].

There are several types of pollutants that cause fouling: colloidal (clays and flocs), biological (bacteria and fungi), organic (oils, polyelectrolytes and humics) and scaling (minerals) [11].

The pollutants have several ways of interacting with the membrane. Firstly, an accumulation of particles can occur by adsorption (Figure 2.1.3.1 a) or deposition (Figure 2.1.3.1 b). The former is caused by interaction between the membrane and the particles, whereas the latter is rejected particles building up at the surface of the membrane. Pollutants can cause pore blockage (Figure 2.1.3.1 c), where partial closure of pores causes reduction in flux. Lastly, some macromolecules can form a gel, when the concentration at the surface of the membrane is high enough [15].

Figure 2.1.3.1. Different scenarios of fouling [15].

The occurrence of fouling depends on many factors such as the type of membrane, the properties and surface properties of the membrane, the type and the characteristics of the pollutants and the mode of operation [15]. If generalized, the particles that have the tendency to cause fouling, are often of hydrophobic nature and carry a surface charge. This does mean the hydrophobic membranes are more sensitive towards fouling compared to hydrophilic, but in no way, it means the latter are not susceptible to fouling. The surface charge on a membrane is another important property to fight against fouling. As organic matter in water at neutral pH carries often a negative charge, the membranes should also be modified to have a negative charge to encourage repulsion [16]. Lastly, the roughness of the membrane plays a role, as membranes with smoother surfaces tend to experience less fouling compared to rougher surfaces [15, 17].

If particles do manage to cause fouling the disruption can be either reversible or irreversible. In the former case, the pollutant can be removed with backwashing, which requires additional systems to be built in for this purpose. The latter is a strong attachment, which cannot be removed by physical cleaning, but only through chemical means [9].

There are a variety of chemicals to choose from that may be used for membrane cleaning, and each of them is targeted to remove a specific form of fouling. For example, citric acid is used to remove inorganic scaling. Strong bases are typically used to dissolve organic material. Detergents and surfactants can also be used to remove organic and specific foulants, especially those that are difficult to dissolve. Chemical cleaning may also use a strong chlorine solution to control biofouling. Due to the variety of the pollutants presence, it is often necessary to use a combination of different chemicals to address multiple types of fouling [18]. Some membranes have poor resistance towards chlorine and other chemical used for cleaning, which reduces their life time. In case of severe fouling, excessive backwashing or chemical cleaning, a replacement of the membrane is needed. Issues as such bring up the cost of the treatment and are the main problem of why membrane technology is costly. Therefore, the incorporation of nanoparticles with photocatalytic properties such as titanium dioxide (Section 2.5) have been investigated to find alternatives ways to fight against fouling and expand the lifetime of a membrane.

To sum up this section on membrane technology, a list of characteristics for an ideal membrane applied in UF, NF and RO operations should possess is presented:

- High water flux, which would keep the capital cost low
- High solute rejection, resulting in premium quality water
- Long-term stability of water flux and rejection, minimum fouling
- Mechanical, chemical and thermal stability
- Minimum pretreatment
- Can be produced into large-scale membranes and modules
- Low-priced

2.2 GRAPHITE OXIDE

This part is to introduce the main material used for membrane production – graphene oxide. Its origins, most popular models, commonly used synthesis methods and formation are discussed in detail. In addition, the theory section is finished by introducing previous investigation done concerning the developed membrane.

2.2.1 GRAPHENE

Graphene is considered as the simplest form of carbon element compounds. It has been given the title as the thinnest material ever produced as it is made of a single atomic layer of sp^2 carbon atoms in a hexagonal lattice structure, which can be displayed as a honeycomb as shown in the figure below [19]. In this hybridization state the carbon atom has 3 sigma bonds, which it shares with the neighboring carbons. Carbon also has an additional fourth bond, which is made of two π orbitals, orientated out of the graphene plane (Figure 2.2.1.1 left image), and is called the π bond. The fourth bond is the reason why graphite has the C-C double bond and conjugation with in the hexagonal rings.

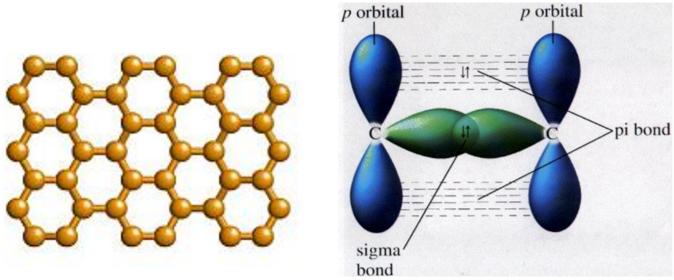

Figure 2.2.1.1 An image of the honeycomb structure of graphene and a model of its sp^2 hybridization [20]

Due to its unique structure, it can form an array of shapes such as a nanotube, a sphere, known as fullerenes, or build a three-dimensional block by layering graphene on top each other as shown on Figure 2.2.1.2.

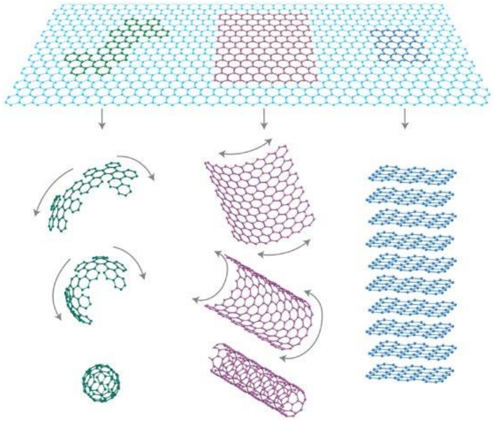

Figure 2.2.1.2 Different shapes made of graphene plane. [19]

Graphene with minimal defect has some great characteristics such as high thermal conductivity and Young's modulus, a large specific surface area and an optical transmittance of up to 98% [21, 22, 19].

2.2.2 GRAPHITE

Graphite is made of graphene layers that are stacked on top of each other and kept together by weak Van der Waals forces. The typical bond lengths and distance between the planar graphene can be seen on Figure 2.2.2.1.

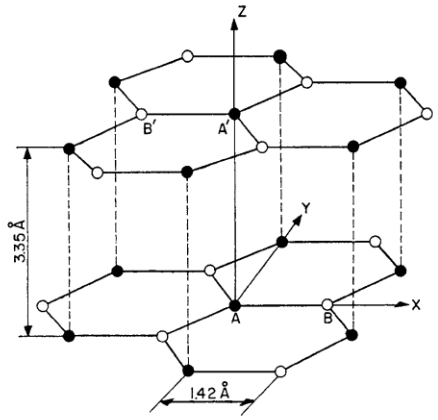

Figure 2.2.2.1. The crystal structure of graphite [23].

The structure of graphite gives it an anisotropy property, which means that its physical properties differ along the plane. It is marked in the x-y surface on the figure above, and z-axis direction, which is pointing out from the plane of the graphene sheet. In other terms, it means the layers of graphene can slide over one another, creating an opportunity where the weak interlayer force could be overcome, thus making graphite apt to be chemically converted.

Graphite compounds and their production have some specific terminology that need to be addressed as they are used in the following paragraphs. A reactant that permeates between the layers of graphene is also referred to as intercalate and composite which is formed this way is called intercalation compounds and the whole process is referred as intercalation [23].

2.3 GRAPHENE OXIDE

Graphite oxide (GO) does not occur naturally and was synthetically produced in 1855 [24]. Since its discovery, it has presented challenges to the research community concerning how it is formed and how the structure of the compound looks like in detail. Throughout the years, graphite oxide’s structure has remained mostly unagreed because the result of its material complexity, although several models have been presented in an attempt to clarify it. Graphene oxide is defined as a two-dimensional compound made from a layer of carbon atoms in sp2 hybridization, with the occasional variation of functional groups, that have formed during the oxidation at the edges and vacancy defects in the material [25]. In this report, in the next two sections, the production of the compound and the two most widely spread and dissimilar models are discussed in detail. In both sections, possible reaction pathways are presented to give explanations to several properties of GO.

2.3.1 GRAPHENE OXIDE SYNTHESIS

The introduction to the graphene oxide and its characteristics is started by presenting the methods of production as it lays a good foundation for the next section where the different models are discussed. As mentioned above, the compound is synthetic and on the next figure the evolution of the manufacturing methods is shown, which end with the two most popular production methods.

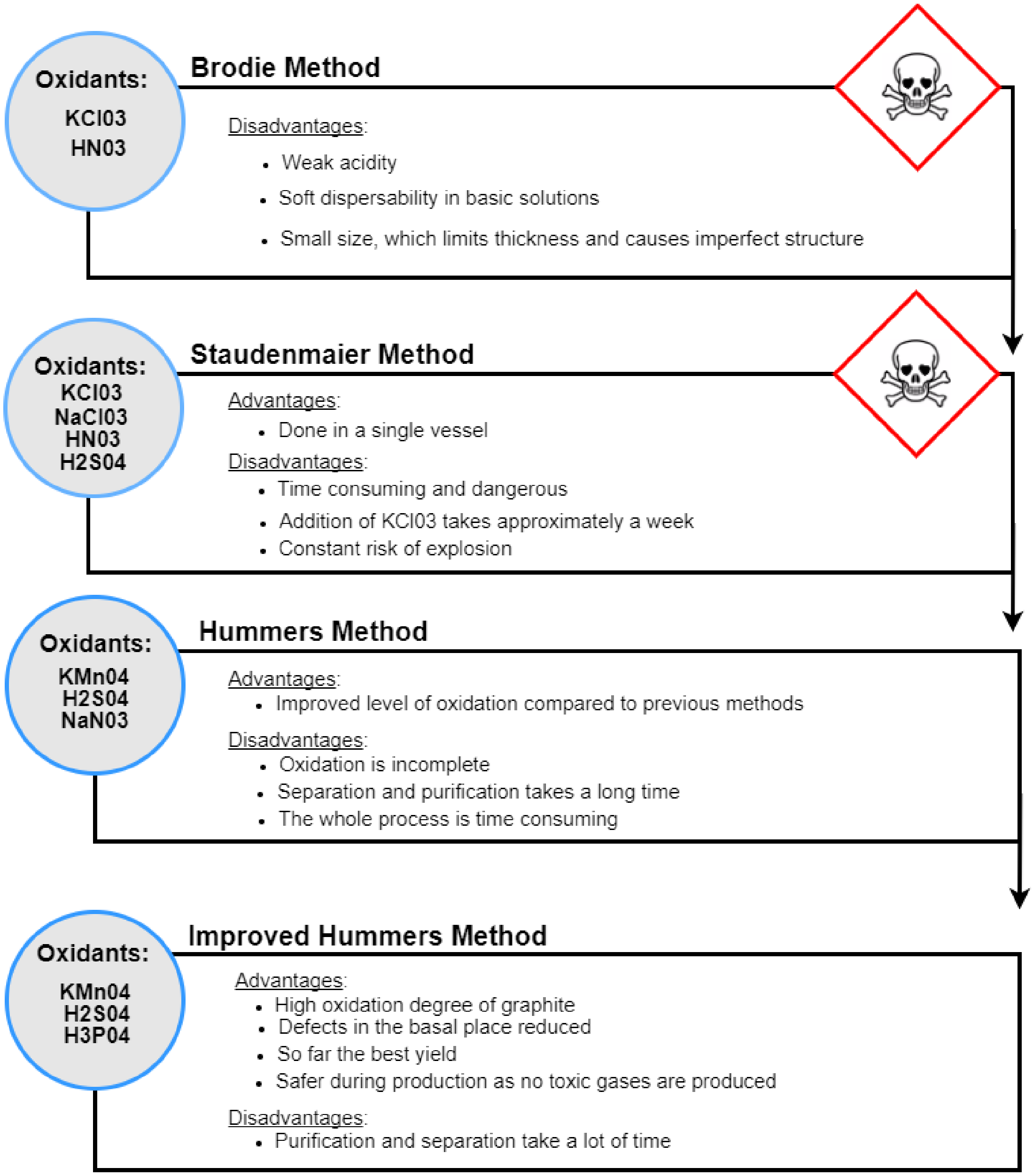

Oxidants:
KCl03
HN03

Brodie Method

Disadvantages:
- Weak acidity
- Soft dispersability in basic solutions
- Small size, which limits thickness and causes imperfect structure

Oxidants:
KCl03
NaCl03
HN03
H2S04

Staudenmaier Method

Advantages:
- Done in a single vessel

Disadvantages:
- Time consuming and dangerous
- Addition of KCl03 takes approximately a week
- Constant risk of explosion

Oxidants:
KMn04
H2S04
NaN03

Hummers Method

Advantages:
- Improved level of oxidation compared to previous methods

Disadvantages:
- Oxidation is incomplete
- Separation and purification takes a long time
- The whole process is time consuming

Oxidants:
KMn04
H2S04
H3P04

Improved Hummers Method

Advantages:
- High oxidation degree of graphite
- Defects in the basal place reduced
- So far the best yield
- Safer during production as no toxic gases are produced

Disadvantages:
- Purification and separation take a lot of time

Figure 2.3.1.1. Most commonly used synthesis methods of GO.

The Figure 2.3.1.1 above shows the developed methods of the production of the GO up until 2010. Afterwards numerous small modifications to the Improved Hummers method have been established, although the essential structure remains the same: concentrated sulfuric acid, permanganate and perhaps nitrate forming a highly oxidizing environment [26, 25]. Few attempts to find an environmentally friendlier way of production has also been made using K_2FeO_4 as an oxidant [27].

The details concerning the mechanism of the formation of GO are still not completely clear, but few investigations have given good insight of some of the steps involved.

Nowadays the Hummers method is the most common way for the synthesis of GO, therefore making it the target for most investigations of the reaction mechanism compared to alternative ways. The findings concerning the steps during the production of GO are relevant and easily applied to this project, although the original Improved Hummers method, also referred to as Tours, was used to produce GO.

The oxidation of graphene into GO has been found to consist of three distinct steps as shown on Figure 2.3.1.2 [28].

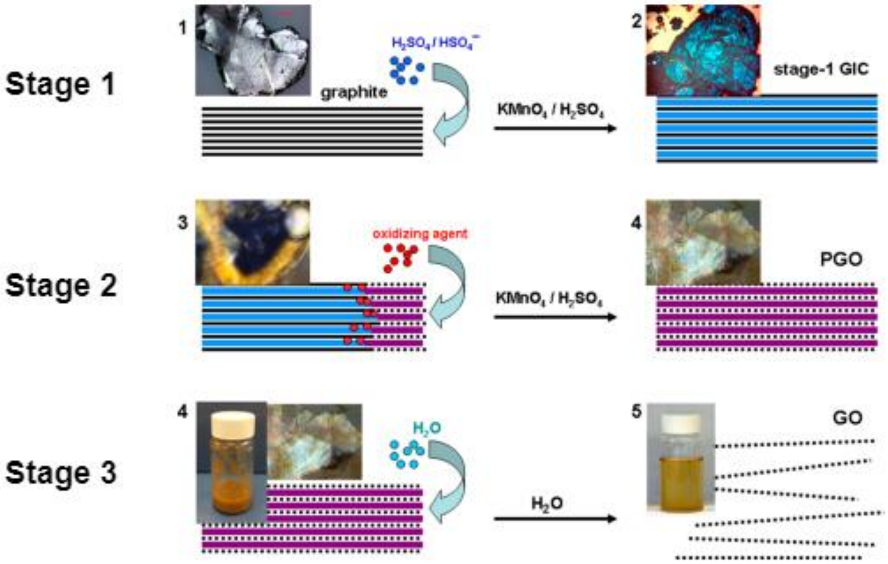

Figure 2.3.1.2. Conversion of bulk graphite into pristine graphene oxide [28].

2.3.1.1 FORMATION OF INTERCALATION COMPOUND

The first part (stage 1) is dedicated to the preparation for the oxidation stage (stage 2) because, in order to oxidize graphite, the oxidant needs to make its way between the graphene layers. At first, the distance between the layers is too narrow for the oxidant to penetrate the structure, creating the need to modify graphite to an intercalation compound. Sulfuric acid has shown to form a sulfuric acid-graphite intercalation compound (H_2SO_4-

GIC) when combined with graphite as shown on Figure 2.3.1.2 in steps 1-2. The suggested formula of the stoichiometry of the stage is:

$$C^{+}_{(21-28)} \cdot HSO_4^{-} \cdot 2.5H_2SO_4$$

The intercalation process is instantaneous from the moment graphite is exposed to the acid medium, taking less than 10 minutes to be complete, depending on the size of graphite flakes and applied reaction conditions. On Figure 2.3.1.2 stage 1 the colour change from grey to blue has been linked to the formation of the GIC [29, 30]. The intercalant penetrates the graphite from the edges and makes its way towards the middle of the flake over time. The wavy nature of graphite oxide is formed mostly during the intercalation stage of the synthesis.

2.3.1.2 FORMATION OF PRISTINE GRAPHENE OXIDE

The second stage (Figure 2.3.1.2) is the occasion of the oxidant entering between the planes of graphene resulting in the conversion of GIC into pristine graphene oxide. Although the formation of the PGO has been shown to start almost simultaneously with the formation of H_2SO_4-GIC [30], which shows that as soon the oxidation agent makes contact with carbon, it reacts immediately. But, the completion of the whole process of oxidizing graphite can take from few hours up until few days and has been shown to be dependent on the morphology of the graphite flakes [28, 31]. The transformation from GIC to pristine GO was visually perceived by reflective light, under what the blue color gradually changes to light-yellow-pearl (Figure 2.3.1.2 stage 1 and 2). The space between the graphene layers after the formation of GIC are suggested to be filled with H_2SO_4 molecules and HSO_4^- ions leaving no extra room for the oxidizing agent to enter. The only way in is through replacing the intercalated molecules or placing itself between them. The reaction moves the same way as the intercalation process – from the edges of graphite towards the center. Based on the experimental data the diffusion rate of the oxidant has been shown to be much slower compared to the oxidation reaction [28]. Therefore, the explanation for the long reaction time is due to diffusion between the densely-populated graphene layers. As the process is diffusion controlled, it brings up the importance of the size of the graphite flakes and the uniformity of the size distribution. In addition, the morphology of graphite has an impact to the reaction kinetics, emphasizing the necessity to have graphite from the same source. Already different flakes in the same reaction mixture have been reported to have a large variation in the progression of the reaction simply due to the structure, where samples with high crystallinity take longer to oxidize compared to samples with disorder and defects [28, 31]. The oxidizing agent which makes its way in is suspected to stay trapped between the layers of graphene up until exfoliation because the addition of water takes place [28].

An oxidation threshold (TOD) has been found to be approximately 4 weight equivalents as anything below the amount doesn't result in high enough density of functional groups and increasing doesn't seem to influence the structure and composition of GO significantly [32].

Common functional group forming during the oxidation of the graphite are epoxides, ketones, hydroxyl groups, on the basal plane, carboxyl and hydroxyl groups, covering the edges of the layers of graphene as seen on Figure 2.3.3.1 [33, 26]. Regardless which method for the synthesis has been used the same functional groups have shown to form in the material, expect sulfates, that originate from the application of H_2SO_4 during synthesis [34, 35, 32].

For a long time, the presence of sulfur had been neglected and thought of as impurity, but now the formation of sulfates or hydrogen sulfate from the previously formed epoxides is believed to occur during the oxidation of graphene and a possible formation route shown on Figure 2.3.1.3 [32].

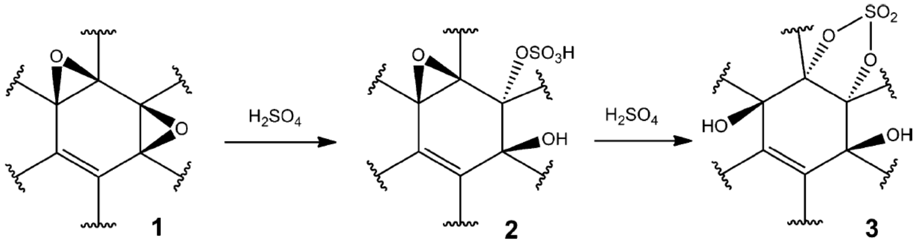

Figure 2.3.1.3. Formation of covalent sulfates [32].

It is suggested sulfuric acid or hydrogen sulfate acts as a nucleophile towards epoxides and results in an intermediate state of a sulfate ester (**1-2**). The reaction can continue if the ester reacts with another neighboring epoxide forming a 1,2-cyclic sulfate (**3**). Alternative product to 1,2-cyclic sulfate is 1,3-cyclic sulfate. As a result of these reactions the formation of two hydroxyl groups is occurring.

In addition, CO_2 production as a byproduct during the synthesis has been confirmed, which can either originate from the permanganate reduction into MnO_2 (Equation 2.3.1.4.1), where water and carbon dioxide is also formed or but from another reaction path, which has not yet been identified.

2.3.1.3 FORMATION OF GRAPHENE OXIDE

The third stage is where the PGO is converted into GO after it has been exposed to water. Pristine graphene oxide has been identified to have white to light yellow coloration, which will start to change as soon as larger quantities of water has been added, rising suspension of an initiation of chemical reactions [32]. The original need for the addition of water and peroxide is to quench the reaction and exfoliate graphene oxide.

The purpose of the peroxide is to deal with the leftover quantities of $KMnO_4$, by transforming it to salts (Equation 2.3.1.3.1), which can be then easily removed due to their affinity to dissolve in water.

$$5H_2O_2 + 2KMnO_4 + 2H_2SO_4 \rightarrow 5O_2 + K_2SO_4 + 2MnSO_4 + 8H_2O \quad \textit{Equation 2.3.1.3.1}$$

The few other reactions triggered by the addition of water is discussed in Section 2.3.4, where the observations on the material's behavior was used to come up with a new model to describe graphene oxide [33]. In a separate investigation the change of color during the quenching and purification was under taken. Changes in compounds color is often an indication of a chemical transformation and it is seeming to be the case with GO as well. The brown color, which is gained in time, possibly suggests increased conjugation of the π-system as polycyclic aromatic domains with 6 and above ringed systems tend to be colored deeply [36]. The proposed reaction sequence of the hydrolysis of the GO is shown on Figure 2.3.1.4.

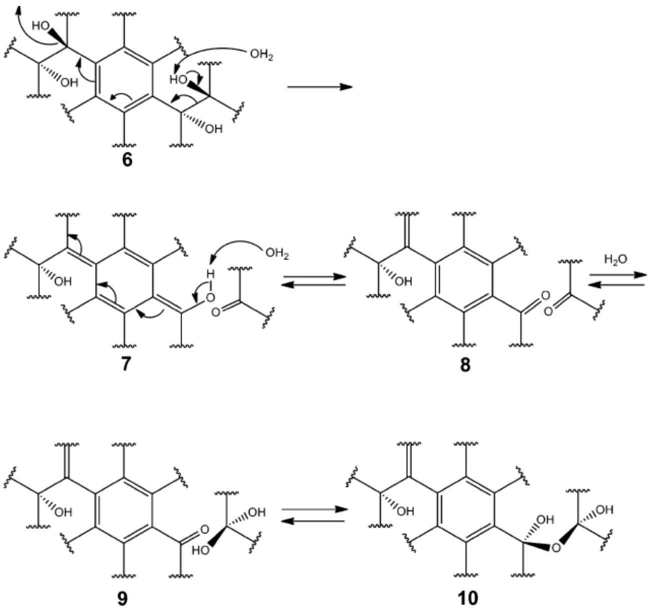

Figure 2.3.1.4. Transformation of GO by reaction with water [32].

The concept is that the quantity of sp2-carbon is increased during the hydrolysis and the process is initiated by the hydrolysis of the protective sulfates. On number **6-7** one of the hydroxyl group are ionized with leads to a C-C bond cleaving. Ketone and an enol is formed as the result. Simultaneously one of the hydroxyl group is eliminated and a carbon-carbon double bond is created. The enol is capable to ionize into an additional double bond. The ketone group in the **8** can undergo hydration and transform into gem-diols **9**. The gem-diols can be transform into hemiacteals **10**.

Another reaction which will be discussed in this section is concerning the identified sulfur moieties. The sulfate esters formed in the last step (Figure 2.3.1.3) are suspected to hydrolyze when water is added into the system. The process of hydrolysis in acidic environment takes hours and result in C-O bond cleavage forming monosulfate (**3-5**). The formed product continues to hydrolyse if it is in acetic media and ends in formation of 1,2-diol (**5**) and the release of a sulfuric acid molecule, which can be one of the reason of the low pH value of GO.

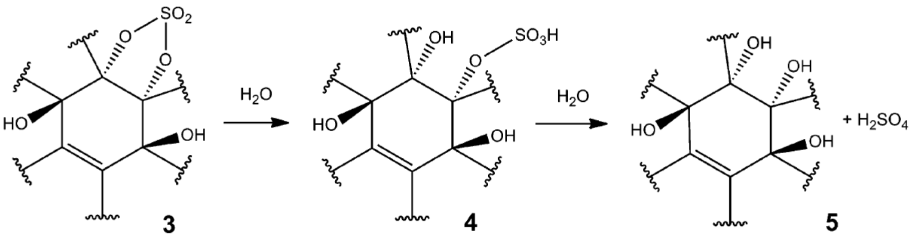

Figure 2.3.1.5. Hydrolysis of the covalent sulfates.

In some cases, incomplete exfoliation of graphene oxide was registered with SEM images and ended in assumptions that covalent sulfates are not only just present as functional group attached to the basal plane of graphene, but they are also suspected to form bridges between different layers of graphene [32].

The change in the structure during the synthesis of graphene oxide is illustrated in Figure 2.3.1.6 below.

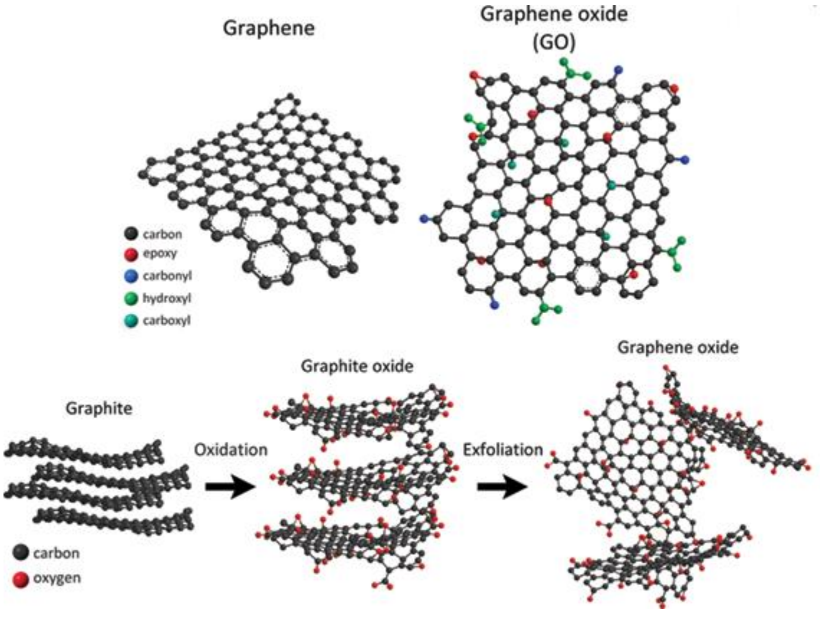

Figure 2.3.1.6. Illustration of the structural changes occurring throughout the synthesis.

2.3.1.4 THE OXIDIZER

The oxidizer used during the synthesis is potassium permanganate ($KMnO_4$) which undergoes transformation when added into the blend of the concentrated acids. The exact details of what is happening to the compound and in what form it oxidizes the graphite is still unclear. At the moment, two attempts have been done to explain the process.

The most popular and referred theory is the formation of diamanganese heptaoxide (Mn_2O_7) [37]. The moment $KMnO_4$ is added to the acids mix, formation of green color can be seen (Figure 2.3.1.7). It could be viewed as evidence for the presence of Mn_2O_7, as it is its characteristic color [38].

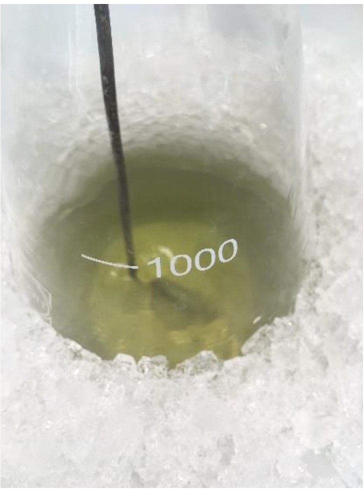

Figure 2.3.1.7. Coloration when $KMnO_4$ is added to the H_2So_4/H_3PO_4 mixture.

The suggested overall reactions between potassium permanganate and sulfuric acid, during what diamanganese heptaoxide is formed, is shown below [38].

$$KMnO_4 + 3H_2SO_4 -> K^+ + MnO_3^+ + H_3O^+ + 3HSO_4^-$$

$$MnO_3^+ + MnO_4^- -> Mn_2O_7$$

Mn_2O_7 has been shown to possess selectivity towards unsaturated aliphatic double bonds over aromatic double bonds [39] therefore it could give explanation of how graphite is converted into GO, although no solid evidence of the existence of the compound has been released. A serious disadvantage of this compound is its tendency to detonate when temperature rises above 55°C or if mixed with certain organic compounds [38].

The second and less spread theory with very limited available information is the formation of planar permanganyl (MnO_3^+) cation that attaches itself to HSO_4^- or SO_42^- ions and forms MnO_3HSO_4 or $(MnO_3)_2SO_4$ molecules. In the environment of concentrated sulfate acid, the compounds are said to exist mostly in nonionized form, but in dilute acids medium ionizations occurs [28].

The oxidation of graphene is complicated and many different reactions are happening simultaneously. What becomes of the reactant potassium permanganate has also been debated and one of the theories is presented as a reaction seen on equation 2.3.1.4.1. It is believed some of the permanganate is converted into manganese oxide, carbon dioxide, sulfates and water [40].

$$4KMnO_4 + 3C + 2H_2SO_4 -> 4MnO_2 + 3CO_2 + 2K_2SO_4 + 2H_2O$$ **Equation 2.3.1.4.1**

2.3.1.5 PHOSPHORUS ACID

Phosphoric acid has been added to the synthesis process as it had revealed a potential ability to protect graphene planes form additional damage in harsh oxidation conditions. Less damage has been registered to the planes compared to different acids used in alternative techniques [41]. The explanation is believed to be due to the formation of five-member phosphor rings, which forbids further oxidation shown in Figure 2.3.1.8.

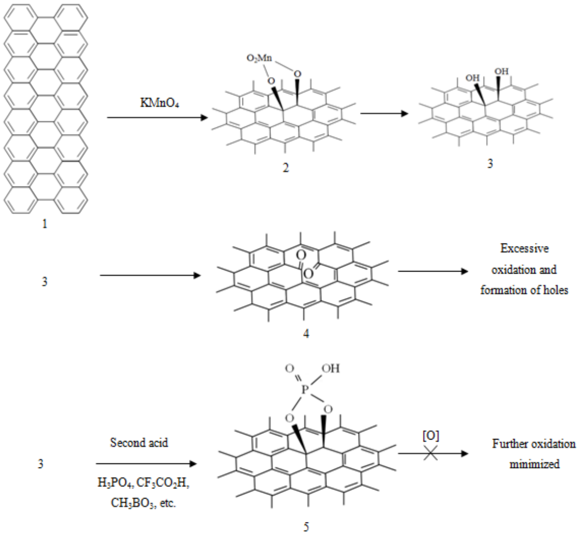

Figure 2.3.1.8. Reaction mechanism by H_3PO_4 to protect the carbon layers [41].

2.3.2 IMPROVED HUMMER'S METHOD

As mentioned in section 2.3.1.3 above that qualitatively similar graphene oxide is obtained with different synthesis methods, displaying some consistency in its behavior. The morphology of graphite has shown to affects the kinetics of the oxidation and the purification procedure has been demonstrated to have much a larger effect on the structure and properties of the material that expected.

During this project, the Improved Hummers method (also referred to as Tour's method) is used to keep the option of comparison between the previous projects possible. Tour's method has also demonstrated higher yield compared to other popular methods [26] and doesn't have toxic gases such as NO_2 and N_2O_4 released during the synthesis as sodium nitrate is not used. The manuscript for Tour's method is also straightforward, easy to follow less time consuming and has the potential to be applied in large-scale production [26].

2.3.3 LERF-KLINOWSKI MODEL

The most widely spread and agreed upon model (Figure 2.3.3.1) of GO was proposed by Lerf-Klinowski (LK) in 1998 [42]. According to their experimental data they suggested the structure to consist of two types of randomly distributed regions. One of them being aromatic areas with unoxidized graphene in sp^2 hybridization and the second being a domain of oxidized carbon in sp^3 hybridization. They also concluded the relative size of the domains to be dependent on the level of oxidation. Epoxide and hydroxyl functional groups were hypothesized to be located between the graphene layers and larger carboxyl groups on the edges of the structure. In addition, the wavy behavior of GO was signed to be caused by the OH-groups converting the hybridization of carbon into sp^3, which does not have a planar nature compared to sp^2 state [34, 43].

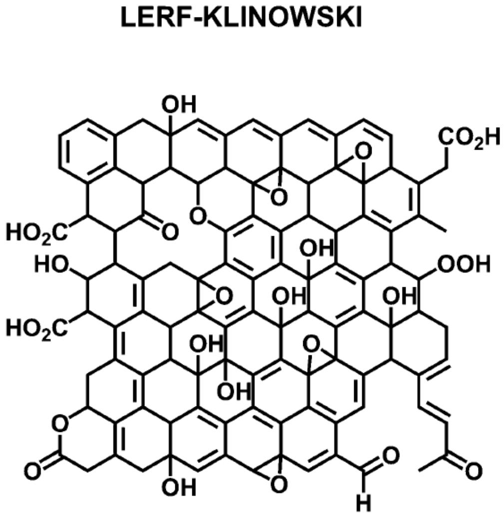

Figure 2.3.3.1 Structural model of GO and the functional group [43].

Most other models have minor difference compared to the LK model concerning the extent of sp^2 hybridization of the carbon and the presence of some specific functional groups for example the existence of hydroxyls and four membered rings 1, -3 or the presence of carboxylic acids versus quinones [43].

The Lerf-Klinowski and alternative models give good insight of the GO, but do not provide an explanation to all of the properties of GO, such as its acidity or its ability to reduce under strong alkaline conditions.

2.3.4 THE DYNAMIC STRUCTURAL MODEL

A new approach to explain GO is using a dynamic structural model (DSM) by Ayrat Dimiev's group [33]. Based on their experimental data, they have concluded GO to be a system which is continuously changing its structure as a result of its interactions with water. The model suggests GO to develop most acidic groups only when exposed to water, which results in the change of pH over time and a low pH of the GO gel. Their model has been able to provide the explanation to two properties of GO, which had not been done before - the low acidity and the ability to reduce under basic conditions.

Their first observation of continuous processes was concerning the moment during the synthesis of GO when water is added to the reaction mixture to quench and terminate the process. A gradual transformation in color over time was noticed possibly indicating expansion of conjugated areas [32].

The second insight was connected to the constant presence of sulfur when analyzed with EA. For a long time, researches signed it off as sulfuric acid's residue, which isn't completely removed during purification. Only later it was noticed that at a certain point the concentration of sulphur remains persistent (0.5-2%) no matter how many times GO was washed with water [44]. The evidence leading to a discovery of covalently bond sulfates within the structure of GO (Section 2.3.1.3).

The detection of sulfur moiety has contributed one possible explanation to the low pH of GO, which has not been address successfully until the moment, although it is definitely not the only contributing factor. Graphene oxide has a pK value between 3-4 in aqueous environment, which is significantly lower than the suggested carboxyl or hydroxyl groups can achieve, but it is achievable if there are enough sulfate groups [43].

They made a detailed investigation of the acidic properties of GO and expanded the understanding of the types of reactions, which are potentially undergoing, especially reactions with water.

A typical titration curves of GO are shown on Figure 2.3.4.1 where the lack of distinguishable inflection points can be seen. This phenomenon has been explained to be caused by the overlapping of numerous acidic functional group [45, 46]. It is common for several properties of GO to vary severally between different batches and different synthesis methods, which make it not reliable and difficult to work with. However, qualitatively same or very similar analytical data is collected with SSNMR, FT-IR and XPS of all the GO samples, which indicates the presence of reoccurring oxygen-containing functional groups despite the production method used or other variances, meaning the conclusion for the absence of inflection points to be not correct. Dimiev's group suggests the reason for such behavior is GO's reactions with water that results in gradual generation of acidic functional groups and an additional contribution originating from the electrical double layer at the GO's interface.

The calculated average value for the content of acidic sites for an aqueous GO was determined to be around 1 per 25 carbon atoms, but for the GO obtained after forward titration with basic solution the value is reduced to 1/17, showing an increase value of acidic sites during analysis. In addition, during the reverse titration less HCl solution was used than expected giving evidence to conclude activated acidification during the insertion of basic solution. The generation of protons was a continuous process as the pH kept lowering when the GO was left to rest.

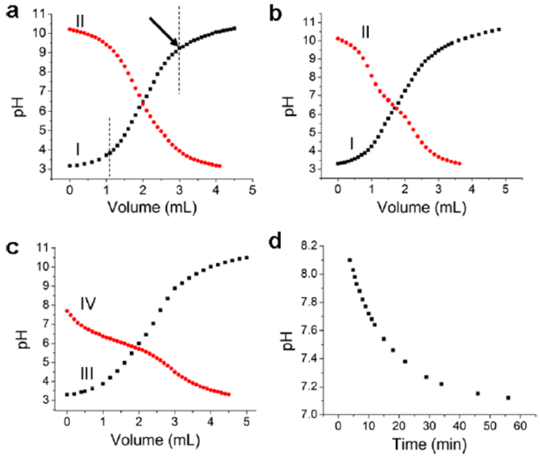

Figure 2.3.4.1. The forward and reverse titration curves of graphene oxide [33].

Although the existence of sulfates was already established and their role of the materials acidity was obvious, analyzing the collected data from titration it became apparent that it was not plausible for this functional group to be the only cause of the intriguing behavior explained above. In addition, GO which has been synthesized without using H2SO4 (Brodie's method) and doesn't have existing sulphates in its structure, still has the same low acidity. The reached conclusion was that the main factor for the acidity of GO is the generation of protons when the compound is exposed to water and the reaction is exaggerated by the addition of strong bases.

The GO was investigated in a basic environment using analytical tools such as XPS, FT-IR, TGA and UV-Vis to find the answer to the constant change in pH. The gathered data gave complementing results to each other showing the decrease of the oxygen containing functional group during the increase of pH, which lead to the conclusion that the process is GO disproportionation.

In addition, the formation of CO_2 was detected giving an indication that carbonate, and bicarbonate could be formed after the addition of basic solution.

Firstly, when pH is below 10 and the conditions are mild the deoxygenation of GO is happening, where the epoxides and OH groups are converted from oxidation state +1 to 0 as elemental carbon and as a ketone with oxidation of +2:

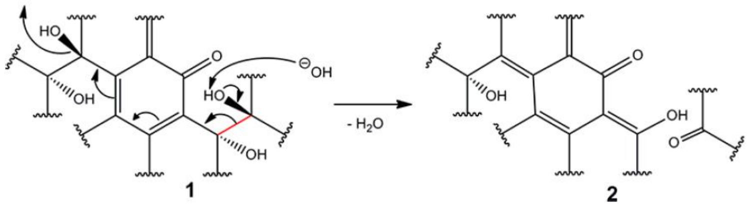

Figure 2.3.4.2. Deoxygenation of GO under mild conditions.

The scheme demonstrates deoxygenation of GO, where a fragment of GO with two vicinal diols and a ketone is present. The process involves cleave of the carbon – carbon bond, loss of two hydroxyl groups and a creation of one ketone, which results in the decrease of oxygen atoms in the structure.

Secondly, under strong alkaline conditions and elevated temperature, decarboxylation happens where CO2 is produced as byproduct and highest oxidized form of carbon:

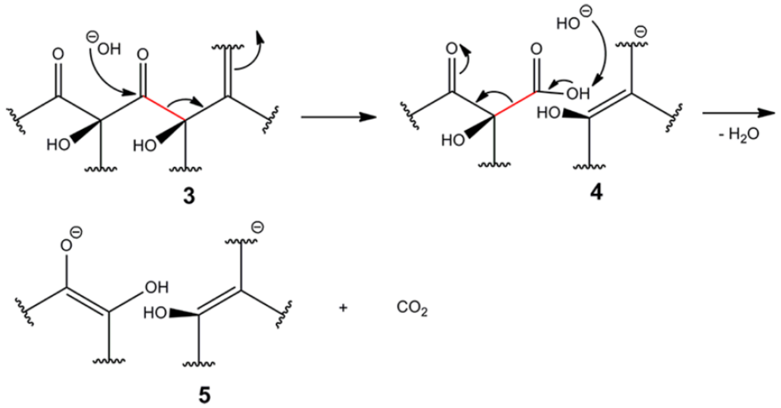

Figure 2.3.4.3. Decarboxylation of GO under strong conditions.

The second explanation to the shifting pH is the GO's colloidal nature. GO's surface charge has been measured to be negative [47, 48, 49, 50] in water medium where the zeta potential (ζ) is ranging from -15 to -45 mV. The large negative charge stabilises the colloidal solution and keep the particles from coagulation. GO with its negative charge is countered by positive ions to balance out the charge. This layer consists of two subparts: the Helmholtz plane and diffuse layer (Figure 2.3.4.4).

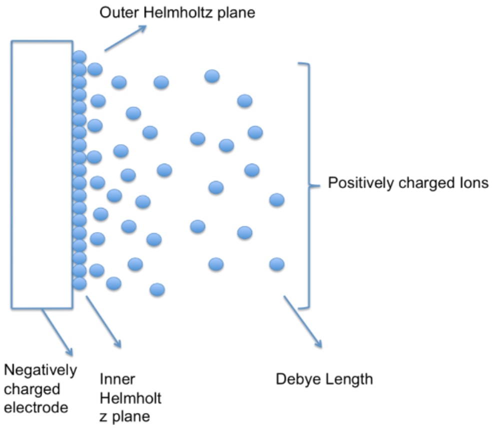

Figure 2.3.4.4. Distribution of ions near negatively charged surface [51].

The diffuse layer is made of ions that are not bonded to the GO permanently and actively exchange ions from the surrounding medium. This behaviour possibly has an additional effect on the acetic properties of GO such as the lack of inflection point (Figure X) and the gradual drop in pH over time. For example, when the concentration of protons in the bulk solution has decreased due to neutralization reaction when NaOH is added to GO, some of the protons from the diffuse layer can move into the bulk solution and the vacancy is filled by a similar ion such as Na+. The addition of Na+ was shown to generate higher negative charge compared to pure GO in water demonstrating the ability to possibly build a more effective counterion layer resulting in accelerating the reaction between GO and water. In addition, the addition of NaOH into GO solution brings up the negative charge even more strongly. Therefore, the Na+ ions have been concluded to be used as building blocks for the electrical double layer and by increasing the negative charge of GO surface they intensify the reaction between GO and water, which would still occur even without the cations, just at lower reaction rates. The occurring process can therefore be categorized as acid to salt conversion, where vinylogous carboxylic acid is transformed into its corresponding salts.

Two possible scenarios for reactions which end up in the build-up of electrical charge and production of protons are shown on Figure 2.3.4.5 and Figure 2.3.4.6. The first reaction route is in a neutral aqueous solution.

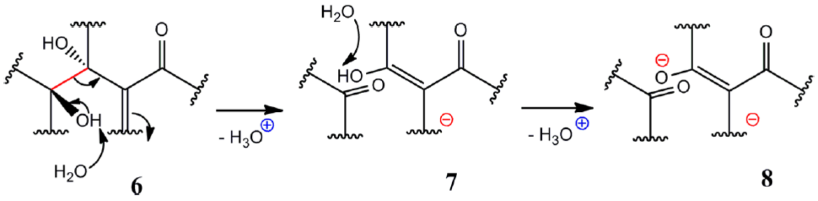

Figure 2.3.4.5 C-C bond cleave due to ionization of the alcohol group [33].

The structural state number 6 shown on the scheme above is a small part of GO, that has developed by the opening of epoxides and a ketone to form a vicinal diol at the vacancy defect. As the environment has been declared to be neutral, a water molecule is the transporter for the proton, which makes the process slower, and results in the acidification of the solution. As in a basic solution the hydroxyl ions would gladly extract the proton and the reaction would be proceeding at a faster rate. The process results in vinylogous carboxylic acid (7), which brings down the pH when ionized (8). The structural state shown in 8 is stabilized by resonance, where the negative charge is delocalized over the graphene domain. The accumulative negative surface charge is neutralized by the electrical double layer.

During the reactions described on the scheme above the proton is produced from the hydroxyl functional group. The next hypothetical route to produce the proton is its formation from water molecule, that ends up becoming part of the GO structure during the process.

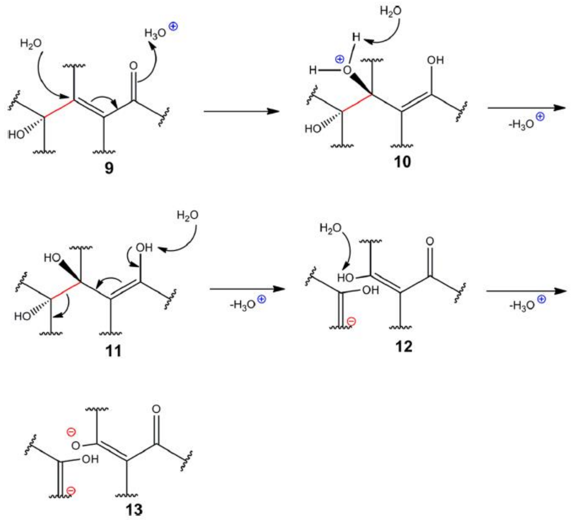

Figure 2.3.4.6. C-C bond cleave due tp extrinsic water molecule [33].

The structure of GO on Figure 2.3.4.6 number 9 has only one sp3 hybridized carbon atom close to a vacancy defect. The graphene layers consisting of the sp2 hybridized carbon atoms is resistant to chemical reactions, but the carbon atoms in sp3 hybridization are susceptible to a chemical attack. Hence the place for the water molecule to attack is the carbon next to the sp3 hybridized one. By doing this the water molecule becomes an intermediate cation (10), which will push the structure to transform into the shape on 11, resulting in the release of one proton. The next step is the cleave of C-C bond which leads into the formation of vinylogous acid (12), which when ionized will turn into the form shown on 13 [33].

To sum up, a new type of model created about the GO material, which states the system to be in a state of constant development due to its weakness towards water. Interactions between the compound and water generates protons and a negative charge on the surface of the GO, which is neutralized by resonance and electrical double layer. In addition, all the above proposed reaction schemes demonstrate a C-C bond cleave, meaning the material seems to be degrading over time if exposed to water medium. It has been suggested that in acidic environment the destruction happens at a slower rate [33].

2.4 THERMAL REDUCTION OF GRAPHENE OXIDE

Many different methods have been developed to reduce graphene oxide to graphene. The techniques can be split into two categories: chemical and thermal reduction. Thermal reduction is of interest in this project as two other projects have been previously committed in the relevant area in Aalborg University Esbjerg Campus. Thermal reduction is simple to perform and contaminates the material less with impurities compared to chemical reduction. In addition, the effect of chemical and thermal reduction on the properties of graphene oxide fibers was investigated by Zheng, X., et al. group [52]. The fibers reduced by thermal annealing obtained better tensile strength and electrical conductivity compared to the samples reduced using chemical means. The reason for the difference was said to be due to the decrease in the interlayer distances and defects in the material and growth of the ordered graphite crystallites, which gives material with better mechanical properties compared to the compound obtained through chemical reduction.

An investigation with XRD was done to see the temperature dependent evolution of the interlayer distance of GO in the range from room temperature (RT) up to 1000°C. To help with the interpretation of the obtained results a model is introduced, which explains how the interlayer distances differ from graphite and an intercalation compound.

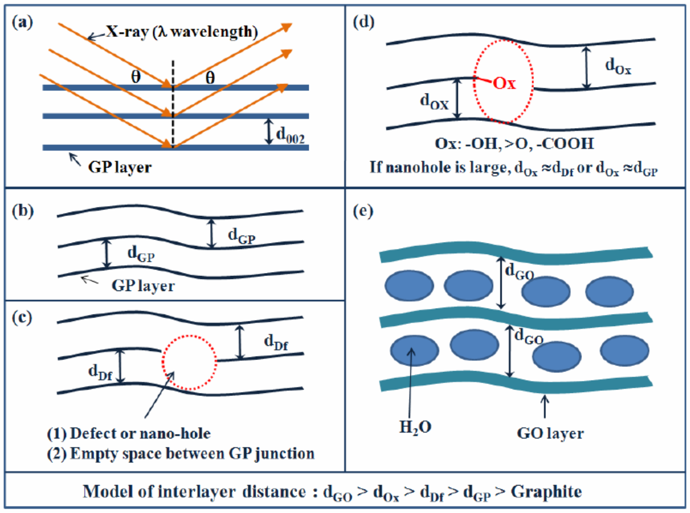

Figure 2.3.4.1 Model for the graphene (a), graphene oxide (e) and thermally reduced graphene (b-d) [53].

On Figure 2.3.4.1 (a) the orientation of graphene layers in bulk graphite can be seen in their organized manner, where the GP represents a graphene layer, d_{002} the distance between the layers and θ the scattering angle. The GP layers have been shown to own a nanocurvature distortions [53], which means the distance between the layers (d_{GP}) is slightly larger compared to bulk graphite (d_{002}). Graphene oxide has been reported to have defects and holes in its structure, which is represented on Figure 2.3.4.1 (c). This means the graphene obtained through reduction will also have defects in its structure. The holes also give room for oxygen functional groups (Figure 2.3.4.1 d) to be present, which increases the distance between the layers (d_{Ox}) significantly. The highest value for the interlayer distance does belong to GO (Figure 2.3.4.1 e), as in addition to the oxygen groups, water is infused into the system, which expands the material. The range for d_{GO} is between ~5 to 9 Å, depending on the number of intercalated water molecules. The increasing order of the defined interlayer distances is $d_{GO} > d_{Ox} > d_{Df} > d_{GP}$ > graphite. As seen on the figure the three middle stages $d_{Ox} > d_{Df} > d_{GP}$ are similar to each other and if the defects in the structures are large enough, functional groups and water could be only placed in the empty spaces, which would mean $d_{Ox} \approx d_{Df}$ or $d_{Ox} \approx d_{GP}$. The authors of the article believe that during thermal reduction GO has intermediate structure made of d_{Ox} and d_{Df}, but the crystal structure grows by the removal of d_{Ox} and d_{Df} as graphene oxide devolves towards graphite.

Figure 2.3.4.2 is the sum of all the XRD plots gathered during the investigation and shows a shift from left to right is occurring during the increase of the temperature. The characteristic peak of GO around 11 2θ varies in intensity and FWHM values as the temperature is brought up.

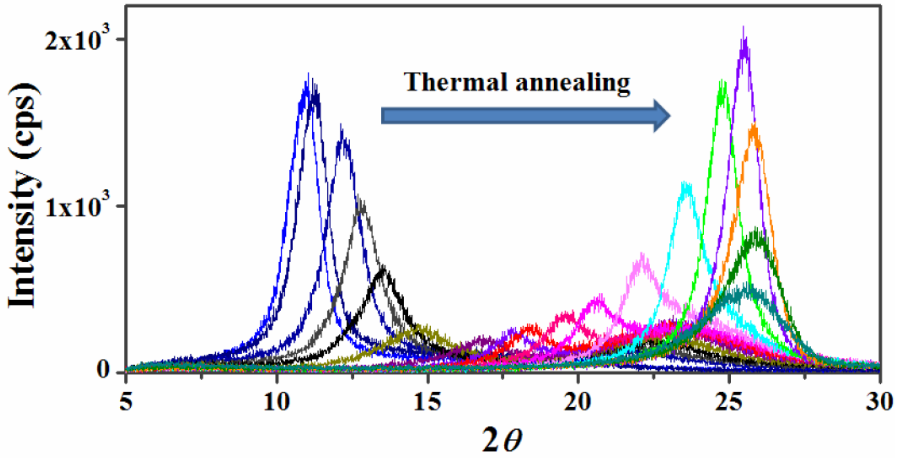

Figure 2.3.4.2. Combination of all XRD plots of the GO reduction from 25-1000°C [53].

Analyzing the plots individually shows the data to divide into four segments during the thermal reduction. The first stage is from RT-130 C, where only one peak is present and belongs to GO (Figure 2.3.4.3). Only a small decrease in the values of interlayer distance and in the FWHM were registered. The miniscule change in measured values were signed to belong to mild evaporation of H_2O. The second stage is between temperature 140-180°C. The peak I values for d and FWHM change severely and a new peak appears (peak II Figure

2.3.4.3) next to it. The reduction in the size of d and the widening of the FWHM is due to drastic vaporization of intercalated water molecules. The vaporization of the water molecules can be seen on Figure 2.3.4.3 (b), where the plots obtained by FT-IR become flatter as the temperature rises. During the removal of the H2O gases exfoliation occurs and the size of the GO crystals are decreasing, which is the reason a new peak with broad FWHM is registered in the XRD plot. The exfoliation of the material happens when the decomposition rate of the epoxy and hydroxyl groups exceeds the diffusion rate of the evolved gases, which creates pressure that surpasses the van der Waals forces holding the sheets together [54].

The third stage is from 180-600°C, during which the values for d and FWHM are reduced even more due to the removal of oxygen functional groups such as -COOH and -OH. The fourth stage, which happens above 600°C, where the values for the interlayer distance seems to rise again and the FWHM narrow, is explained by complex lattice relaxation and disordering processes.

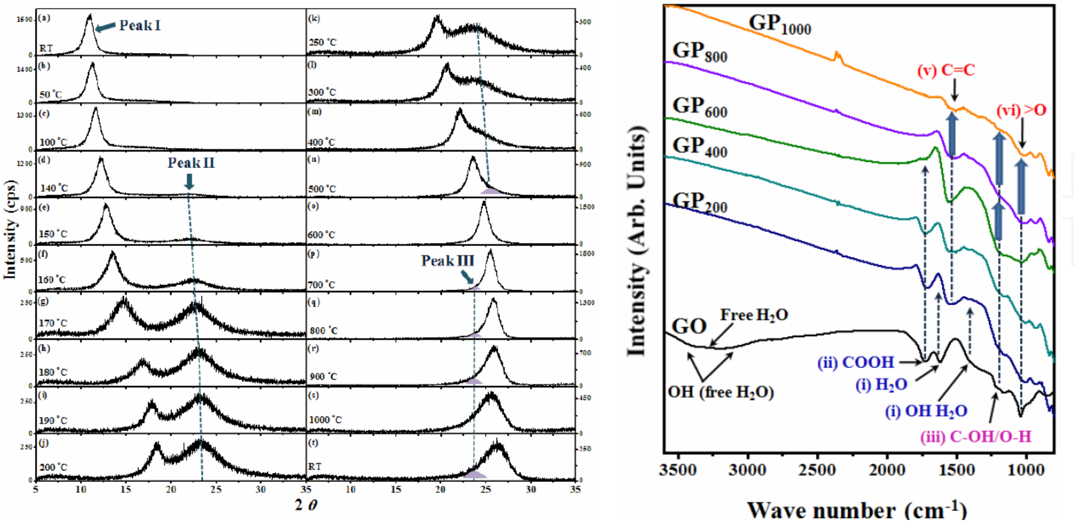

Figure 2.3.4.3. Left: The evolution of GO during thermal reduction from 25-1000°C [53]. Right: FT-IR spectra changes during thermal reduction [53].

Based on gathered results from several methods (XRD, FT-IR, Raman, FE-SEM and FE-TEM) a thermal reduction process for GO was formed and the scheme of it can be seen on Figure 2.3.4.3.

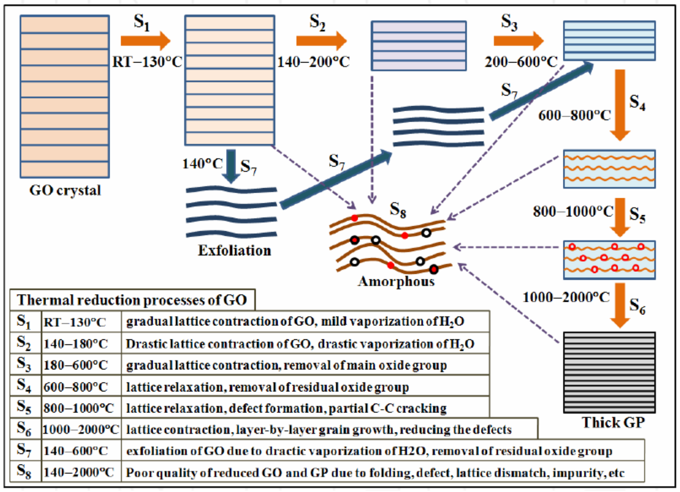

Thermal reduction processes of GO		
S_1	RT–130°C	gradual lattice contraction of GO, mild vaporization of H_2O
S_2	140–180°C	Drastic lattice contraction of GO, drastic vaporization of H_2O
S_3	180–600°C	gradual lattice contraction, removal of main oxide group
S_4	600–800°C	lattice relaxation, removal of residual oxide group
S_5	800–1000°C	lattice relaxation, defect formation, partial C-C cracking
S_6	1000–2000°C	lattice contraction, layer-by-layer grain growth, reducing the defects
S_7	140–600°C	exfoliation of GO due to dractic vaporization of H2O, removal of residual oxide group
S_8	140–2000°C	Poor quality of reduced GO and GP due to folding, defect, lattice dismatch, impurity, etc

Figure 2.3.4.4 Model of the developments during GO thermal reduction [53].

Five important temperatures were pinpointed: 140, 180, 600, 800, and 1000°C. In the first stage the d_{002} value of GO is gradually lessened within the range of RT–130°C due to earlier mentioned vaporization of the intercalated water molecules. The d002 value is severely reduced within 140–180°C, where the evaporation of water (S2) and a partial exfoliation of GO sheets (S7) is responsible for it. In the range 180–600°C due to the removal of the main carboxyl groups (S3), GO (S2) and exfoliated GO (S7) gradually reduce their lattice. In the range of 600 – 800°C (S4) out-gassing of the leftover carboxyl and hydroxyl groups is happening as partial lattice relaxation is occurring. 800 – 1000°C (S5) the epoxide group is removed, which causes load of defects in the lattices, and the in-plane C=C plane cracking is going on. 1000-2000°C growth of the crystal, which also results in the decrease of defects in the layers (S6). The processes of thermal reduction of GO always has small number of amorphous structures (2θ = ~23–25°) within the 140-2000°C, that come from the complex folding structures, combination of different hybridizations, defects and impurities within the material.

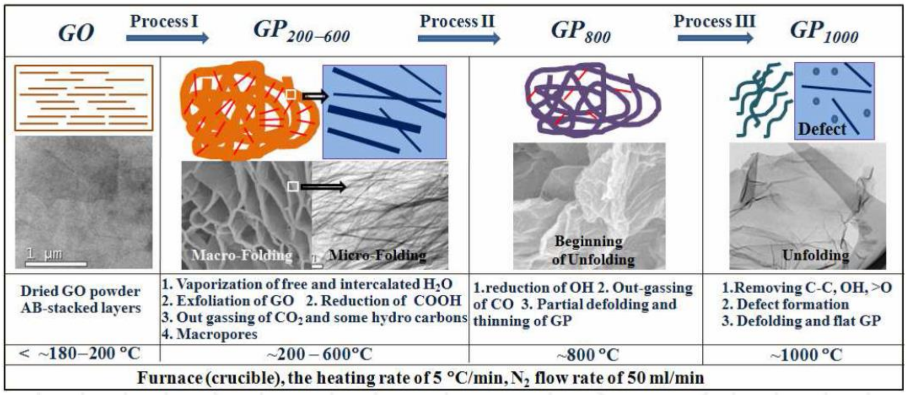

Figure 2.3.4.5. Schematic of folding and unfolding processes in the ranges of 200–600°C, 800°C, and 1000°C [53].

The folding and unfolding (Figure 2.3.4.5), which are said to be taking part in the higher temperature ranges depend heavily on the existence of chemical and hydrogen bond between the interlayers.

Another investigation done by M. M. Storm during which the thermal reduction of graphene oxide was monitored using in situ XRD analysis, came up with a theory based on the results where the material seems to be going through three stages during the thermal reduction [55]. The defined stages are: a GO stage, a disordered stage and an ordered rGO. The conclusion was done based in the plots seen on Figure 2.3.4.6, where three distinct ranges are pointed out on the left side of the plot.

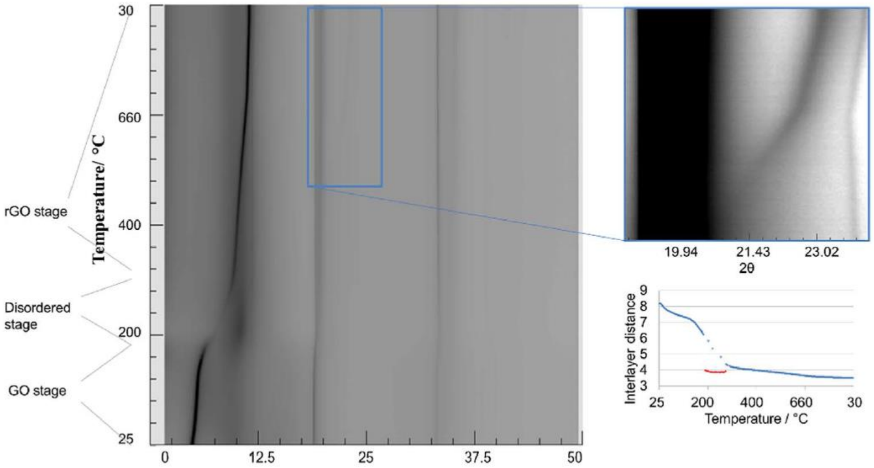

Figure 2.3.4.6. A 2D plot of the diffraction patterns during conversion of GO to rGO, 5°C/min heating rate, where the approximate duration of the GO, disordered and rGO stage have been indicated in the left of the plot [55].

The disordered stage falls into the temperature range, where the water molecules are rapidly exiting the material and causing exfoliation of the material, as discussed in the previous section, which indeed can explain the disorganization. The peak II seems to be the visual evidence of the disordered stage within the graphene oxide. The temperature range, where the disordered state dominated, shifted when different ramps were used for heating, but it was seen during all the tests, even at very low ramp rates. The application of high ramp rates such as 50°C/min resulted in material with widespread disordered state and the formation of more ordered material when heated more seemed to be inhibited, which was not the case during the application of lower ramp rates. The formation of outspread amorphous phase when shock heating is applied has been mentioned by Mcallister et al [56]. The behavior is signed to be caused by the rapid diffusion of the intercalated water and gasses from the membrane, which rips apart the crystals. In case of low heating ramp (less than 5°C/min), the diffusion is slow enough to avoid exfoliation of the graphene oxide and allows formation of ordered rGO.

Membranes made out of GO has been reported to have a risk of explosion during thermal reduction. This behavior has also been reported during the previous projects done at Aalborg University [48], where the membranes when exposed to temperature above 200 °C were ripped apart to pieces. The identified cause for rapid exfoliation is said to be the exothermic reduction of graphene oxide in cooperation with the ratio of mass to size, which results in limitations in heat and mass transfer leading to a thermal runaway reaction [57]. Heat from decomposition reaction cannot dissipate fast enough to the surrounding medium, resulting in localized temperature rise.

2.5 TITANIUM OXIDE

The properties of TiO2 which will be discussed in the next sections are the main reasons for its applications in the membrane production. The biggest problem with membranes to this day is fouling, where organic matter blocks the system. The superhydrophilicity of TiO2 could decrease the danger of fouling by making the material more hydrophilic, as the fouling material often tends to be hydrophobic, and if something still ends up attached to the membrane the photocatalytic process could take care of it. Implications as such would mean savings in money, time and increase in the lifetime of the membranes. In addition, TiO2 have other great attributes such as thermal stability and antibacterial properties, which would only benefit the product.

Titanium oxide (TiO2) is naturally occurring in different kind of rocks and sands. In addition, the production of the compound already has a long history as its manufaction started in the early 20th century [58]. It means there are numerous studies throughout the years concerning the characteristics of the compound. Some of the valued properties of TiO2 are its chemical inertness, thermal stability, ability to be resistant against UV degradation and few more, which will be discussed in more details below [59]. The compound also has high refractive index, whose value is even higher than a diamond's, giving its high brightness and the ability to scatter most of the light [60].

TiO2 can exist in three types of crystalline form – anatase, rutile and brookite [58, 59]. In this project only anatase type of TiO2 has been used and will be mostly focused on. The compound is a semiconductor and the anatase configuration has a band gap of 3.23 eV. The size and morphology of the particles, that make up TiO2, can be varied by controlling the conditions during synthesis, which gives the compound a wide range of application possibilities [59]. TiO2 often finds implications in different products as nanoparticles to establish self-cleaning and anti-bacterial properties on different surfaces [58], which are great assets to add to water purification membranes.

2.5.1 PHOTOCATALYTIC PROPERTIES OF TIO2

The first characteristics of TiO2, that is discussed in more detail is its photocatalytic property. As mentioned earlier TiO2 is a semiconductor with the band gap of 3.23 eV (in anatase form). By converting the 3,23 eV energy of a photon into a wavelength, the results is 388 nm. This is in the range of the UV light, meaning the compound can be categorized/labeled as UV-activated catalyst.

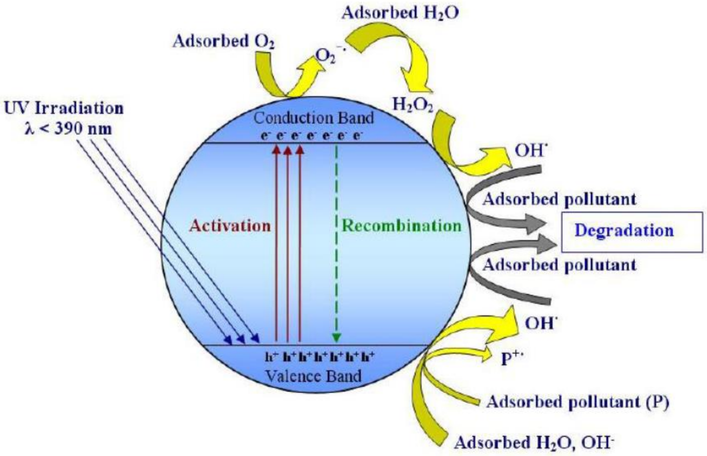

Figure 2.5.1.1. Activation of the TiO2 nanoparticles and its photocatalytic active types [58].

When light with wavelengths less than 388 nm hits the surface of TiO2 particle, an excitation of an electron can occur. If the photon has energy, that is equal or higher compared to the band gap of the compound, a jump from valence band onto the higher energy state conduction band can happen (Figure 2.5.1.1). As a result of the relocation, a hole is created in the valence band, which is called the electron-hole pair. There are two possible ways the excited electron is used.

The first possibility is called recombination, meaning the excited electron falling back to its original location. The process of generating electron-hole pair and the recombination are continuous processes during the exposure to the UV light. The second possibility is due the favorable duration of the electron-hole pair generation that creates a circumstance where the electron-hole pair could be transferred to species that have adsorbed itself on to the surface of the TiO2 [61]. The excitation process is shown below [58]:

$$TiO_2 + hv(\lambda < 390\ nm) \rightarrow TiO_2(e^- + h^+)$$

The potential of the conduction band is negative, which could reduce oxygen molecule, and the positive potential of the valence band could produce hydroxyl radicals through redox reactions at the surface if the TiO2. The reaction to occur two requirements need to be fulfilled. The conduction band potential needs to be thermodynamically higher than the redox potential of the acceptor molecule, so to accept the electron. Secondly, the potential of the valence band must be thermodynamically lower compared to the donor molecule to donate an electron to the vacant hole [61]. The production of hydroxyl radicals on the surface of the TiO2 particles based on the concept above is shown on the equations below [58, 62].

$$TiO_2(e^-) + O_{2(ads)} \rightarrow \bullet\, O^-_{2\,(ads)}$$ **Equation 2.5.1.1**

$$TiO_2(h^+) + H_2O_{(ads)} \rightarrow TiO_2 + H^+ + \bullet OH_{(ads)}$$ **Equation 2.5.1.2**

$$TiO_2(e^-) + H_2O_{2\,(ads)} \rightarrow TiO_2 + OH^- + \bullet OH_{(ads)}$$ **Equation 2.5.1.3**

The electron-hole pair is capable of redox reactions with adsorbate as shown in the reactions above. An oxidized electron donor and a reduced electron acceptor are formed during the processes. The photocatalytic activity of TiO2 has been shown to heavily depend on the involvement of molecular oxygen, which in addition serves as a trap for the photo generated electrons [62].

TiO2 has been often said to possess a so called self-cleaning property under UV light. This ability is brought up by the redox reaction on the surface of TiO2, which produces hydroxyl radicals. These radicals are powerful oxidizing agents, which can degrade nearby organic matter (OM) into harmless species such as CO2 and H2O [62]. Simplified reactions of the process are as followed [58]:

$$h^+ + OM \rightarrow OM\bullet^+ \rightarrow Oxidation\ of\ OM$$

$$\bullet OH_{(ads)} + OM \rightarrow Degradation\ of\ OM$$

2.5.2 PHOTO INDUCED SUPERHYDROPHILICITY

The second important property of TiO2 is superhydrophilicity. The definition of the term is extra attraction to water, excess hydrophilicity. In superhydrophilic materials, the contact angle of water is equal or very close to zero degrees.

In the case of TiO2 the state of increased hydrophilicity is achieved with the help of UV light [63]. This phenomenon is explained firstly by the structural changes triggered by the UV irradiation and secondly by the process of eliminating organics from the surface of the material by photocatalysis [61].

The superhydrophilicity due to exposure to the UV light has been investigated with high resolution X-ray photoelectron spectroscopy (XPS) [63], atomic-force spectroscopy (AFM) [61], contact angle [63] and Fourier-transform infrared spectroscopy (FT-IR) [61]. All the above-mentioned methods have resulted in data, that shows signs of change in behaviors and patterns when TiO2 is exposed to UV light. The compound has shown to have increase of hydroxyl groups and water adsorption when UV light is applied. In addition, if TiO2 is surrounded by molecular oxygen environment the superhydrophilic state is still achieved by the UV irradiation [64], which demonstrates the importance of the presence of O2. The number of hydroxyl groups present on the surface of TiO2 has shown to directly affect both the photocatalytic activity and the superhydrophilicity [61], which indicates some sort of a synergy between these two.

The superhydrophilicity of TiO2 is a property which needs to be initiated. It is triggered as mentioned above with UV irradiation and the property, after activation, has shown not to be affected by the increase of irradiation. The property can also be stopped, and the original state of the material has been shown to be restorable. UV treated TiO2 can convert back to its original hydrophobic state by simply storing it in dark conditions [64].

A theoretical surface of TiO2 and all the three stages – non-activated TiO2, activated TiO2 and after UV irradiation are shown on Figure 2.5.2.1.

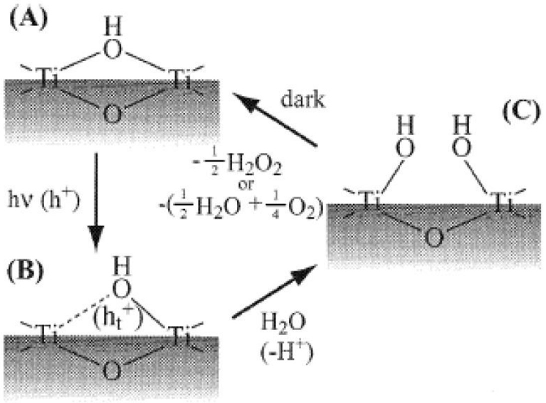

Figure 2.5.2.1. The nonactive state (A), the activation state (B) and activated TiO2 nanoparticles (C) [63].

2.6 GO AND GO/TIO2 COMPOSITE MEMBRANE

In the chapter below the previous three projects committed at Aalborg University Esbjerg and brief literature study on the development of the GO and GO/TiO2 membranes are introduced.

Two projects [48, 49] were done two years ago at Aalborg University Esbjerg, where the synthesis of graphene oxide and the optimal temperature for thermal reduction was investigated. Two of the most popular synthesis methods were tested – Hummer's and Tour's – with the conclusion of the Tour's superiority in safety and simplicity.

Graphene oxide has a layered structure from its original state as graphite. This structure has various functional groups, which have increased the interlayer distance between graphene layers, and defects, inherited from graphite and from harsh oxidation process. These properties create pores and channels which could be used as transportation ways for particles through the material (Figure 2.5.2.1).

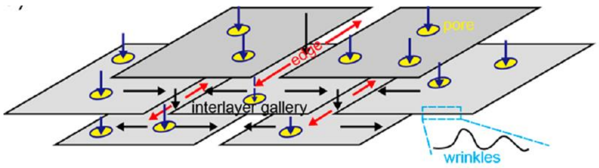

Figure 2.5.2.1. Possible transportation ways through graphene oxide material [65].

The pristine graphene oxide membranes has been found to be unstable in water environment, which meant an addition of a reduction step was necessary. Therefore, the second stage of the investigation was to find a way to treat the membranes where a balance between the amount of hydrophilic functional groups and graphene hydrophobic backbone was to be found.

There are two general options to choose from when reduction of graphene is considered. To either choose among numerous chemical reduction methods, or thermal reduction. The second option was found to be more appealing due to its simplicity and least contaminating to process the GO membranes. The effects of thermal reduction on the membrane are discussed in the Section 2.4.

Firstly, the threshold for the beginning of the thermal reduction was found. Based on results gained from XRD and FT-IR one of the project reported 100°C to be the starting point [49], while 135 C° based on TGA testing was said to be the lowest temperature thermal reduction occurred by the other group [48].

As mentioned above in one of the projects the effect of the reduction was evaluated using mostly XRD and FT-IR methods. The XRD results will be demonstrated in this chapter as some of the goals for this master thesis evolved from it. From Figure 2.5.2.2 the behavior of graphene oxide when reduced under different temperatures is seen in the form of XRD plots. It seems the higher the reduction temperature, the more amorphous the material structure seemed to be. The decrease in crystallinity can be seen as the plot loses its sharp peak as the reduction temperature rises.

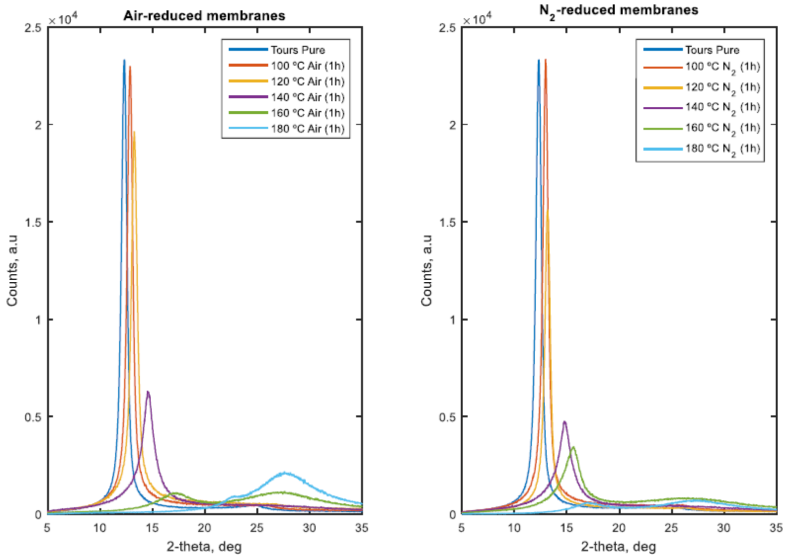

Figure 2.5.2.2. Collection of XRD plots from different reduction temperatures in different environments [49].

The temperature 120°C stands out, as its peak's location is midway between non-reduced and membranes in mostly amorphous state. This phenomenon raised a question of how the implication of different reduction temperature affects the structure of the membrane. Is reduction occurring at 120°C at all? Or if the reduction is committed at a lower temperature and an over longer period, could it influence the poor size of the membrane compared to the rapid crystallinity transformation during the reduction at higher temperatures? These were some of the questions, which emerged from the data. To sum their results, the optimal duration for thermal reduction was said to be 1 hour and the optimal reduction temperatures for air and nitrogen environment were found to be between 140 - 160°C [48, 49]. GO membranes, which were reduced under these circumstances, were found to be most durable in water environment. The membranes did also have vapor permeability higher than the pristine GO and were found to be insoluble in water from 4-9.5 pH.

Membranes made either completely out of graphene oxide or incorporation of the material has been successfully tested in several filtration and separation processes. The research concerning GO as a membrane material is in its beginning stage as the number of investigations is still quite small, but increasing gradually. The membranes with GO have shown to be impermeable to assortments of liquids, vapors and gases with the exception for water [66]. Ultrathin reduced GO membrane supported by a microporous substrate has demonstrated high pure water flux of 21.8 Lm-2h-1bar-1, high retention (>99%) of organic dyes and retention of ion salts of 20-60% [67]. In addition, development of GO membranes for water desalination are undergoing [68].

The second project took the development of the membrane even further by incorporating TiO2 nanoparticles [48]. This innovation opens the possibility to develop membranes with abilities to fight fouling and reduce operation costs of the membrane technology. The photocatalytic activity was tested by exposing the membranes to UV light and seeing if the surface properties of the membrane were affected by it. A decrease was registered in the zeta potential as shown on *Figure 2.5.2.3* below, which indicated the possibility of increase in the amount of oxygen functional groups due to TiO2 photocatalytic properties (see section 2.5).

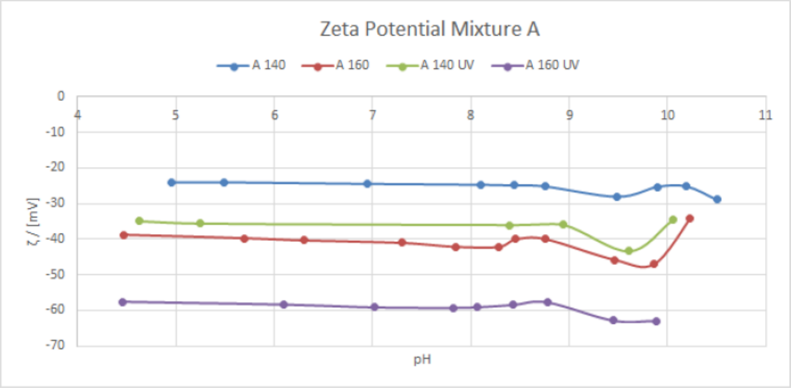

Figure 2.5.2.3. Zeta potential of mixture A membranes, with and without UV irradiation [48].

Drop shape analysis (DSA) results also showed an increase in the membranes hydrophilicity, providing evidence of its state of superhydrophilicity. For example, one of the membranes contact angle changed from 78.9 to 20.8 after being exposed to UV-C light for 30 min [48].

In the literature GO and TiO2 have been tested as part of different membrane configurations. They are mostly incorporated in small quantities into a membrane to enhance its properties or they are layered on top of each other and other membranes. The addition of GO and TiO2 has demonstrated photocatalytic activity by degrading synthetic dyes in aqueous solution [69, 8, 70, 71]. In addition, different membranes, which have been modified with the two materials, have shown improved hydrophilicity, higher pure water flux, flux recovery ratio and antifouling abilities compared to the results before the addition of the two [72, 73].

Unfortunately, the membranes developed at Aalborg University Esbjerg has a serious disadvantage - its lack of strength. The membrane is too fragile to sustain any pressure what so ever, which leads to the third project.

The third project [74] was mostly focused on finding a support material for the previously developed membrane. The selected mode for the membrane is plate-and-frame, where GO/TiO2 membrane would be cast on top a support membrane and be bonded together. Nylon membranes were found to be suitable for the support role and the two membranes became fixed upon each without any assistance.

The pore size of the GO/TiO2 membrane was found to be 9.5 nm, which make the membrane to categorized among the nanofiltration. This membrane doesn't only work based on its pore size, but also its functional groups on the surface of graphene make the membrane to carry a negative charge and are used during the particle transportation across the membrane, making it an electrically charged membrane. Due to incorporation of several materials to produce the GO/TiO2/Nylon membrane, it can be categorized as anisotropic membrane.

Based on the chapters above a sum of good properties GO/TiO2 membranes have been found to own are demonstrated in the Table below.

Table 2.5.2.1. Properties of GO and TiO2.

Property	**GO/TiO2 membrane**
High water flux	X
High solute rejection	X
Antifouling properties	X
Photocatalytic activity	X
Thermal stability	X
Antibacterial property	X
Large-scale production	X

3 PROJECT OBJECTIVES

Filtration is considered as a promising separation and water purification technology due to its easy operation, energy saving property and high efficiency. A potential material for water purification membranes investigated is graphene oxide due to its great properties and relatively low cost.

Graphene, that is the backbone of graphene oxide, is hydrophobic and the oxygen functional groups attached to graphene layers in graphene oxide modify the material to have a hydrophilic nature. Researchers have reported the combination of graphene oxide and anatase TiO_2 to form a membrane, which exhibits properties such as superhydrophilicity. This leads to increased antifouling, and photocatalytic properties. This type of membranes is produced and investigated during this Master's thesis.

Below are the objectives to be investigated during this project:

- Changes in the composition of graphene oxide during the purification stage. Insight into the purposes, effects and efficiency of the two washing solutions used to purify the synthesized gel.

- Structural changes to graphene oxide during application of different reduction temperature and duration. Based the section 2.4, where thermal reduction's effect on the structure is discussed, the membranes are predicted to have different crystalline structures between the different thermal reductions.

- Experiments concerning the effect of thermal reduction temperature and the length of the process on the pore size of the composite membranes. Thermal reduction done at mild conditions should leave room for the material to readjust itself and possibly affect the membrane properties such as the pore size.

- Investigating the effect of different reduction temperature and duration on the photocatalytic properties by exposure using UV-C lamp of the developed membrane. UV light is used to activate TiO_2's photocatalytic properties, which results in the photoinduced superhydrophilicity property that increases the hydrophilicity of the membrane. The photoinduced superhydrophilicity should result in a smaller contact angle with DSA and increased zeta-potential.

- Testing and quantifying the photocatalytic activity using methylene blue solution and UV irradiation. TiO_2's photocatalytic properties can degrade organic matter. Therefore, a difference between the membranes under the UV lamp and the membranes without the lamp is theorized to happen. The membranes with UV irradiation will degrade the dye as the non-activated membrane will not affect the concentration of the dye.

4 EXPERIMENTAL DESIGN

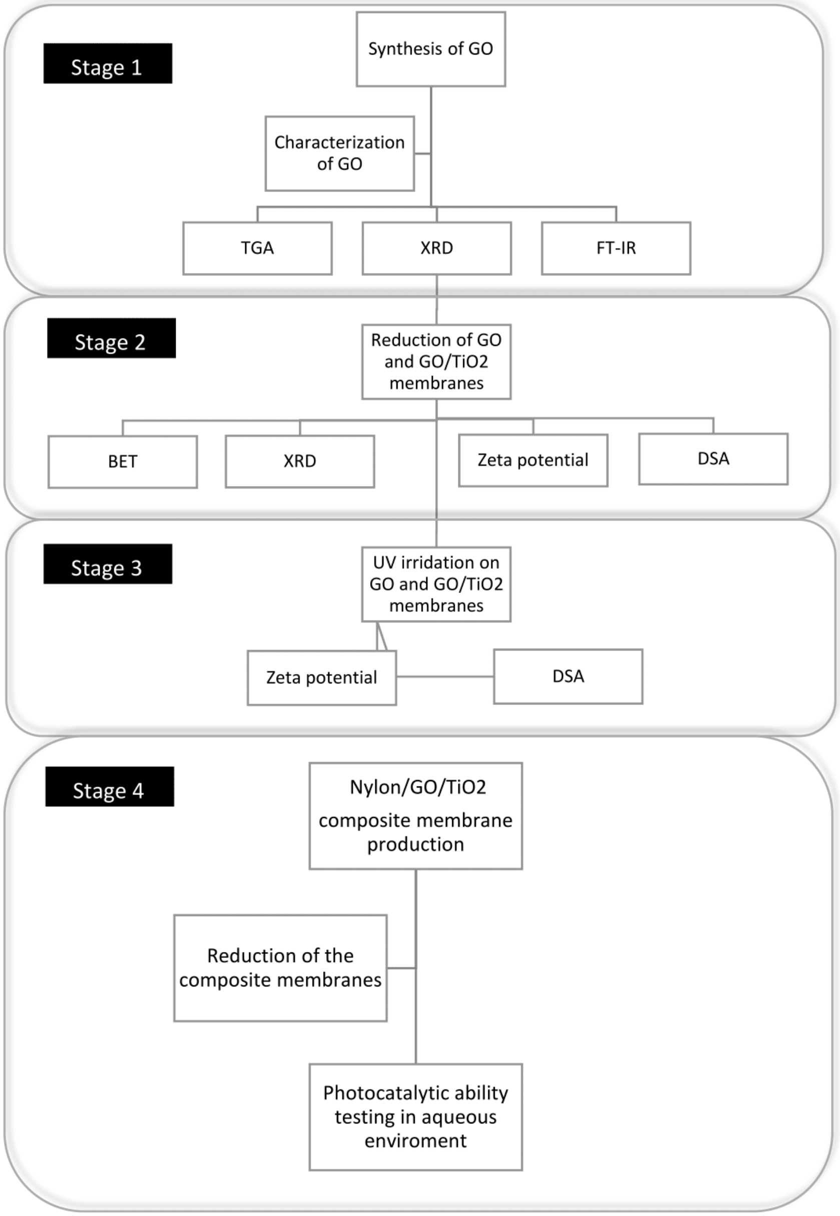

Figure 2.5.2.1. The outline of the project.

The project can be divided into 4 general stage, as seen on Figure 2.1.1.1. The first part is solemnly dedicated to produce the graphene oxide gel and its characterization to make sure it has the necessary qualities.

The second part is the thermal reduction stage, where temperature 120 and 140°C were applied, with durations of 15, 30, 60 and 120 minutes. The reduced membranes were characterized and investigated with several analytical techniques to register the changes to the membrane.

The third part is the investigation of the effect of UV exposure to the incorporated properties of TiO_2 nanoparticles and the changes it brings to the properties of the whole membrane.

The last part is about the quantification of the reduction of methylene blue under UV lamp in an aqueous environment.

All the methods for the production of the materials and membranes, thermal reduction and the analytical methods are briefly introduced in the next chapter.

5 METHODS

This chapter is dedicated to provide all the scripts with commentaries for the laboratory work and analytical techniques.

5.1.1 IMPROVED HUMMERS METHOD

1.) *A 9:1 mixture of concentrated H_2SO_4/H_3PO_4 was added to a mixture of graphite flakes and $KMnO_4$ in ratio of 1:6.*
Firstly, the two solid reactants, approximately 3 g graphite flakes and 18 g $KMnO_4$, were weighed, mixed and added into 1000 ml flask equipped with a magnetic stirrer. A blend (360:40 ml) of concentrated sulfuric acid (H_2SO_4) and phosphoric acid (H_3PO_4) was prepared mixed together separately and let to cool down to room temperature before adding it the solids in the flask. The flask containing the solids was placed into an ice bath as the addition of acid produces an exothermic reaction (35-40 °C). The temperature during the addition part was kept between 5-10 degree. The mixture of acid was added to the solids very slowly using disposable pipettes and the speed of the magnetic stirrer was held on minimum during the first 100 ml of acid. The color of the solution was green as shown on Figure 2.3.1.7.

2.) *After the addition of acids, the solution is removed from the ice and left to be stirred overnight at 50 °C for approximately 14 hours.*

The solution should be of brown color by now and be more viscous than before.

3.) *The reaction was cooled to down to room temperature using an ice bath. 400 mL of water was slowly added to the reaction solution while the temperature was kept below 40 degrees. Finally, 30% H_2O_2 was added to finalize the reaction.*

The ice bath was used during the whole process. During addition, a color change occurs again from brown into red/purple. The mixture may be removed from ice before the termination of the reaction step where 30% H_2O_2 is added to the mixture. The volume needed depends on the level of oxidation of GO and can be between 3–5ml. The addition of peroxide must be stopped, when the solution´s colour changes into yellow.

4.) *GO is left to settle overnight.*
The obtained solution was divided into two measuring cylinders in order to settle the GO, which was completely dispersed in water/acid mixture. Around 200ml of solution was transferred into the cylinders and topped up with additional 200ml of deionized water. After a day or two the slurry had separated into two layers and the colour had turned from orange to brown. The majority of the top layer was removed by decanting and with the help of 5ml automatic pipette.

5.) *Over the course of 3-4 days the obtained GO is washed with 1 M HCl solution 3 times and with deionized water 4 times using centrifugation.*
The purification stage was done firstly with acid solution. GO was dissolved in approx. 25ml of the acid solution using spatulas and vigorous shaking followed by centrifugation

at 6000 RPM for 10 minutes. This procedure needs to be repeated 3 times. Following the HCl wash, the GO was dissolved in the same volume as before of deionized water and followed by centrifugation at 6000 RPM for 4 hours. The washing with water must be done 4 times.

5.1.2 OPTIMIZED IMPROVED HUMMERS METHOD

The amounts had to be reduced compared to the description in the article due to the limited amount of reactant available at the time.

1.) 200ml of concentrated H_2SO_4 acid is placed into a flask and 1:3 weight ratio (5g and 15g) of graphite/$KMnO_4$ is added into the liquid phase in small dosages while keeping the temperature less than 10 degrees.
2.) The reaction mixture is left to be stirred for 3h.
3.) The reaction mixture is cooled down to room temperature and placed into an ice bath for the addition of 400ml of water. Water is added slowly and close attention was kept on the temperature to be below 40 degrees. This was followed by adding 30% H_2O_2 to bring an end to the reactions with in the system.
4.) The obtained solution was split in two measuring flasks and approximately 200ml of water was added into each of the containers. It was left to settle overnight in the fume hood.
5.) The purification step should be done using vacuum filtration with 200ml of deionized water, 200ml 1 M HCl solution.

5.1.3 TiO_2

The TiO_2 nanoparticles used for the experimentation was synthesized during a previous project. The discussion about the synthesis of TiO_2 can be found in the separate report [47], where the manuscript and theory are written down in detail.

Before every membrane production the TiO_2 solution was sonicated with probe-type sonication at 40% power setting for approximately 1 minute to ensure the nanoparticles are dispersed into smaller particles.

5.1.4 MEMBRANE PRODUCTION

All the membranes were produced the same way, with the same weight ratio of 1:15 TiO_2/GO. 10 grams of GO gel and 0.6 µl of TiO_2 mixture was poured into a petri dish, which was used as the cast (Figure 5.1.4.1 A-C). The membrane was left to dry in the fume hood for at least 48 hours. A very detailed description of the production process and of the removal of the membrane from the mould can be found in a separate report [47] done at Aalborg University Esbjerg.

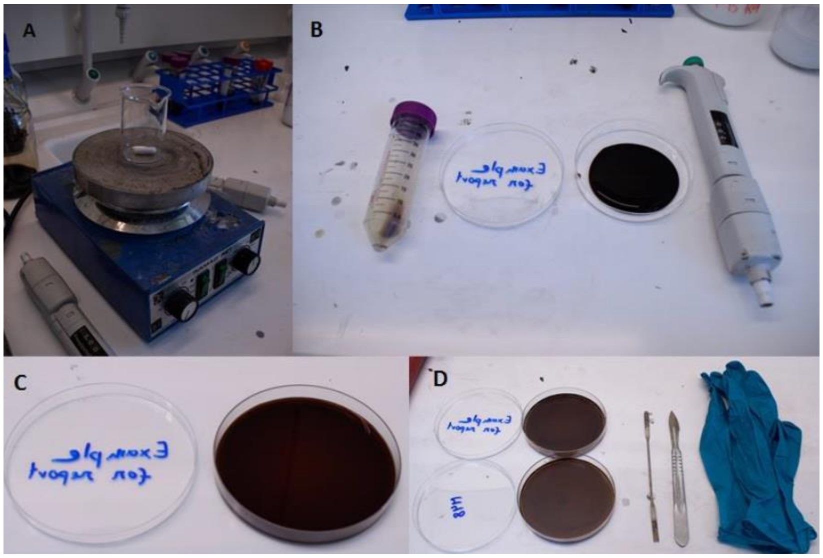

Figure 5.1.4.1. The procedure to produce the GO/TiO2 membranes [74].

5.1.5 COMPOSITE MEMBRANE PRODUCTION

Membranes with the support material are done similarly to what was described in the membrane production part. Based on the diameter of the nylon membrane the amount of GO was decreased proportionally to have the same thickness as the full-sized membrane.

3 grams of GO gel was mixed with 0.2µl of TiO_2 solution. The mixture was poured on top of the nylon membrane and left to dry in the fume hood for at least 48 hours. To quicken the drying of the membrane, layers of filtration paper were put under the nylon membrane. On Figure 5.1.5.1 the cast for the membrane production is shown.

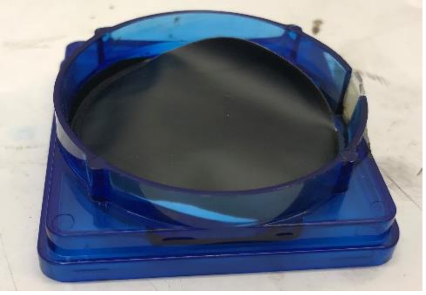

Figure 5.1.5.1. The plastic cast used for the GO/TiO2/Nylon membrane production.

5.1.6 THERMAL REDUCTION

The dried membranes were reduced with different durations in nitrogen purge at 200ml/min using the Carbolite (Figure 5.1.6.1 left) oven at 120 and 140°C.

The membranes were set in the oven at room temperature. The heat rate was kept at 5°C /min. The "rough" side of the membrane is recommended to be situated outwards, while inserting the membrane in the oven. Doing this has shown to help the membrane to relax back into flat surface better after the removal from the heating system. An example of a reduced membrane can be seen in Figure 5.1.6.1 (right).

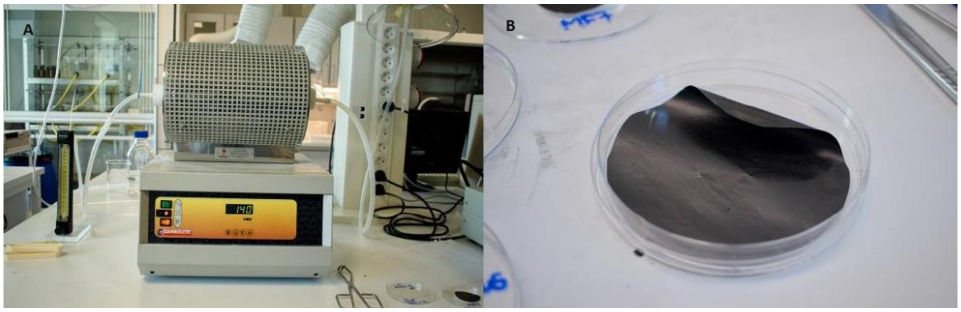

Figure 5.1.6.1. Left: the Carbolite oven used for reduction. Right: A photo of a reduced membrane.

5.1.7 ACTIVATION OF TIO2 PARTICLES WITH UV LIGHT

The lamp used for experimentation is equipped with UV-C light with wavelength of 254 nm. The UV exposure was kept to 30 minutes, where the intensity on the membranes was around 2 mW/cm^2. The experiment set up was surrounded with a wooden box to have control over the surrounding environment for more precise measurements. These parameters were kept constant throughout the experimentation. The UV-C lamp setup is illustrated in Figure 5.1.7.1.

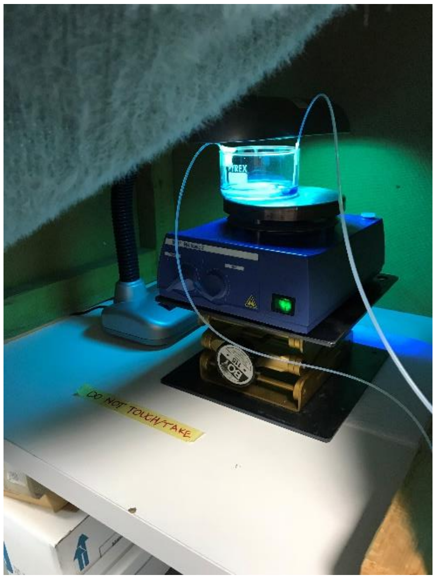

Figure 5.1.7.1. The experiment setup for the UV irradiation of the membranes.

5.1.8 THERMOGRAVIMETRIC ANALYSIS (TGA)

TGA is a technique, where the weight percentage (wt. %) of a sample is monitored as a function of temperature or time in controlled atmosphere. The duration, final temperature, the heat rate and other parameters are user defined. The programme used for the analysis of GO can be found in the Table below.

Table 5.1.8.1. The program for the concentration of GO.

Starting temp. 1 (°C)	Heating rate (°C/min)	End temp. 1 (°C)	Starting temp. 2 (°C)	Heating rate (°C/min)	End temp. 2 (°C)
25	10	150	150	25	550

5.1.9 X-RAY DIFFRACTION (XRD)

For most analysis the Panalytical X' Pert Pro MPD X-ray Diffractometer with a cobalt-sealed tube (Co Kα X-rays of 0.179 nm) operating at 45 kV and 20 mA was used. The measurements concerning GO were done with a method named KRA50, where the scanning was only done up until 50°. A sample mounted into the solid's sample holder can be seen on Figure 5.1.9.1.

Figure 5.1.9.1. The XRD sample holder with a membrane.

The collected XRD data can be used to calculate the characteristics of the crystal structure. The distance between the crystalline layers is calculated using the Braggs's Law:

$$n * \lambda = 2 * d * \sin\theta \rightarrow d = \frac{n * \lambda}{2 * \sin\theta}$$

Where n is a positive integer number, λ the specific wavelength, d is the distance between crystalline layers and θ is the diffraction angle.

The Scherrer equation is used to calculate the average height of the laminar layer of GO:

$$H = \frac{K * \lambda}{\beta * \cos\theta}$$

K is the Warren shape constant, that is taken to equal 0.9, and β is the measured full width at half maximum (FWHM). FWHM can be found form the XRD plot (Figure 5.1.9.2).

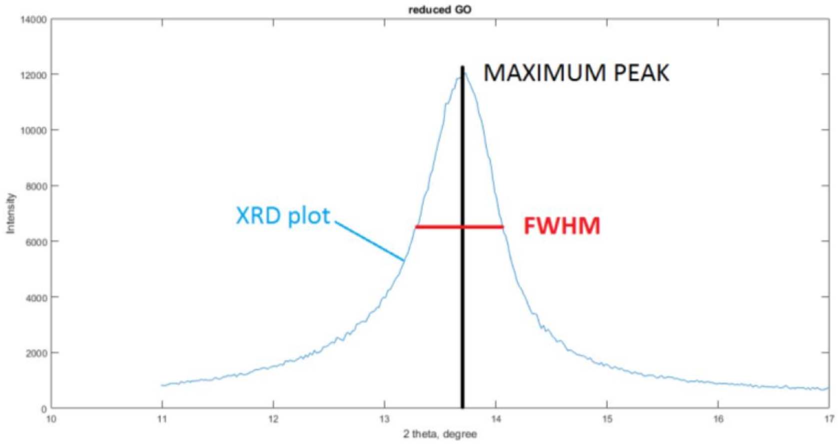

Figure 5.1.9.2. XRD plot with the full width at half maximum.

Lastly the number of crystalline unit cells forming a laminar layer is calculated using the previously calculated values:

$$n = \frac{H}{d}$$

5.1.10 DROP SHAPE ANALYSIS (DSA)

The Krüss DSA equipment was used for the analysis. The used solvents were deposited onto the membrane by a sessile drop method. An image of the drop is recorded with a camera and transferred to the drop shape analysis software. The program performs a contour recognition based on the grey-scale analysis of the image. The data is then fitted to a geometrical model to the contour. Young-Laplace-Fit method was chosen to calculate the contact angle during this project. The contact angle is estimated between the drop shape and the baseline (Figure 5.1.10.1).

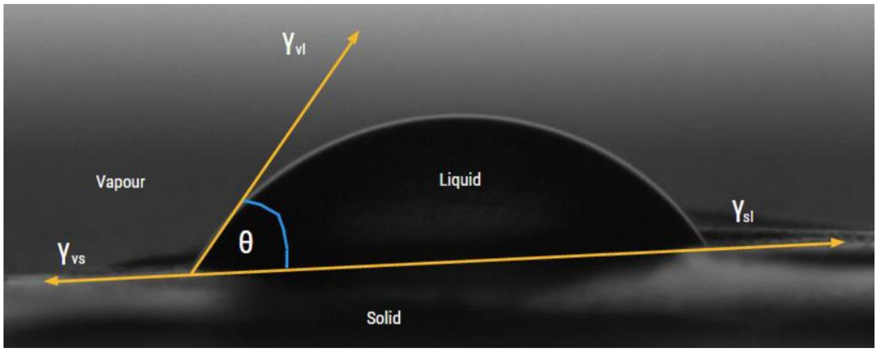

Figure 5.1.10.1. Contact angle at the three-phase contact point.

Membranes were characterized using two solvents - distilled water and diiodomethane, to be able to perform the two-component surface energy characterization. The membranes must be attached to a microscope glass slider with double sided tape for the duration of the analysis. This ensures the membrane remains flat and does not change shape during measurements.

To evaluate the surface energy the two-components surface energy theory based on Good's equation was used. The solid's dispersive component was calculated using the equation below.

$$\gamma_s^D = (\gamma_l/4)(\cos\theta + 1)^2 \qquad \textbf{Equation 5.1.10.1}$$

γ_s^D is the dispersive component of surface energy for the solids, γ_l is the overall surface tension of the liquid and the θ is the measured contact angle. The value of γ_l for diiodomethane is taken 50.8 mN/m.

The polar components of the surface energy for the solid was evaluated using the equation below.

$$(\gamma_s^D * \gamma_l^D)^{1/2} + (\gamma_s^P * \gamma_l^P)^{1/2} = \gamma_l \frac{(\cos\theta+1)}{2} \qquad \textbf{Equation 5.1.10.2}$$

γ_l^D is the dispersive component of the surface tension for the liquids, γ_s^P is the polar components of the surface energy for the solids, γ_l^P the polar component of the surface tension for the liquids and γ_l is the overall surface tension of the liquid.

The values for γ_l^P=46.4 mN/m, γ_s^D is calculated with Equation 5.1.10.1, $\gamma_l^D$is taken as 26.4 nM/m and γ_l is 72.8 mN/m.

The surface polarity was calculated by:

$$Surface\,polarity = 100\% * \frac{\gamma_s^P}{\gamma_s}$$

5.1.11 ZETA POTENTIAL

When an electrode surface is brought into contact with an electrolyte, an electrical charge is created. Zeta potential (ζ) is an electrokinetic measurement of the electrical charge, which is created at the interface between the liquid phase and the membrane. The created potential is measured at the shear plane, which is the slipping location of the moving liquid phase compared to the stationary liquid phase as demonstrated on the Figure 5.1.11.1. The zeta potential of a particle or surface is the physical property that describes the electrostatic stability of a particle in a colloidal solution.

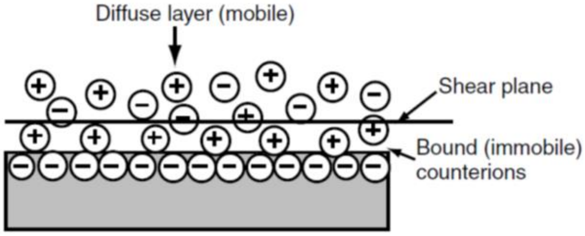

Figure 5.1.11.1. Surface with a negative charge, that is balanced by positively charged counter-ions. The position of the shear plane and the diffuse layer [75].

Depending on the chemical structure of the material or particle, the surface charge can either be positive or negative. For a solid surface such as membranes, the zeta potential gives information about the surface functionality, specific interaction of dissolved compounds with the solid surface and liquid-on-surface adsorption processes [76]. By changing the pH, the zeta potential will change due to ionization of the surface groups. When the pH is increased, the surface charge of a sample becomes neutralised and the electrostatic repulsive forces decrease between surfaces causing a colloidal solution to become unstable and a porous structure to breakdown [77]. The pH at which the zeta potential reaches zero is the isoelectric point and is the point where the system is least stable.

Hence the analytical tool gives us the information about the stability of the GO/TiO2 membranes. In addition, their capabilities of repelling sudden ions as well as minimize fouling and degradation can be evaluated. The decreasing effect to fouling is in the range, where the zeta potential is highest and nonchanging as the surface charge is at its maximum and thus, the membrane is capable of repulsing more of the fouling with the same charge sign (negative or positive), which acts as a barrier of the membrane efficiency. The SurPass analytical equipment was used for the investigation.

5.1.12 BRUNAUER–EMMETT–TELLER (BET)

BET is a characterisation tool, which is used to measure the surface area and the pore size distribution of a sample. The BET analysis uses gas adsorption, which is measured as a function of relative pressure, to evaluate the specific surface area. The gas needs to be physically adsorbed on the surface of the sample by weak bonds, for example by the Van der Waals forces. No permanent bonding should occur as desorption by the decrease in pressure at the same temperature is required to happen. As the result of adsorption and desorption techniques, determination of pore area and specific pore volume is possible to be evaluated.

The pore size of the GO/TiO2 membranes determines which type of particles are rejected during purification processes and the categorization of the membrane. The surface area gives an idea of how exposed are the nanoparticles as the greater the surface area, the more organic matter could be exposed to the TiO2's photocatalytic reactions.

The BET equipment used in this project is of the brand CE Instruments Sorptomatic 1990 Series. For one measurement 2,5 full sized membranes were cut into fine pieces and transferred into the sample holder. Each sample is needed to be degassed to remove gas and vapors which might have been adsorbed onto the surface from the air. This is normally done by using a vacuum system. The degassing process for the GO/TiO2 membranes are done at 80°C, to make sure no further thermal reduction is occurring, for until the pressure in the sample holder is zero.

5.1.13 PHOTOCATALYTIC ACTIVITY TESTING WITH SPECTROPHOTOMETER

This procedure is based on a standard testing DIN 52980. The method is meant to quantify the activity of photocatalytic surface through degrading organic matter in aqueous environment. The necessary step to prepare and set up the experiment are as follows:

1.) The sample need to be tested for its stability in water, as it will be submerged for 5 hours. A perfect sample should have higher density than water, so the sample would not float. The active surface should have a size between 100 and 1500 mm^2, thickness between 1-5 mm and a maximum of length of 60 mm at the longest point.

2.) The samples are first immersed in an aqueous 20 μM methylene blue solution in a dark environment for 2 hours. The samples need to have the methylene blue preabsorbed on the surface so the adsorption during testing deteriorates only due to photocatalytic activity.

3.) Wash the tubes and cuvette with 10 μM methylene blue solution, to make sure no water is left into the system from previous testings. About 20 minutes before the beginning of the experiment switch on the UV-light (365 nm), so it would be warmed up and make sure the membrane will be situated in a location, where the intensity of the lamp is 2 mW/cm^2.

4.) After the two hours of pretreatment the sample transferred into a separate container and immersed in 30 ml of 10 μM methylene blue solution. The spectrophotometer is prepared by selecting the kinetics mode. The most suitable wavelength for the experiment with methylene blue is 660 nm and the length of the experiment can be between 3-5 hours. During this project the spectrophotometer is set to take measurements every second, but the time can be set up to 2 minutes. The photocatalytic activity of the sample can be seen on the graph which is shown on the computer screen. If the sample is photocatalytically active, the graph will decrease over time, which means that methylene blue is degraded.

5.) After the experiment wash the system with deionized water to keep the system from saturation of methylene blue.

The experiment setup can be seen on Figure 5.1.13.1 . The area with the lamp and the membrane was covered with a wooden box, to be more in control over the surrounding area for the purposes of precision.

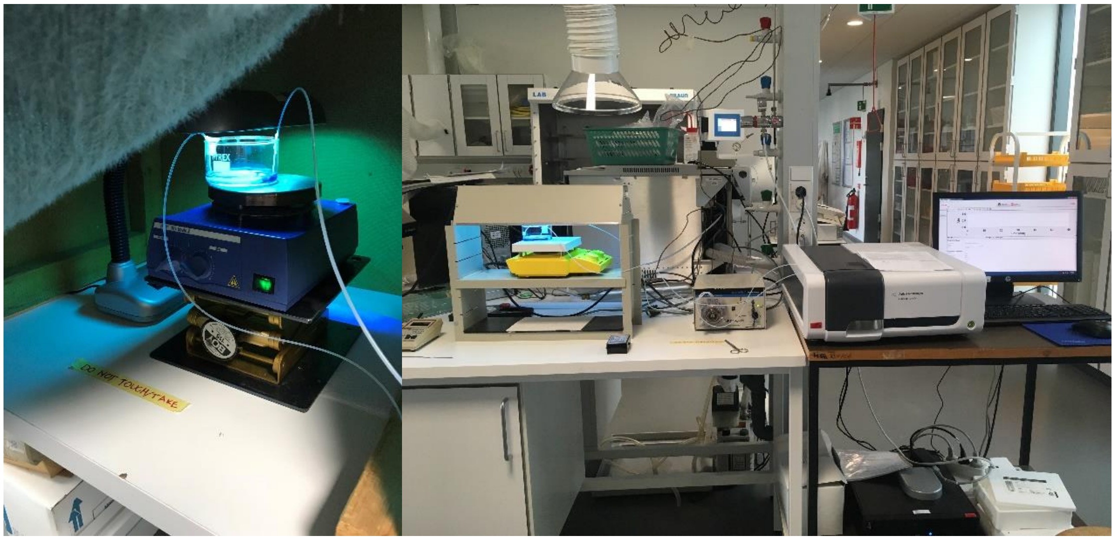

Figure 5.1.13.1. The setup for the quantification of photocatalytic activity testing.

5.1.14 CALIBRATION CURVE OF METHYLENE BLUE

Calibration curve for methylene blue was done to provide the opportunity to convert absorption value from UV-Vis to concentration. A stock solution of 20 µM was done, which was used to make other necessary solutions. In total 5 calibration solutions (Table 5.1.14.1) with known concentration were made and measured.

Table 5.1.14.1. Calibration solutions of methylene blue.

Concentration (µM)	Methylene blue solution (ml)	Water (ml)	Final volume (ml)
20	25	0	25
15	18.75	6.25	25
10	12.5	12.5	25
5	6.25	18.75	25
2.5	3.125	21.875	25

Two calibration graphs (Figure 5.1.14.1) were done to make sure all experiments can be included. Most of the experiments were done at 660 nm, except one, which was measured at 680 nm. The obtained trendline equations are used for the evaluation of concentration.

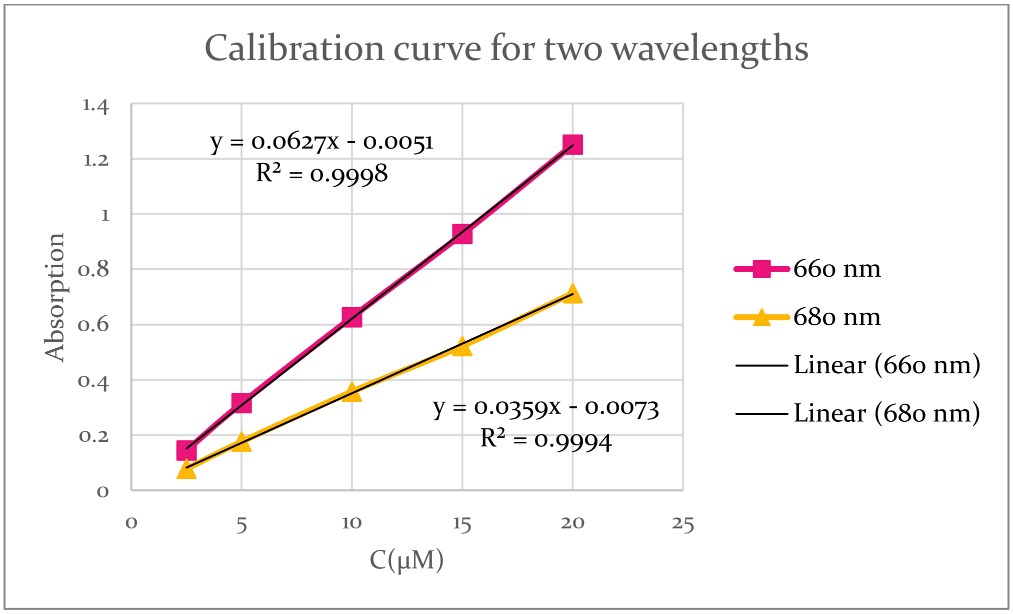

Figure 5.1.14.1. Calibration curve for 660 and 680 nm.

6 RESULTS AND DISCUSSION

In the following sections all the gathered results are presented. The first part is focused on the synthesis and purification of the graphene oxide. The second chapter introduces the process of characterization of the synthesized graphene oxide. Thirdly the effect of different temperatures and duration applied during thermal reduction on the membrane characteristics is discussed. The part after that will be focusing on the effects and quantification of the photocatalytic activity. And lastly, the miscellaneous results section report on data, which didn't fit in any of the previous sections.

6.1 GRAPHENE OXIDE SYNTHESIS

Throughout the results sections the abbreviation GOS_ will be used, which stands for Graphene Oxide Synthesis and is used to differentiate between different attempts of making the material for membrane production. In Table 5.1.14.1 an overview of all the trials of making graphene oxide, including the method, what was varied during the experiment, amount of H_2O_2 used to finish the reaction and if the synthesis was successful in the end, is shown.

Table 5.1.14.1 Sum of all the synthesis committed throughout the project.

GO batches	Method	Variable	H_2O_2 used	Successful
GOS1	Impr. Hummers	No ice bath	-	No
GOS2	Impr. Hummers	Ice bath	6.5	Yes
GOS3	Opt. Impr. Hum.	Concentration	7	No
GOS4	Impr. Hummers	Solids into acids	6.5	Yes
GOS5	Impr. Hummers	Acid onto solids	6.5	Yes
GOS6	Impr. Hummers	No changes	6.5	No
GOS7	Impr. Hummers	No changes	6	Yes

6.1.1 GOS1

GOS1 was the first attempt to synthesize graphene oxide. Another project [47] that dealt with graphene oxide synthesis had a suggestion concerning the unnecessity of the ice bath during the addition of acids. This idea was tested to see if it is possible to add the acids slow enough to avoid a burn out. To test it out the solids were placed in a 1000 ml flask and the acid mixture was slowly added to the blend of the solid compounds. After adding 1 ml of the acids blend, the reaction mixture burst into flames resulting in the eruption of burned graphite and $KMnO_4$ from the flask. The main trigger for the explosion was the magnetic stirrer that added unnecessary heat due to friction when the solids were smeared against the glass flask and too vigorous stirring between concentrated acids and the reactants. The detonative behavior of the reaction blend is consistant with the theory of the existence of the dimanganese heptoxide (Mn_2O_7), that is said to be explosive when the temperature exceeds 55 °C. In addition, the colors seen during the addition of the acid mixture matches with the reported green color of the compound (2.3.1.4). It can be concluded that an ice bath is strongly recommended for safety purposes.

6.1.2 GOS2

The second attempt to synthesize graphene oxide (GOS2) was done by following the steps explained in Section 5.1.1 with the cooling during the addition of the acids. The synthesis was successful and resulted in GO gel with good properties. In most of the articles concerning the synthesis of the compound, the obtained gel is usually exfoliated using an ultrasound probe as one of the last steps before its application in various situations.

This hadn't been tested yet during the previous projects and an attempt was done during this project. The settings for the probe were chosen to be mild and the time for the procedure was 3 min. This test ended up damaging the gel and making it unusable.

There are few possible ways to explain the effect. Firstly, the gel could have been damaged by the temperature rise during the procedure. Although, the exposure of the gel to the sonification was not long and the rise of the temperature was not drastic, yet noticeable by touching the container, the procedure still could have had resulted in reducing the gel enough for it to be not suitable to make membranes.

The second explanation could be the process decreased the crystal size of the GO. Often the size of particles of the materials used for membranes production are preferred to be of a smaller size as it deposits better on other surfaces and provides a smoother surface. GO could be an exception, which needs to have larger sized particles to be able to form a membrane.

The damaged gel was analyzed with XRD and DLS to test which of the theories is a better fit to describe what happened. XRD results obtained (Table 6.1.2.1) by examining a membrane before and after sonification do show a slight difference.

Table 6.1.2.1 XRD results from analyzing a membrane made of the gel before and after sonification.

Sample	d (nm)	H	n
GOS2 – before	0.8411	11	13
GOS2 - after	0.8276	12	14

Thermal reduction decreases the height between the interlayers (d-value) and could be the potential explanation. Yet the value 0.8276 nm is higher than what was obtained in one of the previous projects, where a gel with the d-value of 0.802 nm [47] was successfully used to produce membranes. So theoretically the gel should be good enough for membrane production.

To test if the size of the crystals is reduced during the exfoliation of the gel, DLS analysis was done to a gel before and after sonification. Two dilutions – 1:50 and 1:100 - of the stock GO gel were done and analyzed.

	1/100 G6 before (nm)	1/100 G6 after (nm)	1/50 G6 before (nm)	1/50 G6 after (nm)
	341	262	384	308
	301	287	375	272
	269	268	359	283
	255	239	356	297
	237	258	348	294
	237	253	358	273
	231	249	347	282
	235	256	355	292
	241	255	348	284
	262	260	352	274
	285	242	359	284
	296	233	-	272
	326	244	-	273
Average	270	254	358	283

In the case of both dilution the size of the particles decreases after sonication, which means the reason GOS2 was not usable after sonification was most likely due to the reduction of the particles size, not thermal reduction. Two membranes were made, where one of them was sonicated before casting. On Figure 6.1.2.1 the difference in their appearance is shown.

Figure 6.1.2.1. Left: membrane made using sonicated GO gel. Right: membrane made of the same GO gel before sonication.

6.1.3 GOS3

GOS3 was synthesized using suggestions from an article [78] which was focused on the optimization of the Improved Hummers method (Tour's method) and presented great results and ideas to make the production process quicker and more effective. The manuscript for the synthesis can be found in Section 5.1.2. The optimized method for GO production was not successful and here is why.

The first claim in the article was the accomplishment of reducing the reaction time from 12h to 3h while maintaining the same level of oxidation of the raw material. The conclusion about the level of oxidation was made based on spectrum gathered with Raman, which indeed showed very similar patterns and the intensity of the D band indicating similar structural disorder and great number of defect in the graphene layers in both cases. By replicating the condition from the, different results were found because a lot of the graphite has not as the kinetics of the reaction has been shown to be time consuming due diffusion of the oxidant between the crowded layers of graphene as explained in section 2.3.1.2. The graphite which did oxidize during the 3 h can possibly be equally good compared to the graphene oxide obtained by 12h reaction, but the yield of the whole process was severely affected by it. In addition, using only one analytical method to analyse a complex compound such as GO, which hasn't yet been completely understood by the research community, is not always enough.

The second implemented optimization was the ratio of solids and liquids. The usual amount of the solid reactants used are 3g of graphite and 18 g of $KMnO_4$, which are combined with total of 400ml of H_2SO_4/H_3PO_4 (9:1 ratio) mixture as explained in section 5.1.1. Based on the discussed article the optimum combination was found to be 400ml of H_2SO_4, 15g of graphite and 45g of KMnO4. Due to limited availability of graphite during this project the repeat experiment was done with proportionally reduced amounts. In general, the viscosity of the reaction mixture during the oxidation using the normal 3g of graphite has always been something to keep an eye on as it increases with time and has caused the magnetic stirrer to be blocked. So, with the additional amount of solids suggested in the article caused the mixture’s viscosity to increase so much that the very needed stirring was seriously hindered from the beginning of the reaction and ended up in completely stopping the mixing as time passed by. The lack of stirring made the graphite to “sit” at the bottom of the flask and resulted in it not being exposed to the acid/oxidant mixture as much as it should have been, again affecting the overall yield of the process.

Another optimization proposal was made concerning the purification stage, where the steps and quantities were suggested to be halved. The data based on what the conclusion of the unnecessity of longer purification was gathered using Raman spectra. Only one analytical method is not enough to back the statement of the efficiency of the smaller quantities ability to remove impurities from the product and Raman is not a direct method to investigate the compound’s purity. During this project EA analysis was done throughout the purification part to see the changes in composition and to check the validity of shorter procedure. The details concerning the exact obtained results will be discussed in section 6.2.1, but the conclusion of the paragraph is the suggestion not to decrease the quantities of the purification. Perhaps an increase in the amount should be applied to make sure the impurities are removed. The gel should be as clean as possible, so no harmful or unwanted compounds would not seep into water, if the material is used to produce water purification membranes.

The authors of the discussed reported a higher yield of the final product (graphene oxide) compared to the original Tour’s method and lower manufacturing costs, but based on the experiments committed during this project the obtained results did not match with what was reported in the discussed article. In addition, the synthesized gel didn’t turn out to have good enough quality ending up being unusable again.

6.1.4 GOS4

GOS4 synthesis was done following instructions from the section 5.1.1. The only change made to the prescript was concerning the ending of the reaction, where the original method said to add water in small quantities into the reaction mixture which mostly consists of concentrated acids, but instead a switch was made where the reaction mixture was slowly added into the cooled water. The switch didn’t seem to have any severe effect on the synthesis outcome as the obtained results were identical to previous tests where the opposite was done. In the end, it seems it doesn’t matter which way around the addition of water occurs and based on the numerous experimentations with Tour method adding water to the acetic mixture is a cleaner and easier procedure although it goes against the basic knowledge of the acid into water concept. The experiment turned out to be a success and a good quantity of quality GO gel was obtained, which was used for membrane production.

6.1.5 GOS5

The fifth synthesis (GOS5) was done following the prescript from section 5.1.1. The reaction was left to be stirred over night for 12h. At some point during the night the magnetic stirrer had stopped working due to either malfunction of the equipment, the viscosity of the solution or the combination of both. The GOS5 product, while purified, behaved in a new way, as a large amount of white precipitation was noticed for the first time ever (Figure 6.1.5.1 left photo).

The usual silver-grey precipitation (Figure 6.1.5.1 right photo) is signed to belong to unreacted graphite, which can be noticed often in small quantities in the solution throughout the purification. The dissimilarity between the newly detected white and the usual graphite grey precipitation indicates a different origin.

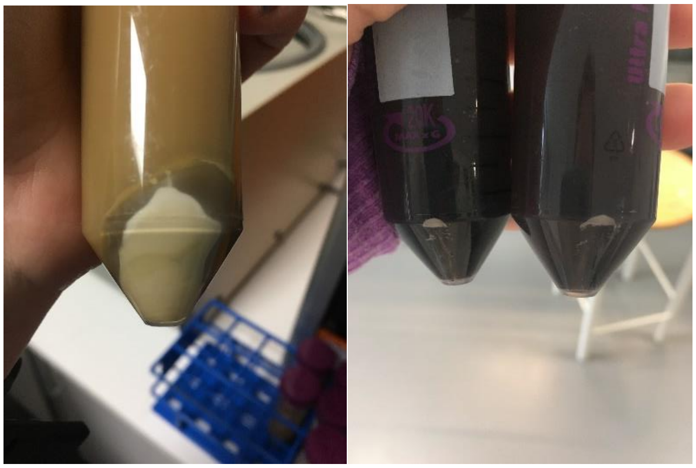

Figure 6.1.5.1. Right: photo of the never seen before white prcipitaion. Left: unreacted graphite residue

The amount of the white precipitation lessened with each wash and in some cases, it disappeared completely from the solution. There are two possible explanations for this. In the section 2.3.1.2, the color of pristine graphene oxide has been detected to range between white and light yellow, if no significant amount of water has been added to initiate the hypothesized hydrolysis. The fact that the quantity decreases with each wash and taking into consideration the time it takes to perform one wash (4 hours with water and 10 min. with 10% HCl solution) and the slightly elevated temperature in the solution during centrifugation, could create an environment where the material is reacting with water in accelerated speed.

The second explanation could be the conditions of the solution made some of the impurities in their salts form to precipitate and their quantity is lessened during each wash as they are gradually removed from the solution. Potassium sulfate (K_2SO_4) is one of the existing salts and is known to have white color. In addition, $MnSO_4$ has also been reported to have a pale pink color, which could appear whitish in the background of the brown graphene oxide solution (section 2.3.1.3). As the priority at that point was to obtain GO gel so membranes could be produced, no analysis was done to identify the chemical characteristics of the precipitation leaving only the option theoritize of what it could have been.

Although the experiment was expected to be ruined because of failed stirring, the purified GO gel was unpredictably good enough for production of membranes and was used for further experimentations.

6.1.6 GOS6

In the contrast to the fifth synthesis, where usable GO gel was obtained although crucial part of the synthesis failed, and anomalies occurred during purification, GOS6 that was done following the same prescript, during which everything went without any problems, ended in a gel that was unusable. The gel produced membranes which were too fragile to work with an example how the appearance of the gel varies can be seen on Figure 6.1.6.1 on the right. All the membranes are done using 10 g of the GO gel. The darker membranes are made using GOS5 and the light-colored membrane is done from GOS6.

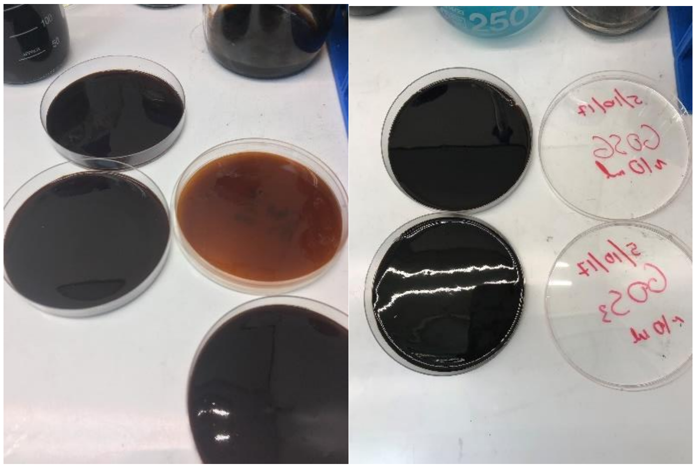

Figure 6.1.6.1. Left: produced membranes using GOS5 and GOS6. Right: the bottom membrane done using GOS6 after resting time of 4 months.

The GOS6 gel was revisited for testing 4 months later. The gel's colour in the storage unit and the membranes produced from it have much darker colour (Figure 6.1.6.1 left). In addition, the membranes produced from GOS6 are not fragile anymore and with a smooth surface (Figure 6.1.6.1 right). It could be indication of changes occurring over time to the material, which matched with the proposed theory in section 2.3.1.3., meaning GO is not a stationary material, but a dynamic one. A second explanation could be the aggregation of the GO particles over time, which also would mean darkening in colour as light is reflected less.

6.1.7 GOS7

The last synthesis of graphene oxide is the GOS7. The synthesis was done by following the manuscript from section 5.1.1. The whole process went as planned and no deviations occurred. The gel was left to sit for 3 full days and during the standstill the solution had again the white precipitation and new addition in the form of bubbles (Figure 6.1.7.1) were registered. The white precipitation disappeared quickly during the wash with HCl or H2O solutions.

Figure 6.1.7.1. White precipitation and bubbles after the synthesis of the gel.

6.1.8 PURIFICATION OF GRAPHENE OXIDE

The persistent failure to come up with a manuscript, that would result in consistent supply of similar composition and structured GO gel still raises the question what is not being regulated yet.

The focus so far has been mostly on the first part of the production, the synthesis, thinking a mistake of some sort is being repeated. During one of the previous project [47] a mistake was done indeed by not keeping the temperature under control, but it has been corrected during this project due to an article, in which a group reported their discovery of the most important factor affecting the synthesis is temperature and that high temperature causes harm to the graphene oxide [79]. Although everything seems to be taken into consideration when it concerns the synthesis of graphene oxide, but still the obtained gels vary largely between batches.

The only part of the production that does not include a detailed description is the purification step, which based on section 5.1.1, could be the actual time when most changes to the structure of GO are occurring. None of the projects done at Aalborg University Esbjerg [48, 49, 47] have recorded a detailed description over what time period and how exactly purification was done, making it likely to be the point where the biggest variation occurs. For example, was the purification stage started as soon as the gels were ready or were they left to sit for a while? It is not clear if the gel, when left into the fume hood overnight, is topped up with the solution used for washing or not. Was one wash done per day or were several? How long did it take before the purified gel was used for membrane production? These are the most important questions to find answers to because if the compound reacts with water as reported in section 2.3.1.3, time is of the essence and should be defined.

The second sign of potential changes to the gel during purification is seen when the sequence of the washing solutions is changed. When water is used for washing, gelation is triggered as the compound seems to swallow it throughout the whole process and the volume of the gel increases with each wash as shown on Figure 6.1.8.1.

Figure 6.1.8.1. The change in the appearance of GO while washing with water.

If water is the last solvent the gel is washed with, the GO gel will stay in a state as demonstrated on the last picture above. The gelation can be easily explained by the fact that the compound's affinity to dissolve in water. The gels colour starts to change as soon it is exposed to water. The light brown colour becomes darker over time when in aqueous solution. The colour change is hypothesized to be caused by chemical process and the phenomenon is explained in section 2.3.1.3 or aggregation of the GO particles over time.

On the other hand, when HCl solution is used for washing, the material stays relatively compact, meaning expansion doesn't occur the way it does with water, and the colour change is not as noticeable and drastic as with water (Figure 6.1.8.2).

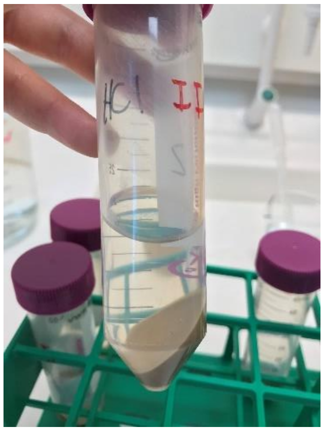

Figure 6.1.8.2. GO after the last wash with HCl solution.

6.1.9 SUMMARY

As demonstrated in the above sections the unpredictable nature of the synthesis of graphene oxide has been a big issue not only during this project, but is a common theme throughout all the relevant research done within this field at Aalborg University Esbjerg Campus [48, 49, 47].

On one hand the material shows sign of insensitivity, where it is still applicable even though the reaction conditions weren't ideal (GOS5 synthesis during this project). Yet again GOS6 where every requirement and condition were carefully followed, with no mistakes, resulted in unusable gel, with no obvious explanation why, indicating as if it is sensitive.

The random behavior of the compound refers strongly to the fact its mechanics are still not fully known and rises the demand for investigations. At this stage, the process has very low chance of replication, which needs to be solved before mass production is put in motion.

In addition, the purification part of the synthesis is not well defined yet, meaning the variation of the gel between different batches could be the origins of the variation in properties problem.

6.2 GRAPHENE OXIDE CHARACTERIZATION

The synthesized graphene oxide gel goes through a series of analytical techniques to evaluate its properties to verify the quality and to check if it fits with previously collected data. In addition, the changes in the composition of graphene oxide during purification part is presented.

6.2.1 ELEMENTAL ANALYSIS (EA) OF THE GRAPHENE OXIDE

The produced graphene oxide gel needs to be cleaned from impurities. This is done by washing the material with 1M HCl solution and distilled water. The different stages of purification of gel GOS2 and GOS7 were analyzed with Elemental Analysis (EA) to investigate the changes in the elemental composition. In addition, if it is possible to reduce the quantities used for the washing of the gel.

The coding systems for the samples in Table 6.2.1.1 and Table 6.2.1.3 T stands T for tube, W for water wash and A for acid wash. The last number represents the sequence number of the washing step.

All the samples were left out to dry minimum for 48h in the fume hood which was followed by 1 hour at 105°C in an oven to make sure most water has been removed. The two following tables have the obtained results from both investigated gels.

The purification of the gel GOS2 was a continuous process and was done as soon as possible, while the time period for washing GOS7 was longer, where there were few days in between washing with acid and water. A variation in the sequence of the washing stages were made, where half of the gel was purified with the normal way of acid wash first followed by water wash and other half where water wash was applied before the acid wash.

Table 6.2.1.1. Composition of GOS2 with sequence of water – acid wash.

Purification stage	Sample codes	Carbon	Hydrogen	Sulfur
Pre-purification	T6	7	5	17
Water	TW	45	1	2.3
Water + acid	TWA	45	0.5	1.9

Table 6.2.1.2. Composition of GOS2 with sequence of acid-water wash.

Purification stage	Sample codes	Carbon	Hydrogen	Sulfur
Acid	TA	41	1.2	3.3
Acid	TA	41	2	3.3
Acid	TA	41	1.3	3.7
Acid+water	TAW	45	1.5	2

Table 6.2.1.3 Composition of GOS7 during water-acid wash.

Purification stage	Sample codes	Carbon	Hydrogen	Sulfur
Pre-purification	T0	7.2	4	18.37
Water	TWS2	40.4	-0.99	2.21
1st Water + acid	TWA1	41.1	-2.11	1.44
2nd Water + acid	TWA2	41.9	-1.09	0.95
2nd Water + acid	TWA2	42.9	0.01	0.94
3rd Water + acid	TWA3	43.0	-1	0.78

Table 6.2.1.4. Composition of GOS7 during acid-wash wash.

Purification stage	Sample codes	Carbon	Hydrogen	Sulfur
1st Acid	TA1	26	2.83	11.21
1st Acid	TAS1	32.9	3.36	6.63
2nd Acid	TA2	38.4	0.71	5.59
3rd Acid	TA3	40.8	-1.42	4.715
1st Acid+Water	TAW1	44.3	-1.18	2.04
2nd Acid+Water	TAW2	44.8	-1.61	2.79
4th Acid+Water	TAW4	44.9	2.14	2.3

The first sample was taken before the beginning of the purification and is marked as T6 or T0 in the tables above. The numerical values are similar to each other in both cases and show the high levels of sulfur and oxygen. It is sensible, as the synthesis requires large amount of sulfuric acid to be used, which in this case has not yet been fully removed. The acid's presence is also indicated with the large amount of hydrogen percentage if you compare the value to the other results obtained after purification steps and take into consideration the size/weight of the hydrogen element.

The percentage of sulphur element content changes during each wash, decreasing from 17 to 1.9 (Table 6.2.1.1 column 5). This is very common as explained in section 2.3.1.3 where the leftover acids and salts are being washed out. In addition, at some point, the level of sulphate should become stable due to the permanently bonded functional groups.

In the case of GOS2 no matter what sequence, the same level of sulphur (approx. 2% from Table 6.2.1.1 and Table 6.2.1.2) was achieved after the purification. The percentage of sulphur behaves differently with GOS7, where the results for water-acid (Table 6.2.1.3 - 0.78 %) sequence is significantly lower compared to acid-water (Table 6.2.1.4 - 2.3%). The different values could be a result of unstable machinery as the values for H2 in the Table 6.2.1.3 and Table 6.2.1.4 are nonsensical because it is highly unlikely hydrogen is not present in some of the samples. But if the obtained results are taken as trusted, a fitting explanation can be found. As mentioned in the beginning of this results section, the time period for the washing of GOS7 was longer than what was spent on GOS2. The acid-water wash part for GOS7 was done with the similar speed as GOS2 gels and the results are indeed comparable to each other. There was a week's gap between the water-acid wash, where the water wash was completed, and the gel was left to sit in a fume hood before acid wash was done. If the ideas presented in section 2.3.1.3 are true, it is possible that the sulphates were slowly hydrolysed during the time period into H_2SO_4 and were removed during the water wash resulting in overall lower sulphur level.

6.2.2 TGA OF THE GRAPHENE OXIDE

At the moment, the only way to evaluate the concentration of the graphene oxide in the gel is using TGA method. A typical plot describing the process can be seen on Figure 6.2.2.1. Up until the temperature has reached 100°C a gradual change can be seen, which could be assigned to the evaporation of water. After the water has been removed the weight percentage reaches a stable value, which is considered to be the rough concentration of the GO in the synthesized gel. The reason it is described as the rough concentration is the fact the gel still includes other compounds, such as impurities, than just GO.

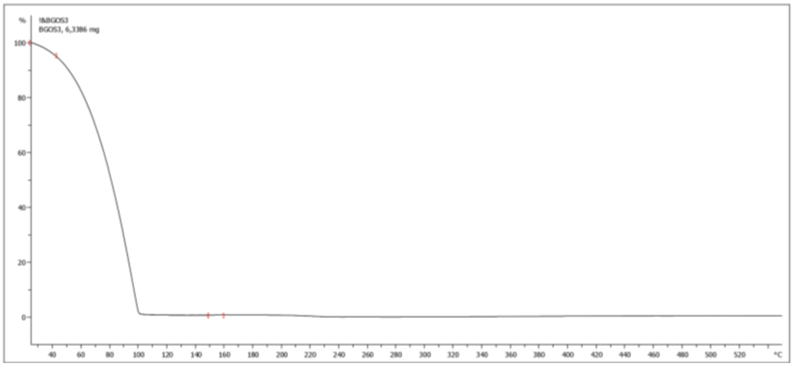

Figure 6.2.2.1. Typical plot obtained when GO concentration is measured with TGA.

The averaged result for the successful GO gels synthesized during this project has been found to be 2.1%, which matches well with results obtained during previous projects [48, 49, 47].

6.2.3 FT-IR OF THE GRAPHENE OXIDE

The evaluation of the presence of the typical functional groups is done by analyzing a membrane produced from the synthesized graphene oxide with FT-IR method. Preprocessed spectra of one of the membranes can be seen on the figure below.

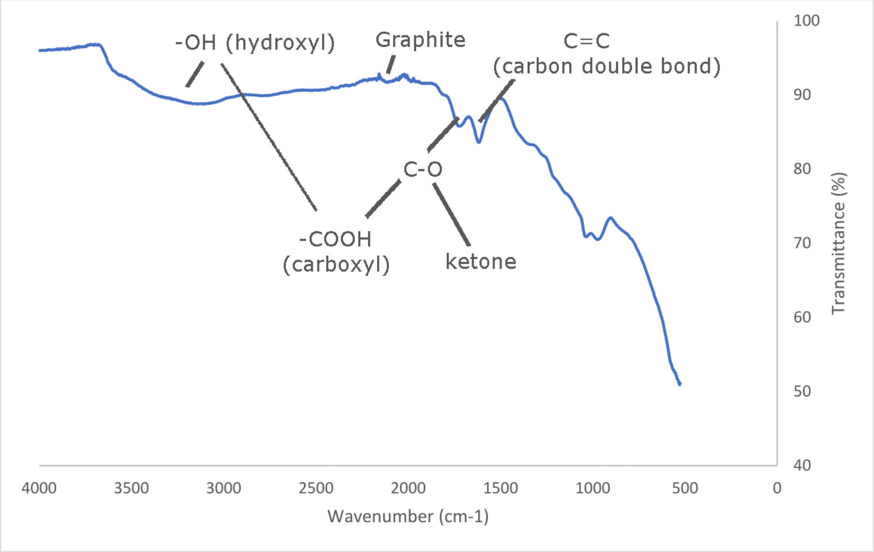

Figure 6.2.3.1. Spectrum of non-reduced graphene oxide membrane.

In general, the qualitative composition of the GO has shown to be consistent and not depending on the method of synthesis. Nevertheless, the spectrum is a difficult one to interpret as many of the functional groups tend to overlap or affect each other. The collected spectrum of the material synthesized during this project is analyzed to see if the usually reported bonds and functional group are present.

The first bond to be identified in the material is typically O-H. By starting to read the spectrum (Figure 6.2.3.1) from the left to the right a broad peak can be seen between 3500 – 2700 cm-1. It is typical placement for the oxygen – hydrogen (O-H) bond. The bond can represent the presence of alcohol group, which usually leaves a mark on the FT-IR spectrum between 3500-3200 cm-1. The second possibility is it belonging to a OH- fragment within carboxyl group (COOH-), that adsorbs in the range of 3330-2500 cm-1. The extra broad absorption range on the spectra on Figure 6.2.3.1 is from 3500 – 2700 cm-1, in which both of the functional groups ranges fit into leading to conclusion where it is believed to show the existence of both alcohol and carboxyl groups in the material.

The next small absorption can be seen in the range of 2300-2000 cm-1 and up until now the existence of the peak on other FT-IR spectra has not been discussed in the relevant literature. It has been identified to originate from the reactant graphite [47], but it is not clear what it shows exactly. It could indicate the presence of graphite as impurity, which was not completely removed during the purification of the GO gel. The second hypothesis presents the possibility of it representing the existence of conjugated carbon bonds within the graphene layers which are supposed to have sp^2 hybridization. In many of the articles concerning the analysis of the GO compound the carbon in sp2 hybridization is associated with the peak found at 1600 cm-1, that is said to belong to carbon-carbon double bond [26].

It is also a known theory that during the reduction of the material these areas with sp2 hybridization should increase as some of the oxidized graphene is converted back into its original form (Section 2.4). In one of the previous projects [47] a slight increase in adsorption was seen with the peak at 2300-2000 cm^{-1}, but a noticeable decrease was seen with the peak at 1600cm-1. Patterns as such leads the trail of though more towards the peaks at 2300 cm-1 to represent carbon in sp2 hybridization and raises question which functional group does the peak at 1600 cm-1 characterize. The answer to the question is believed to be water [80, 45, 81]. The peak is associated with the adsorbed water molecules in the material, which during the thermal annellation would decrease as water is exported from the compound resulting in noticeable decrease in the peak's size.

Next typical bond which should be present is the carbon- oxygen double bond. The peak located at 1700 cm-1 is believed to belong to it. This fragment is the second part of the carboxyl group, when combined with the earlier discussed presence of -OH adds more confidence in the existence of the carboxylic functional group. The second functional group it can represent is ketones, whose existence in the material is very probable. It has been reported that the only way to register the presence of ketones is after the reduction of the compound, as the first groups which tend to reduce are -OH and -COOH, leaving more thermally stable functional group such as ketone behind [82].

6.2.4 XRD

XRD is used to characterize the crystalline structure of the synthesized graphene oxide. This method allows to measure the distance between the layers of graphene (d), the average height of one laminar layer (H) and an estimation of how many graphene layers are in one laminar layer (n).

The first step after every synthesis is to measure how much has the distance between the graphene layers expanded compared to the reactant. Before starting to report on the numerical values calculated from the measurements gathered with XRD, a small explanation about the relationship between the level of oxidation and the d-value is relevant. The d-value, which will be discussed much, has been used to evaluate the level of oxidation. The idea behind is: the larger the gap between the two layers of graphene, the more functional groups have been formed during the oxidation [25]. In the previous project the d- value for graphite was measured to be 0.335 nm [47], which is the exact value reported in the literature [25]. The gathered results are presented in the Table 6.3.4.2, where different batches of non-reduced graphene oxide were examined.

Table 6.2.4.1. Crystalline properties for different membranes calculated from XRD plots.

Composition	Sample name	d (nm)	H	n
Graphite		0.335		
GOS4 + addi. H20	M17	0.8438	11	14
GOS4	M10	0.8383	12	14
GOS4+TiO2 + addi. H20	M25	0.8739	12	14
GOS4+TiO2	M18	0.8636	12	14
GOS5	M29	0.8608	14	16
GOS6 spring	M48	0.8504	10	12
GOS6	G6	0.8346	10	11
GOS6+TiO2	M51	0.8735	9	10

The transformation from graphite to graphene oxide can be seen on Figure 6.2.4.1, where the peak on the right originates form the reactant graphite. The narrow sharp feature of the peak shows an organized crystalline structure in graphite. The discreet peak on the left belongs to graphene oxide. Comparing the two peaks, there is no doubt a chemical conversion has happened as the shape and location has changed noticeably. The broadened shape of the peak is conveying a message the crystalline structure has been disturbed and the order has been broken, which result the formation of an amorphous state. The addition of TiO2 particles seem to decrease the order even more as the intensity of the blue peak is lowered compared to the other two graphene oxide peaks, where TiO2 is not added (Figure 6.2.4.1).

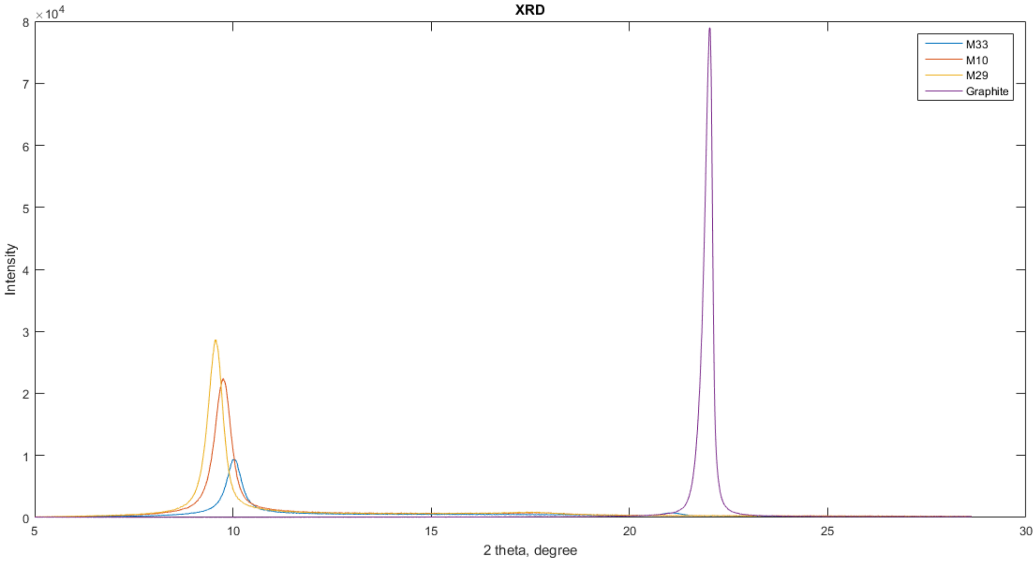

Figure 6.2.4.1 XRD plots of graphite (purple), graphene oxide (yellow and red) and reduced graphene oxide (blue).

During the autumn 2016 project the reported d-value for the GO was 0.802 nm, which was so far, the lowest obtained value. The measured distances during this project are significantly higher and a better match with the reported values of 0.825 nm from autumn 2015 [49] and 0.848 nm from the Master's thesis 2016 [48]. The reason for the higher d results during this project are due to being very attentive towards the temperature during the addition of the acid blend and later the water, as it has found to severely affect the compound [79], which was mostly neglected in the autumn 2016 project [47].

An unexpected result is the measurement obtained analzying the GOS5 as the synthesis didnt go according to plan and had a stirring malfunction (Section 6.1.5). The synthezed GO gel was showing unusual signs during the purification and was excpeted to result in a failure. Contrary to the expectation, it ended in a gel, which not only was fine to work with, but apparately the oxidazion had been very successful as the distance between the layers was measured to be the highest it has ever been (Table 6.2.4.1, row 6).

GOS6 gel was analysed right after its synthesis and the d-value was calculated to be 0.8503 nm. The same gel was used months later to produce and analyse a membrane with XRD and the value had lowered during the resting time to 0.8346 nm. The gradual reduction in the interlayer distance value can be interpreted to mean a reduction of graphene oxide over time. This theory has been discussed in Section 2.3.1.3, where an explanation is given to the self-reduction of graphene oxide through hydrolysis, meaning graphene oxide is a dynamic material, which keeps developing its properties over time, especially in the presence of water.

Another enlarging factor to the d-values seems to be the addition of TiO_2 particles. The distance between the layers grows noticably as shown in Table 6.2.4.1 comparing rows 2-3 and 4-5.

A small increase in the distance between the layers could be also seen if additional water is added to the membrane (M17 and M25) just before it is poured into the mold and left to dry compared to the others where no modifications were done to GO gel (M10, M18 and M38). The water could be absorbed into the systems due to hydrolysis, which result in the formation of new functional groups. The second reason could be the material's hydrophilic nature, which means it could be adsorbing water into the system and expand the material.

6.2.5 SUMMARY

New insight about the components change during the purification stage was gained by analysing the steps with EA. The successful graphene oxide batches achieved a good level of oxidation based on the calculated d-values. All the reported bonds in the literature – OH, C=O, C=C, C-O - [26] were identified to be present in the synthesized graphene oxide. The concentration of the GO gels was measured to be in average 2.1 wt%, which is in the same range as in previous projects. XRD results showed the d-values obtained during this project to be in good match with previous projects. Also, a change over time in GO gel was registered, which indicates a potential chemical process occurrence. The d-value size is affected by the addition of TiO2 particles and addition of water before casting the membrane.

6.3 THERMAL REDUCTION OF THE COMPOSITE MEMBRANE

In this chapter the effect of different temperature and duration for thermal reduction on the properties of GO/TiO2 membrane is focused on. The analytical techniques used for investigation are XRD, Zeta Potential, Drop Shape Analysis (DSA) and Brunauer–Emmett–Teller (BET).

6.3.1 XRD

The aim for using XRD was to investigate if and how the crystallinity of the material is affected by varying temperature and time. Two different temperatures were studied by varying time of reduction. The explanation for the reasons behind the chosen temperatures can be found in Section GO AND GO/TIO2 COMPOSITE MEMBRANE2.6. The two discreet temperatures are 120 and 140 °C. The gathered XRD plots will be discussed before the numerical values.

On the first plot (Figure 6.3.1.1) the behaviour of GO during the reduction at 140°C is shown. This temperature is in the range of optimal reduction conditions reported in previous projects [48, 49]. The red line on the figure represents reduction done for 60 minutes, which is the reported optimal duration for the thermal reduction [48, 49]. The blue coloured plot shows results gathered from thermal reduction at 140°C for 30 minutes.

When comparing the two plots an effect on the crystallinity of the GO can be seen, where the main peak at 13° 2θ not only shifts, but also loses some of its intensity and sharpness. This type of behaviour usually means either a chemical conversion or crystallinity/phase changes. While the GO peak is lessening, a second very broad peak emerges in the range of 22-28° 2θ. It is reported to belong to the GO crystals, which are lessened in size during rapid evaporation of gasses from the membrane layers, and the disordered phase (Section 2.4). It is direct evidence of GO being converted into rGO. The height of the broad peak is larger during the 60-min. reduction period than the 30-min. one, meaning that more GO is reduced as time passes on. The second highest peak at approx. 30° 2θ belong to TiO2, as reported in project of autumn 2016 [47].

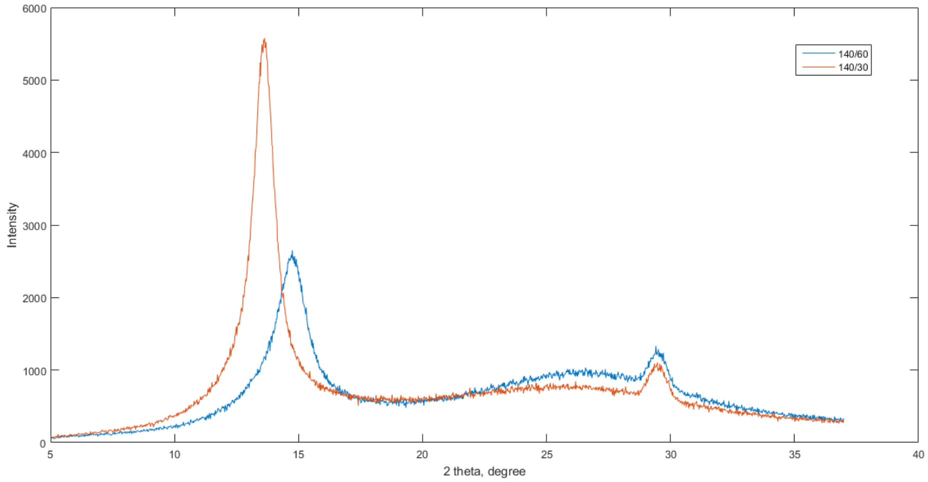

Figure 6.3.1.1. XRD results from thermal reduction at 140°C for 30 minutes (red) and 60 minutes (blue).

The next plots (Figure 6.3.1.2) show the results obtained when the membrane was reduced at 120°C. The plots for the duration 15 (blue) and 30 (red) minutes seem to have no deviation from each other. No appearance of the second large peak is seen, meaning no reduction of graphene oxide is happening within the first half hour at 120 °C.

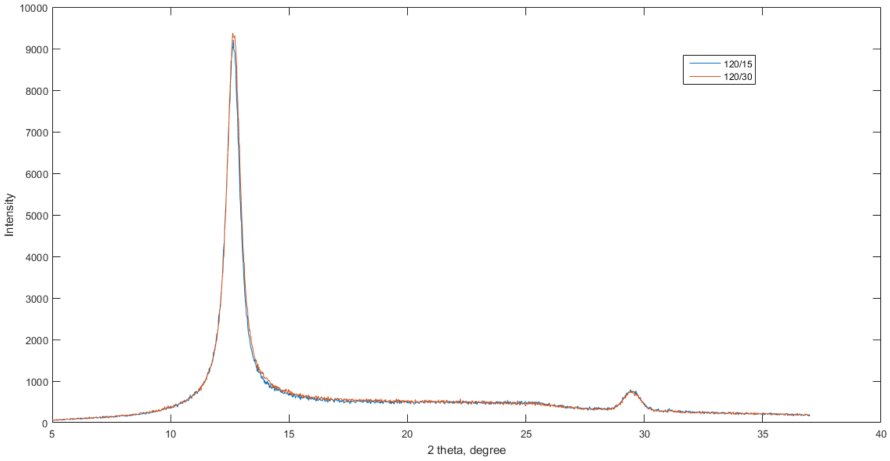

Figure 6.3.1.2. XRD results from thermal reduction at 120 °C for 15 (blue) and 30 (red) minutes.

The third plot is obtained by using a different XRD machine to analyse the third sample and the gathered results are not suitable to be combined with the previous two on the figure above. The third analysed membrane was reduced at 120°C for 2 hours. The thermal reduction has begun as the second broad peak can be seen to emerge just like it does with 140°C.

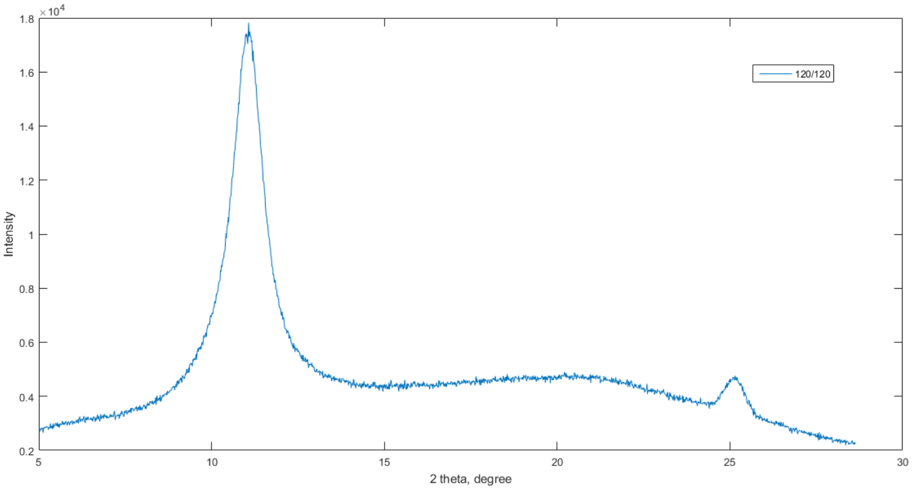

Figure 6.3.1.3. XRD result from thermal reduction at 120 °C for 120 minutes.

The calculated values from the XRD plots are all presented in the Table 6.3.1.1. In the case of the experiments at 140°C, as seen on the Figure 6.3.1.1, thermal reduction is taking place as the d-value is decreasing noticeably. It seems the reduction is triggered very quickly when the membrane is exposed to the 140°C condition. The percentages of reduction are calculated using the value 0.8383 nm for M21-M22 and value 0.8608 nm for M32-33, M40 from Table 6.3.1.1 as the starting point of the reduction. Evidence for the lessening in size of the crystal structure is seen from the decreasing values of H and n. It shows the layers of graphene lessening and the laminar layer thinning as thermal reduction goes on. The reason being exfoliation due to gasses leaving the structure (Section 2.4).

Table 6.3.1.1. Crystalline properties for different thermal reduction conditions.

Temp. (C)	Duratio n (min)	Sample name	d (nm)	H	n	Percentage of reduction (%)
140	30	M22	0.7538	8	11	10.0
140	60	M21	0.6969	5	7	16.8
120	15	M32	0.8119	13	16	5.6
120	30	M33	0.8132	13	16	5.5
120	120	M40	0.7981	5	7	7.2

At temperature 120°C the reduction seems to either have an incubation period of some sort or very slow conversion process. The first hour or so only a small decrease in the d-value is registered. The H and n results stay similar and demonstrate the existence of larger crystalline structure. The minor lessening in the interlayer distance is from the permeated water evaporation process and the evaporation process seems to be mild enough where the exfoliation is not as violent as seen with the results from 140°C. At around two hours, the reduction starts, the crystalline structure is ripped apart just like with 140°C, but the d-values have not been reduced as severely as in the case of 120°C.

6.3.2 ZETA POTENTIAL

The zeta potential and the stability of differently reduced membranes were determined using Surpass Streaming Potential equipment.

The zeta potential value was larger for the membrane reduced at 140°C for 30 minutes then reduction done at same temperature, but for the duration being 60 minutes (Figure 6.3.2.1). The charge of the membrane surface depends on the number of functional groups present. In case of the 30-minute reduction, the process of removal of the functional groups is not as far developed compared to the 60 minutes one, as also discussed in the previous XRD section, resulting in higher surface charge.

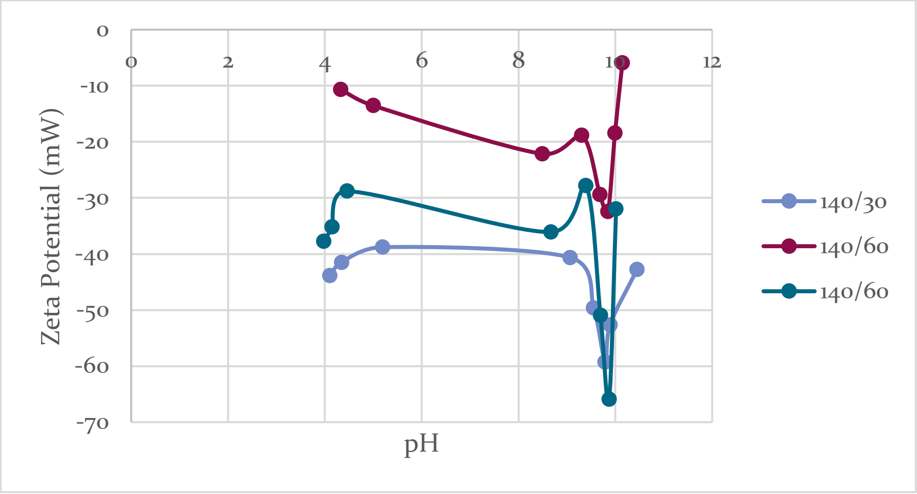

Figure 6.3.2.1. Zeta potential at different pH values for two types of thermally reduced membranes.

The stability of the membrane doesn’t seem to be affected by the different reduction conditions. The instability for both membranes start around the same 9+ pH, showing the construct to be stable in acidic environment and vulnerable if the pH is raised too much.

6.3.3 DSA

The hydrophilicity and surface energy of the differently reduced membranes were investigated using the Drop Shape Analysis. The first result in the Table 6.3.3.1 belongs to non-reduced GO/TiO2 membrane to set a reference point.

The next 3 rows are measurements from membrane reduced at 120°C at different durations. A decrease in the polarity of the membrane has happened when compared to the non-reduced membranes values. The reason being evaporation of infiltrated water molecules leaving the layers of the material. In general, the quantities are very similar to each other and matches with the XRD results, where no thermal reduction was registered within the first 30 minutes. According to the results with DSA no thermal reduction seems to be occurring at the 60-minute benchmark either.

The results obtained from membrane reduced at 140°C has a small variation between the different durations. The surface energy and polarity decrease when the membrane has been exposed to the temperature for more than 30 minutes. More functional groups have been removed from the system as the time passes on resulting in lower hydrophilicity and surface energy of the membrane.

Table 6.3.3.1 DSA results from membranes reduced in different thermal reduction environments.

Temp.	Time	H2O	DIM	Polar c	Dispers c	Overall	Polarity %
0	0	39.8	49.0	24.9	34.8	59.8	42.7
120	15	50.5	36.6	15.3	41.2	56.4	26.7
120	30	44.5	30.1	17.2	43.9	61.3	27.6
120	60	46.7	30.7	16.3	43.8	60.2	27.1
140	15	50.7	30.1	13.8	44.2	58.0	23.8
140	30	47.9	32.5	15.8	43.1	58.9	26.8
140	60	59.9	37.1	10.2	41.0	51.2	19.7

The numerical values in the rows 2-5 (120°C and up to 140°C/30 min) are very similar in its hydrophilicity and surface energy, although structure-wise as seen in XRD Figure 6.3.1.1 and Figure 6.3.1.2, a difference can be seen.

6.3.4 BET

The membrane surface characteristics such as a specific surface area and the average pore size were measured with BET. The results obtained from membranes, which were reduced under 140°C at different durations, are similar to each other as seen in the first two rows in Table 6.3.4.1. In the XRD section 6.3.1, the plots (Figure 6.3.1.1) and calculated crystal properties (Table 6.3.1.1) demonstrated the occurrence of graphene oxide conversion to reduced graphene oxide at 30 minutes. The process seems to be immediate at 140°C, leaving the material no opportunity to rearrange and is just violently shredded. The values for 30 and 60 minutes are most likely to be similar due to the rapidity of the reduction process when 140°C is reached. The third row belongs to a repeatability test, where left over pieces were used, and the measurement gave almost identical quantities to the previous one.

Table 6.3.4.1. Specific Surface and Pore size for different reduction temperature and time.

Temp	Time	Membrane nr	Mono-layer	Specific Surface	C value	Pore V	Max Pore V
140	30	M27	7.3	31.63	39	0.033	0.034
140	60	M28a	6.9	30.09	39	0.031	0.033
140	60	M28b	6.9	30.11	39	0.031	0.033
120	15	M32	6.1	26.76	38	0.028	0.029
120	60	M41	9.1	39.70	42	0.041	0.043

Thermal reduction at 120°C does affect the properties of the membrane more than at 140°C. The reduction at 120°C seems to have a delay or the process is so slow it takes time before the conversion process is registered. During the delay water molecules are exiting the layers of graphene oxide, but no conversion is happening. The properties gained by analysing 120°C/15min. membrane can be considered as non- reduced membrane, because, as seen in the XRD section, the conversion process had not yet begun. Only the membrane reduced for 2 hours at 120°C showed signs of reduction. Based on the measurement results in the table above, a reduction could be seen from 1 hour. In addition, the effect on the surface area seems to be bigger when the reduction is done at a lower temperature, where the material seems to be exfoliated more then with 140 °C.

The pore size distribution was not majorly affected by varying the temperature nor the duration of the reduction as seen in Table 6.3.4.2.

Table 6.3.4.2. Pore size distribution in relative volume in percentage value.

Pore size range (nm)	120°C/15min (%)	120°C /60min (%)	140°C /30min (%)	140°C /60min (%)
100-10	1	1.36	1.17	1.12
10-5	5.46	5.34	5.4	5.42
5-2	49.61	49.28	49.45	49.5
2-1.5	14.59	14.55	14.57	14.58
1.5 – 1	29.34	29.47	29.4	29.38

6.3.5 SUMMARY

Based on the gathered XRD plots and calculations the thermal reduction was found to be almost instantaneous when 140°C is used. Thermal reduction done at 120°C seems to take either some time before the conversion to rGO begins or before the slow conversion is registered by analytical tools. The reduction starts to show up in the results somewhere after 1 hour of exposure as at the 2-hour benchmark the reduction peak on the Figure 6.3.1.3 is emerging. The surface charge for the membrane reduced for shorter duration was measured to lower compared to the membranes reduced for longer time period. The delay in the reduction at 120°C was confirmed with DSA as well, because the polarity and surface energy doesn't change within the first hour of reduction. The membranes reduced at 140°C have a decrease in the polarity of the membrane as the duration of the process increases. The surface area and pore size for membranes reduced at 140°C were similar even at different durations. The surface area was found to vary a little between the membranes reduced at 120°C. The pore size distribution did not change as a results of the variation of temperature and duration.

6.4 PHOTOCATALYTIC AND HYDROPHILIC PROPERTIES

This chapter is dedicated to investigating the photocatalytic activity and hydrophilicity of the composite membranes and pristine graphene oxide using Zeta Potential and DSA. An attempt to quantify the photocatalytic activity was done using UV-Vis.

6.4.1 ASSESMENT OF PHOTOCATALYTIC ACTIVITY USING UV-VIS

Before starting with the presentation of the results few expectations of the behavior are introduced. A difference in the slope was predicted between the samples measure with the UV lamp and samples not exposed to UV light. Based on the theory in section 2.5.1 the membranes with TiO2 nanoparticles are expected to have a steeper slope in the concentration change of the dye compared to membranes with only GO as its material. The dye should be oxidized quicker in the presence of the photocatalyst.

The first testing with the UV-Vis was done with the methylene blue solution and the support membrane, to make sure the components of the composite membrane doesn't have any part in the oxidation of the dye. In addition to a regular nylon membrane, testing with thermally annealed nylon (140°C/60min) membrane was committed to make sure no changes occur to the properties. Miniscule deviation was registered by the nylon membrane on the dye solution during 2 hours of testing. The gathered blank data can be seen Figure 6.4.1.1.

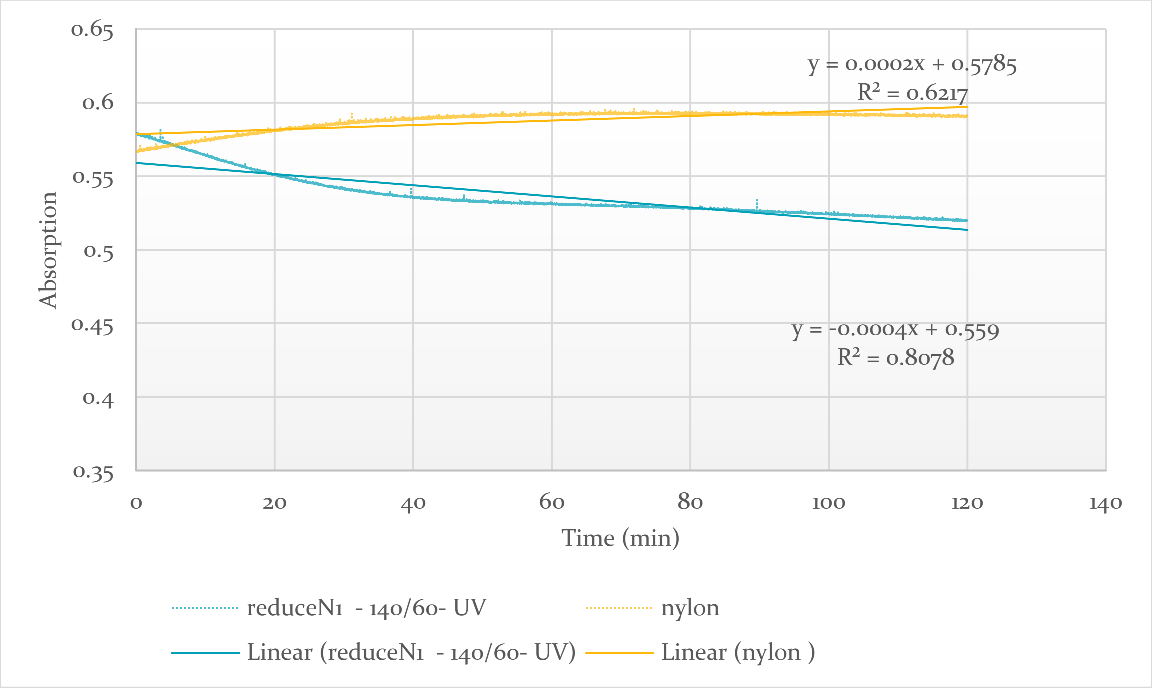

Figure 6.4.1.1. Results from testing the nylon membrane in methylene blue solution.

The list of the investigated samples for the photocatalytic activity is shown in Table 6.4.1.1 below. The gathered data from UV-Vis (original Figure 6.4.1.2) is plotted as the natural logarithm of the concentration of methylene blue versus time, to be able to calculate the slope of the process. For more precise results in terms of concentration of methylene blue, a calibration curve was measured to estimate the exact concentration of the dye at any given moment. The calibration curves and how they were made is introduced in Section 5.1.14. The gathered preprocessed data from the investigation with UV-Vis is demonstrated on Figure 6.4.1.3 and the calculated slopes from the data are to be found in Table 6.4.1.1 below.

The gathered results were unexpected as none of the prediction about the results were met, because change in the concentration of methylene blue was detected during all the measurements. This means the concentration of the dye decreases whether the UV- lamp was on or not, or if TiO_2 was added to the membrane or not.

Table 6.4.1.1. The calculated slopes and R values obtained by measuring the concentration change of methylene blue with and without UV lamp exposure.

Temp.	Time	Sample name	Composition	UV	Slope	R
140	60	N13	GO	No	-0.0133	0.9966
140	60	N2	GO	Yes	-0.0092	0.9943
140	60	N9	GO	Yes	-0.0157	0.9948
140	60	N5	GO/TiO2	No	-0.0098	0.9785
140	60	N6	GO/TiO2	Yes	-0.0097	0.9829
140	60	N0	GO/TiO2	Yes	-0.0092	0.9954
140	60	N7	GO/TiO2	Yes	-0.0122	0.9976
140	30	N10	GO/TiO2	Yes	-0.0183	0.9978

The GO/Nylon membranes were measured with and without UV lamp exposure. No photocatalytic activity was predicted to happen during these experiments due to lack of TiO2 particles, but it turned out to be wrong. The concentration of methylene blue decreases independent from the exposure of the UV light. The calculated slope for just GO/Nylon membrane without the UV lamp exposure is -0.0133. The value is very similar to the slopes calculated when the UV lamp was used (-0.0092 and -0.0157), which means the change in the concentration of methylene blue can be concluded not to be originated from a photocatalytic effect.

To make sure the decrease in methylene blue concentration is not originating from photocatalytic activity, membrane made out of GO were additionally investigated using DSA and Zeta Potential in section 6.4.2 and 6.4.3 GO demonstrated an increase on the zeta potential of the membrane when UV irradiation was done (Section 6.4.2), possibly indicating an increase in the number of functional groups on the surface, but DSA results show no increase in hydrophilicity and surface polarity (Section 6.4.3). No conclusion can be made based on the gathered results if graphene oxide is also photocatalytically active, due to the contrary nature of the data. The fact that the dye's concertation decreased even without the UV irradiation indicates a possibly different type of process than oxidation of methylene blue due to photocatalysis.

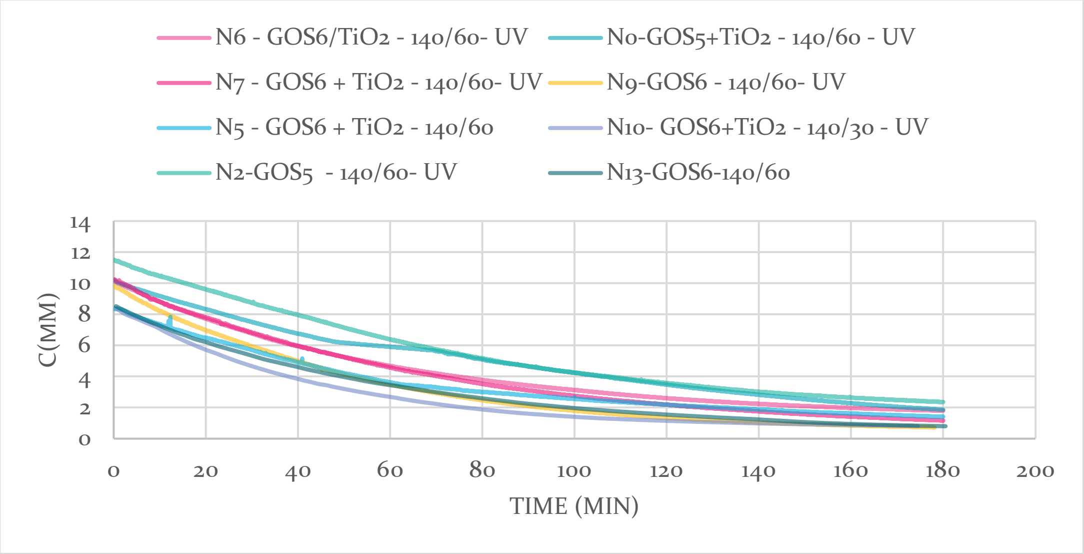

Figure 6.4.1.2. The original data of methylene blue concentration change over time gathered with UV-Vis.

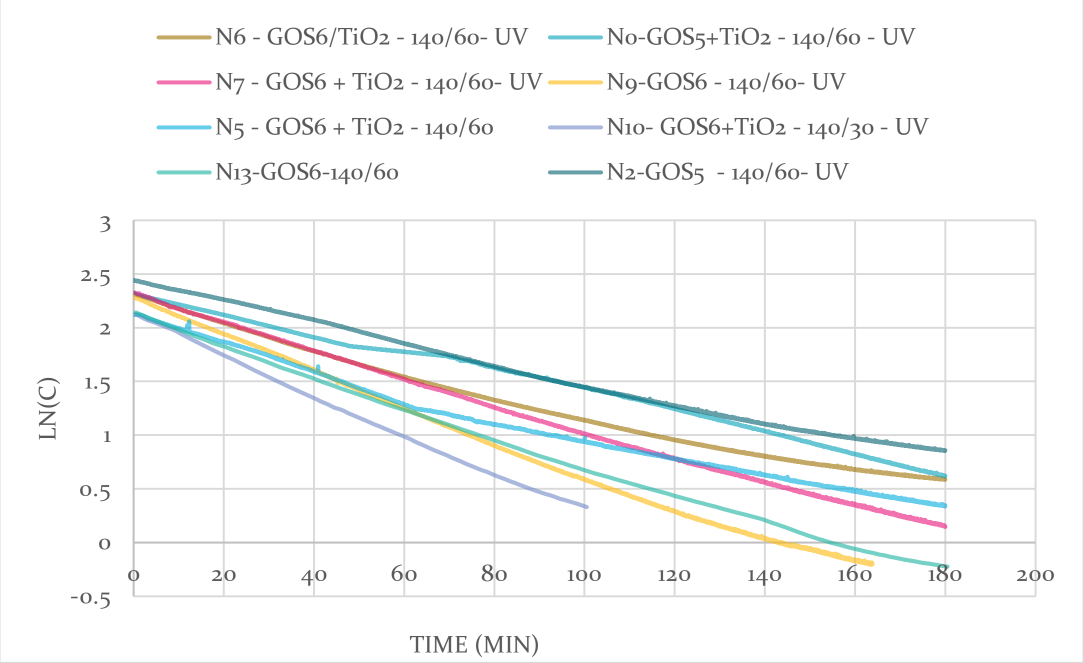

Figure 6.4.1.3. Preprocessed data of the change in concentration of methylene blue over time.

The second unexpected behavior is the lack of difference between the slopes gathered from the membranes, which had incorporated TiO_2 particles. The slopes obtained from UV irradiated membranes have two results, which are smaller or similar (-0.0097 and -0.0092) to the blank test (-0.0098) and only one that is larger in value (-0.0122). The steepest slope (-0.0183) was measured with a membrane made of GO/TiO_2/Nylon and was reduced 30 minutes instead of 60 minutes as all the previous samples were. The increase could be an outlier or an insight to what is really happening to methylene blue.

An assumption of a chemical reaction occurrence was made before the start of the experiments. The focus was mostly set on the photocatalytic properties of TiO_2 particles, which left the other component, graphene oxide, overlooked. Methylene blue (Figure 6.4.1.4) has three N-H groups, which are in its protonated form in aqueous solution at low pH.

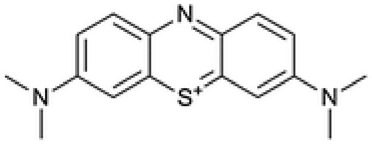

Figure 6.4.1.4. Chemical structure of methylene blue.

Graphene oxide has several oxygen functionalities, which give the membrane its negative surface charge. The negative and positive dipoles resolve in electrostatic interaction, which means the results gathered during this project reflect the dye molecules adsorbing on to the surface of GO [83].

From the adsorption point of view the steeper slope measured with 140°C/30minute (Table 6.4.1.1 bottom row) membrane could be understood purely based on the number of functional groups. All the other membranes have been reduced for an hour, meaning they have less functional groups left in their structure compared to the one reduced less time, meaning less areas where electrostatic interaction can occur. The lack of effect of TiO_2 particles under UV light is still surprising, but the low concentration of TiO_2 in the membranes could be the reason why steeper slopes were not registered.

6.4.2 ZETA POTENTIAL

The composite and graphene oxide membrane's photocatalytic and hydrophilic properties were tested by measuring the zeta potential before and after UV irradiation. Both of the membranes used during the testing were reduced at 140 °C, but at different durations. The same trend can be seen on Figure 6.3.2.1 as in section 6.3.2, where the surface charge of the 30-minute reduction (-40 mV) is higher compared to the 60-minute (approx. -20 mV).

In both cases the membranes' zeta potential is increased after it has been exposed to a UV lamp, possibly indicating the photocatalytic properties of the membrane. The charge of -20 mV of the membranes reduced at 60 minutes is taken down to -25 mV. A similar increase in charge is occurring with 30-minute reduced membranes from -40 mW to – 45 mW. The zeta potential could be increasing due to the TiO_2 particle activation, which adds new hydroxyl groups to the surface of the membrane (Section 2.5.1).

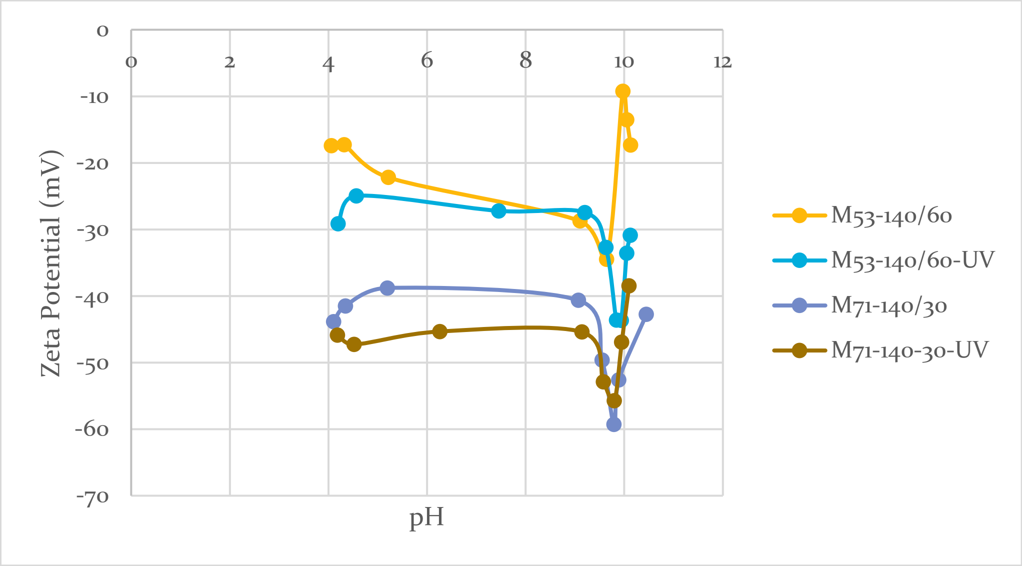

Figure 6.4.2.1. Zeta potential change during variation of pH for differently reduced GO/TiO2 membranes.

The second important investigation is concerning the graphene oxide membrane. The GO membrane was tested the same way as the previous GO/TiO2 membranes, where half of the membrane was exposed to UV irradiation while the other side wasn't. Based on the plot below, an effect on the surface charge of the GO membrane is registered. The surface charge was increased when UV-C light is applied just like in the case of GO/TiO2 membranes. Based on this result only GO cannot yet be concluded to have photocatalytic properties.

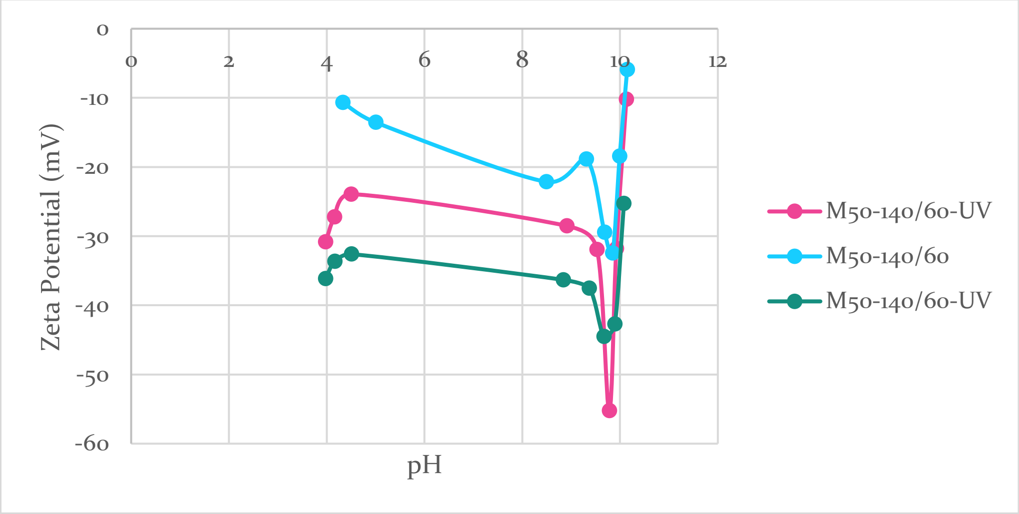

Figure 6.4.2.2. Zeta potential change during variation of pH for GO membrane.

6.4.3 DSA

Lastly, DSA was used to measure the effect of UV light exposure to the polarity and surface energy of GO and GO/TiO$_2$ membranes. The behavior of the irradiated GO membrane seems to be opposite to GO/TiO$_2$ membranes. The composite membrane's contact angle with water severely decreases after its been exposed to UV light. For example, membrane reduced at 140°C/30min. angle changes from 39° to 11° (Table 6.4.3.1). The change in the contact angle with water also means the polarity of the membranes increases compared to before and after the UV lamp application as shown in the last column in Table 6.4.3.1. This trend shows the activation of TiO$_2$ particles, which adds more oxygen functional groups to the surface, resulting in the increase of the hydrophilicity.

This is not the case with membranes made of only GO. UV exposure has the opposite effect, it decreases the contact angle with water (from 41° to 52°). The irradiation seems to lessen the hydrophilicity of the material and its polarity (drops from 30% to 27%). Perhaps a photolytic degradation is triggered for a functional group or an impurity in the membrane, which affects the contact angle with water. The behavior is indicating GO doesn't have superhydrophilic properties, but doesn't rule out photocatalytic property.

Table 6.4.3.1. Collected and calculated results from DSA.

Temp/time	**Material**	**UV**	**H2O**	**DIM**	**Polar c**	**Dispers c**	**Surface energy**	**Polarity %**
140/60	GO		41.1	30.0	18.9	44.2	63.2	30.0
140/60	GO	X	52.1	40.1	15.1	39.5	54.6	27.6
120/60	GO/TIO2		55.6	34.8	12.0	42.1	54.1	22.0
120/60	GO/TIO2	X	41.4	32.0	19.2	43.4	62.6	30.7
140/30	GO/TIO2		39.0	33.1	20.7	42.9	63.6	32.6
140/30	GO/TIO2	X	11.2	21.1	29.1	47.4	76.5	38.0
140/60	GO/TIO2		28.5	34.6	26.4	42.2	68.6	38.5
140/60	GO/TIO2	X	9.0	18.9	29.0	48.1	77.1	37.7

6.4.4 SUMMARY

Quantification of the photocatalytic activity was done to the composite membrane. During the testing, the concentration of the dye decreased with all samples, which lead to believe either graphene oxide has photocatalytic properties or something else was happening than the oxidation of methylene blue. The reason was identified to be adsorption of the dye molecules on the surface of GO due to electrostatic interactions. GO was tested with DSA and Zeta Potential for photocatalytic activity and hydrophilicity changes, but results turned out to be contradictory, which doesn't permit to obtain a conclusion.

The change in zeta potential due to UV exposure for the GO/TiO2 membranes were found to have a similar level of effect, independent from reduction temperature or duration. The stability of the membranes was not affected by the duration of the reduction nor the exposure to UV.

The photocatalytic properties were registered for the GO/TiO2 membranes, where the contact angle decreased, and polarity increased severely after UV light exposure. Membranes made out of graphene oxide did not show signs of superhydrophilicity unlike the GO/TiO2 membranes, the contact angle increased when it was treated with UV light.

6.5 MISCELLANEOUS RESULTS

In this chapter a couple of results are presented, that didn't fit into the sections above, but are worth mentioning. They mostly deal with the membrane behaviours, that makes it difficult to work with, and aspects which needs to be resolved before moving on in the development of the composite membrane.

During the analyses with the zeta potential rapid swelling of the membranes became apparent and caused problems. The swelling during the different analysis were recorded and can be seen on Figure 6.4.4.1 below.

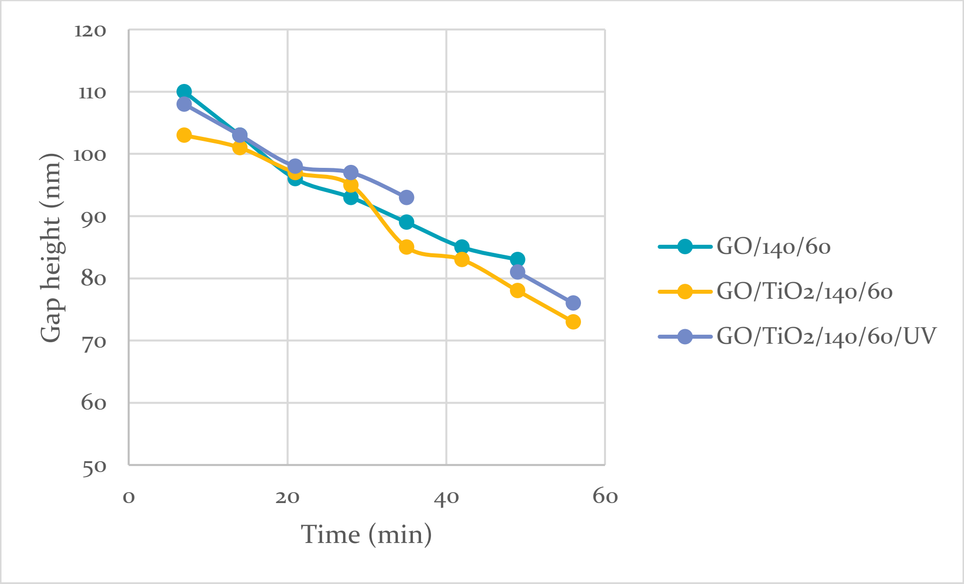

Figure 6.4.4.1 Swelling of the produced membrane.

The gap decreased from approximately 110 nm down to 75 nm, which is 30% change with in 1 hour of operation. Overall the rate of swelling seems to be the very similar, not depending on the composition or exposure to UV. The swelling wasn't only occurring during the change of pH, but started from the moment the equipment was filled with water, where the gap decreased over time, if left to sit. Swelling could cause some changes in the membrane properties, such as pore size and strength. Hence, these factors should be investigated and taken into consideration in the future development.

The second drawback of the composite membrane is the poor bondage between the nylon membrane and GO/TiO_2. This was unexpected as the GO/TiO_2/Nylon membrane was very durable when tested with tensile strength and in Sterlitech cell under elevated pressure during another project [47].

The membranes produced as part of this project were soaked in methylene blue solution for 2 hours, which most of the time ended weakening the bond between the two layers of membrane. The GO layer ended up becoming loose on top of the nylon membrane and if caution wasn't practised, the material fractured (Figure 6.4.4.2).

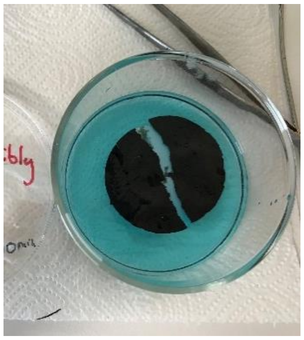

Figure 6.4.4.2. A failed experiment due to breakage of the membrane.

This should be resolved by either investigating how to bond the two membranes better or find an alternative way to support the GO membrane.

7 CONCLUSIONS

During this project several attempts to synthesize graphene oxide was done. The unpredictable nature of the synthesis of graphene oxide became apparent, as not all the attempts were successful.

The temperature control during the addition of acids blend and water is found to be very important. This was seen by obtaining graphene oxide with larger d-values (0.8383, 0.8608 and 0.8346 nm Table 6.2.4.1) compared to another project (0.802 nm [47]), where it was neglected.

The graphene oxide gel has demonstrated a change in its properties over time. A transformation was noticed with the GOS6 as it was not usable for membrane production directly after it had been synthesized, but after few months the gel produced good membranes. The coloration of the gel had darkened and the d-value showed to decreased (0.8504 nm to 0.8346 nm) in size if the gel is left to rest.

The purification stage of the gel production was investigated with Elemental Analysis to see what changes in the composition of graphene oxide occur. A difference between the content of sulfur was registered if the gel was left to rest for a couples of days after purification with water. The reason for the phenomenon is believed to be due to the hydrolysis of the sulphate moieties over time. In addition, the amount HCl solution used for purification is concluded to be enough, but the amount of water should be increased, as the composition didn't reach the level, where the content of elements became stable.

As previously mentioned, the gels used for membrane production, were characterized to have all the reported bonds in the literature – OH, C=O, C=C, C-O - [26]. The concentration of the GO gels matches the data obtained in previous projects and was measured to be in average 2.1 wt%.

The gathered XRD results showed an almost instantaneous thermal reduction when 140°C was used. The exfoliation of the GO crystals is seen on the XRD plots from the reduction duration of 30 minutes and upwards. The pace of the thermal reduction at 120°C is much slower and needs some time before the conversion to rGO is seen on the XRD plots.

The slow speed in the reduction at 120°C was seen in the results from DSA as well. The polarity and surface energy changed very little within the first hour of reduction at 120°C. The membranes reduced at 140°C have a noticeable decrease in the polarity of the membrane as the duration of the process increases.

The conversion rate of GO to rGO could be affecting the surface area of the membrane, but not the pore size distribution. The membranes reduced at 140 °C had similar pore size distribution and specific surface even at different durations of reduction. The surface area was found to vary slightly between the membranes reduced at 120°C, while the pore size distribution remained the same. Zeta potential was measured to be more negative for membrane with shorter reduction duration compared to longer ones.

An attempt to test and quantify the photocatalytic activity using methylene blue solution and UV irradiation was done. During the testing the concentration of the dye decreased with all samples, which lead to believe either graphene oxide has photocatalytic properties or something else was happening than oxidation of methylene blue. The reason in the change of the concentration of methylene blue is believed to be adsorption of the dye molecules on the surface of GO due to electrostatic interactions.

The photocatalytic and hydrophilic properties of GO were tested with DSA and Zeta Potential. The results turned out to be contradictory, where the zeta potential became more negative when exposed to the UV lamp, but DSA did not register any superhydrophilicity occurrence. The gathered results due to their contradictory nature doesn't allow conclusions to be made about the photocatalytic activity of GO.

The superhydrophilicity state of the GO/TiO2 membranes was registered. The photoinduced superhydrophilicity resulted in a smaller contact angle with water when measured with DSA and the UV exposed composite membrane's zeta-potential was measured to become more negative.

8 RECOMMENDATIONS

The seemingly random behavior of the graphene oxide refers strongly to the fact its mechanics are still not fully known and rises the demand for investigations. At this stage, the process has a very low chance of replication, which needs to be solved before mass production is put in motion.

A method for the approximation of the end of the reaction should be developed as now the reaction is left to stir a certain number of hours. There isn't any way to know how far the reaction has gone.

Thorough investigation into the purification of the GO gel should be done, where the effect of time and number of washes is focused on, to define the procedure a little better than it is now.

In addition, the properties of the GO over long-time period should be investigated. The pH, the sulphur content, the d-value, Raman analysis, particle size should be measured to see if any and what changes occur.

The possible photocatalytic activity and the adsorption property of GO needs to be tested in more detail and quantified.

A detail investigation on the swelling of the membrane and its ramification on the membrane properties. A more efficient way to attach the nylon and the GO/TiO_2 membrane should be found to avoid the degradation of the composite membrane. In addition, alternative materials as support material should be looked into.

9 REFERENCES

[1] "Internationa Decade for action "Water for life 2005-2015"," United Nations, [Online]. Available: http://www.un.org/waterforlifedecade/scarcity.shtml. [Accessed 20 11 2017].

[2] "World Wild Life," World Wild Life, [Online]. Available: https://www.worldwildlife.org/threats/water-scarcity. [Accessed 20 11 2017].

[3] B. Handwerk, "National Geographic News," National Geographic, [Online]. Available: https://www.nationalgeographic.com/environment/sustainable-earth/water/. [Accessed 20 11 2017].

[4] D. Dimick, "National Geographic News," National Geographic , 21 august 2014. [Online]. Available: https://news.nationalgeographic.com/news/2014/08/140819-groundwater-california-drought-aquifers-hidden-crisis/. [Accessed 20 11 2017].

[5] Rinkesh, "FF Concerve Energy Future," [Online]. Available: https://www.conserve-energy-future.com/causes-effects-solutions-of-water-scarcity.php. [Accessed 20 11 2017].

[6] "European Enviroment Agency," 2009. [Online]. Available: https://www.eea.europa.eu/media/newsreleases/drought-and-water-overuse-in-europe. [Accessed 3 12 2017].

[7] C. Zhao and et. al, "Highly effective antifouling performance of PVDF/graphene oxide composite membrane in membrane bioreactor (MBR) system," *Desalination,* vol. 340, pp. 59-66, 2014.

[8] Y. Gao, H. Meng and M. Baoxia, "Membrane surface modification with TiO 2–graphene oxide for enhanced photocatalytic performance," *Journal of Membrane Science,* vol. 455, pp. 349-356., 2014.

[9] R. Baker, Membrane technology ans applications, Wiley, 2012.

[10] D. Spuhler and F. Mazille, "Membrane Filtration," SSWM, 2012. [Online]. Available: https://www.sswm.info/content/membrane-filtration. [Accessed 21 11 2017].

[11] J. A. Jensen and P. Kønigsfeldt, Membrane filtration and related molecular separation technologies, APV Systems, 2000.

[12] A. Figoli and A. Criscuoli, Sustainable Membrane Technology for Water and Wastewater Treatment., Dalian: Chinese Academy of Sciences, 2017.

[13] A. SINCERO and G. SINCERO, "Advanced Filtration," Izmir: Dokuz Eyluel University., 2003. [Online]. Available: http://web.deu.edu.tr/atiksu/ana07/arit4.html. [Accessed 21 11 2017].

[14] "Slideshare," 8 9 2016. [Online]. Available: https://www.slideshare.net/Khawwam/lecture12-membrane-filtration.

[15] K. Peinemann and S.Nunes, Membrane Technology, Volume 4: Membranes for Water Treatment. Membranes, Wiley, 2010.

[16] N. Li, W. Ho and T. Matsuura, Advanced Membrane Technology and Applications, Wiley, 2011.

[17] R. Singh, Membrane Technology and Engineering for Water Purifcation: Application, Systems Design and Operation, Elsevier Science, 2014.

[18] "Membrane Filtration," [Online]. Available: https://www.mrwa.com/WaterWorksMnl/Chapter%2019%20Membrane%20Filtration.pdf. [Accessed 21 11 2017].

[19] A. Geim and K. S. Novoselov, "The rise of graphene," vol. 6, no. 3, 2007.

[20] [Online]. Available: http://www.andrew.cmu.edu/user/feenstra/graphene/.

[21] C. Rao, K. Biswas, A. Subrahmmanyam and A. Govindaraj, "Graphene, the new nanocarbon," vol. 19, no. 17, 2009.

[22] C. Soldano, A. Mahmood and E. Dujardin, "Production, properties and potential of graphene." Carbon 48.8 (2010): 2127-2150.," vol. 48, no. 8, 2010.

[23] D. L. Chung, “Review graphite,” *Journal of materials science,* vol. 37, no. 8, pp. 1475-1489, 2002.

[24] B. Brodie, "On the atomic weight of graphite," *Philos Trans R Soc Lond B Biol Sci,* vol. 149, p. 249–259, 1859.

[25] W. Gao, Graphene Oxide: Reduction Recipes, Spectroscopy, and Applications, Springer, 2015.

[26] D. C. Marcano and et al., "Improved synthesis of graphene oxide," Vols. 4806-4814, 2010.

[27] L. Peng and et al., "An iron-based green approach to 1-h production of single-layer graphene oxide," *Nature communications,* vol. 6, 2015.

[28] A. M. Dimiev and J. M. Tour, "Mechanism of graphene oxide formation," *ACS nano,* vol. 8, no. 3, pp. 3060-3068, 2014.

[29] A. M. Dimiev and et al., "Reversible formation of ammonium persulfate/sulfuric acid graphite intercalation compounds and their peculiar Raman spectra.," *ACS nano,* vol. 6, no. 9, pp. 7842-7849, 2012.

[30] A. M. Dimiev and et al., "Direct real-time monitoring of stage transitions in graphite intercalation compounds," *ACS nano,* vol. 7, no. 3, pp. 2773-2780, 2013.

[31] S. Eigler and et al., "Wet chemical synthesis of graphene," *Advanced materials,* vol. 25, no. 26, pp. 3583-3587, 2013.

[32] A. M. Dimiev and et al., "Pristine graphite oxide," *Journal of the American Chemical Society,* vol. 134, no. 5, pp. 2815-2822, 2012.

[33] A. M. Dimiev, L. B. Alemany and J. M. Tour, "Graphene oxide. Origin of acidity, its instability in water, and a new dynamic structural model.," *ACS nano,* vol. 7, no. 1, pp. 576-588, 2012.

[34] A. Lerf, H. He, M. Forester and J. Klinowski, "Structure of graphite oxide revisited," vol. 102, pp. 4477- 4482, 1998.

[35] T. Szabo and et al., "Evolution of surface functional groups in a series of progressively oxidized graphite oxides," *Chemistry of materials,* vol. 18, no. 11, pp. 2740-2749, 2006.

[36] R. A. Harvey, Polycyclic Aromatic Hydrocarbons, New York: Wiley-VCH, 1997.

[37] A. Simon and et al., "The crystal structure of Mn2O7," *Angewandte Chemie International Edition,* vol. 26, no. 2, pp. 139-140, 1987.

[38] K. R. Koch, "Oxidation by Mn207: An impressive demonstration of the powerful oxidizing property of dimanganeseheptoxide," *J. Chem. Educ,* vol. 59, no. 11, p. 973, 1982.

[39] M. Trömel and M. Russ, "Dimanganheptoxid zur selektiven Oxidation organischer Substrate.," *Angewandte Chemie,* vol. 99, no. 10, pp. 1037-1038, 1987.

[40] Y. Chen and et al., "One-pot synthesis of MnO 2/graphene/carbon nanotube hybrid by chemical method," *Carbon,* vol. 49, no. 13, pp. 4434-4442, 2011.

[41] A. L. Higginbotham, D. V. Kosynkin, A. Sinitskii, Z. Sun and J. M. Tour, "High-yield production of graphene by liquid-phase exfoliation of graphite," *Nature nanotechnology,* pp. 563-568, 2010.

[42] A. Lerf and et al., "Structure of graphite oxide revisited.," *The Journal of Physical Chemistry B,* vol. 102, no. 23, pp. 4477-4482, 1998.

[43] D. R. Dreyer, A. D. Todd and C. W. Bielawski, "Harnessing the chemistry of graphene oxide," no. 43, pp. 5288-5301, 2014.

[44] W. Gao and et al. , "New insights into the structure and reduction of graphite oxide," *Nature chemistry,* vol. 1, no. 5, pp. 403-408, 2009.

[45] T. Szabo and et al., "Enhanced acidity and pH-dependent surface charge characterization of successively oxidized graphite oxides," *Carbon,* vol. 44, no. 3, pp. 537-545, 2006.

[46] C. Petite, M. Seredych and T. J. Bandosz, "Revisiting the chemistry of graphite oxides and its effect on ammonia adsorption," *Journal of Materials Chemistry,* vol. 19, no. 48, pp. 9176-9185, 2009.

[47] B. Wright and K. Andersen, "Reinforcement of Go/TiO2 membrane with support material for water treatment purposes," Aalborg University Campus Esbjerg, Esbjerg, 2016.

[48] M. Pedersen and T. Jensen, "Graphene Oxide / Titanium oxide Membranes," Aalborg Univercity campus Esbjerg, Esbjerg, 2016.

[49] K. Andersen, P. Petrarulo, D. Ramos and P. Rooyen, "Investigating the effects of thermal reduction on graphene oxide membrane structure and permeability performance," Aalborg University Campus Esbjerg, Esbjerg, 2015.

[50] D. Li and et al. , "Processable aqueous dispersions of graphene nanosheets," *Nature nanotechnology,* vol. 3, no. 2, pp. 101-105, 2008.

[51] R. Cardona and J. Santiago-Aviles, "INTECH," [Online]. Available: https://www.intechopen.com/books/advances-in-nanofibers/materials-and-processes-for-ion-permeable-separating-membranes-by-electro-spinning. [Accessed 7 12 2017].

[52] X. Zheng and et al. , "Comparing effects of thermal annealing and chemical reduction treatments on properties of wet-spun graphene fibers," *Journal of materials science,* vol. 51, no. 21, pp. 9889-9901., 2016.

[53] S. Huh, "Thermal Reduction of Graphene Oxide," INTECH Open Access.

[54] M. McAllister and et al. , "Single sheet functionalized graphene by oxidation and thermal expansion of graphite.," *Chemistry of materials,* vol. 19, no. 18, pp. 4396-4404, 2007.

[55] M. M. Strom, R. E. Johnsen and P. Norby, "Storm, Mie MøllerIn situ X-ray powder diffraction studies of the synthesis of graphene oxide and formation of reduced graphene oxide.," *Journal of Solid State Chemistry,* vol. 240, pp. 49-54, 2016.

[56] M. McAllister and et al. , "Single sheet functionalized graphene by oxidation and thermal expansion of graphite.," *Chemistry of materials,* vol. 19, no. 18, pp. 4396-4404, 2007.

[57] Y. Qiu and et al. , "Explosive thermal reduction of graphene oxide-based materials: mechanism and safety implications.," *Carbon,* vol. 72, pp. 215-223, 2014.

[58] A. Khataee and G. Mansoori, Nanostructured titanium dioxide materials: properties, preparation and applications, Singapore: World scientific, 2012.

[59] Titanium dioxide., Lyon: World Health Organization International Agency For Research On Cancer, 2010.

[60] TiO2: Uses of Titanium Dioxide, RSC Advancing the Chemical Sciences., 19th July 2013.

[61] E. Søgaard and M. E. Simonsen, Heterogeneous Photocatalysis, Elsevier, 2014..

[62] U. Diebold, "The surface science of titanium dioxide," Surface Science Reports vol. 48, New Orleans, 2003.

[63] N. Sakai, A. Fujishima, T. Watanabe and K. Hashimoto, "Quantitative Evaluation of the Photoinduced," *The Journal of Physical Chemistry B,* vol. 107, pp. 1028-1035, 2003.

[64] M. Takeuchi, K. Sakamoto, G. Martra, S. Coluccia and M. Anpo, "Mechanism of Photoinduced Superhydrophilicity on the TiO2 Photocatalyst Surface," *The Journal of Physical Chemistry B 107,* pp. 15422-15427, 2005.

[65] W. Ning, X. Peng and Z. Xu, "Understanding water permeation in graphene oxide membranes.," *ACS applied materials & interfaces,* pp. 5877-5883, 2014.

[66] R. R. Nair, H. A. Wu, P. N. Jayaram, I. V. Grigorieva and A. K. Geim, "“Unimpeded permeation of water through helium-leak–tight graphene-based membranes.," *Science,* pp. 442-444, 2012.

[67] Y. Han, Z. Xu and C. Gao, "Ultrathin graphene nanofiltration membrane for water purification.," *Advanced Functional Materials,* pp. 3693-3700, 2013.

[68] H. M. Hegab and L. Zou, "“Graphene oxide-assisted membranes: fabrication and potential applications in desalination and water purification.," *Journal of Membrane Science,* pp. 95-106, 2015.

[69] S. Filice and et al. , "Graphene oxide and titania hybrid Nafion membranes for efficient removal of methyl orange dye from water.," *Carbon,* pp. 489-499, 2015.

[70] L. M. Pastrana-Martinez and et al. , "Photocatalytic behaviour of nanocarbon–TiO2 composites and immobilization into hollow fibres.," *Applied Catalysis B: Environmental,* pp. 101-111., 2013.

[71] C. Xu, Y. Cui, Y. Xu and X. Fu, "Graphene oxide–TiO2 composite filtration membranes and their potential application for water purification.," *Carbon,* pp. 465-471, 2013.

[72] M. Safarpour, V. Vatanpour, A. Khataee and M. Esmaeili, "Development of a novel high flux and foulingresistant fouling resistant thin film composite nanofiltration membrane

by embedding reduced graphene oxide/TiO2.," *Separation and Purification Technology,* pp. 96-107, 2015.

[73] M. Safarpour, A. Khataee and V. Vatanpour, "Effect of reduced graphene oxide/TiO2 nanocomposite with different molar ratios on the performance of PVDF ultrafiltration membranes.," *Separation and Purification Technology,* pp. 32-42, 2015.

[74] B. Wright and K. Andersen, "Reinforcement of GO/TiO2 membrane with support materials for water treatment purposes," Aalborg University Esbjerg, Esbjerg, 2016.

[75] T. Cosgrove, Colloid Science Principles, methods and applications., Wiley, 2010.

[76] T. Luxbacher, The ZETA Guide Principles of the streaming potential technique., Anton Paar, 2014.

[77] J. Lyklema, Fundamentals of interface and colloid science: soft colloids., Academic press, 2005.

[78] M. Lavin-Lopez, A. Romero, J. Garrido and L. Silva, "Influence of Different Improved Hummers Method Modifications on the Characteristics of Graphite Oxide in Order to Make a More Easily Scalable Method," vol. 55, 2016.

[79] K. Maab, A. Shokuhfar and S. Ahmandi, "The effect of temperature and type of peroxide on graphene synthesized by improved Hummers' method.," *International Nano Letters,* vol. 6, no. 4, pp. 211-214, 2016.

[80] M. Y. C. a. A. R. Mermoux, "FTIR and 13C NMR study of graphite oxide," *Carbon,* vol. 29, no. 3, pp. 469-474, 1991.

[81] T. e. a. Szabó, "Enhanced acidity and pH-dependent surface charge characterization of successively oxidized graphite oxides," *Carbon,* vol. 44, no. 3, pp. 537-545, 2006.

[82] Z. M. R. K. H. S. Y. A. R. Rasuli, "Wettability modification of graphene oxide by removal of carboxyl," vol. 364–368, no. 589, 2015.

[83] P. e. a. Sharma, ""Kinetics and adsorption behavior of the methyl blue at the graphene oxide/reduced graphene oxide nanosheet–water interface: a comparative study.," *Journal of Chemical & Engineering Data,* vol. 58, no. 12, pp. 3477-3488., 2013.

[84] S. P. C. W. B. R. S. R. Daniel R. Dreyer, "The chemistry of graphene oxide," vol. 39, 2010.

[85] [Online]. Available: https://www.worldwildlife.org/threats/water-scarcity. [Accessed 2017].

[86]

[87] M. L. K. P. a. T. R. Jensen, "Graphene Oxide /Titanium Dioxide Membranes," Aalborg University Esbjerg, Esbjerg, 2016.

[88] P. A. P. D. P. R. a. P. C. v. R. Katrine Andersen, "Investigating the effects of thermal reduction on graphene oxide membrane structure and permeability performance," Aalborg University Esbjerg, Esbjerg, 2015.